Exploring hydrophobic interactions for the purification of the T4 bacteriophage: Phenyl and Phenyl Boronate Chromatography

André Trigo Moutinho Gomes

Thesis to obtain the Master of Science Degree in

Biotechnology

Supervisor: Prof. Ana Margarida Nunes da Mata Pires de Azevedo

Examination Committee

Chairperson: Professor Luís Joaquim Pina da Fonseca

Supervisor: Professor Ana Margarida Nunes da Mata Pires de Azevedo

Member of the Committee: Professor Ana Gabriela Gonçalves Neves Gomes

November 2022

Preface

The work presented in this thesis was performed at the Institute for Bioengineering and Biosciences of Instituto superior Técnico (Lisbon, Portugal), during the period February-July 2022, under the supervision of Prof. Ana Azevedo.

Declaration

I declare that this document is an original work of my own authorship and that it fulfils all the requirements of the Code of Conduct and Good Practices of the Universidade de Lisboa.

Acknowledgments

First of all, I would like to utterly thank my supervisor, Professor Ana Azevedo. Thank you for the trust placed in me, for the encouragement given at each setback I had, for the freedom of ideas given throughout my work. I truly believed in the project given to me and with your aid, we built an interesting story where I felt I had control over my decisions. This was of the utmost importance to me, and I know that my performed work would never be matched if I was under different guidance.

An enormous thank you to all the people at laboratory 8.6.11. Sara Rosa, Jorge João, Ana Rita Santos, and Ricardo Silva, to all, an endless thank you. You played an enormous part in my thesis progress. To Sara Rosa and Ana Rita Santos, thank you for helping me to understand how to work with bacterial cultures and bacteriophage production. Thank you also for always being available to help even with the most basic questions, and for helping me make sense of my many strange results. To Jorge João, all my knowledge regarding the AKTA systems comes from you. Being the foundation of my thesis, you played a crucial role in helping me to succeed. I will not forget the endless patient you had with me. To Ricardo Silva, although we did not see other many times, you always cheered me up, either by talking about football or motivating me. A special thanks to everyone at the seventh floor for helping me to work with the most basic tools. A very special note to Sofia Duarte, who was my partner in crime in the purification of bacteriophages. You were always a great teacher. Overall, I always felt happy and lucky to be together with you guys, we had many great laughs, and I am not lying when I say I will miss you.

To all my close friends, an incredible thank you. The thesis period was rough because we did not see each other much, but I always felt that at the end of the day, you were there to motivate me in the toughest moments. A special thank you to the Galáticos FC, composed of my great friends Bernardo Raimundo, Nuno Filipe Mata, and Miguel Ribeiro. You all know what you mean in my life.

An endless thank you to all my family, including my dog. It was a tough journey and you truly helped and always understood my frustrations. Finally, an incredible and special thank you to my girlfriend that was by my side at each step of my thesis. You truly understood me and encouraged me to pursue and surpass my highest limits.

To all, a truly special thank you!

Resumo

O mundo está à beira de entrar mais uma vez numa era “pré-antibiótico”, associado ao aparecimento de bactérias resistentes a antibióticos. Terapia bacteriofágica apresenta-se como uma das mais promissoras ferramentas para combater este perigo. No entanto, não existe ainda um processo de purificação de bacteriófagos que permita a remoção total de impurezas do hospedeiro. Diversas cromatografias foram testadas sabendo que esta técnica deve estar no centro de uma solução. Cromatografia de fenil boronato (CFB) foi eficiente a adsorver bacteriófagos, via interações hidrófobas, resultando num rendimento de 54.5% e uma remoção de proteínas, dsDNA, e endotoxinas de 94.9%, 95.8% e 98.1%, respetivamente. Cromatografia de interação hidrófoba (CIH) foi utilizada com base nestes resultados. Diferentes concentrações de sulfato de amónio na fase de equilibração foram testadas, sendo que 0.75 M resultou no maior rendimento (93.0%) e uma remoção de proteínas, dsDNA, e endotoxinas de 98.3%, 88.3% e 93.3%, respetivamente. Um gradiente linear serviu como base para o desenvolvimento de gradientes com vários passos mais apropriados para a indústria. Com 0.75 M de sulfato de amónio na fase de equilibração e cinco passos de eluição, um rendimento de 70.2% foi obtido, com uma remoção de proteínas, dsDNA, e endotoxinas de 96.8%, 92.5% e 98.8%, respetivamente. CFB e CIH aparentam ser ferramentas inovadoras para a purificação de bacteriófagos. O que falta perceber é como estas operações funcionariam com outros bacteriófagos e como a CIH pode ser otimizada em termos de ligandos e seleção de sais.

Palavras-chave: Bacteriófago; Bactérias resistente a antibióticos; Cromatografia de Fenil Boronato; Cromatografia de Interação Hidrófoba; Remoção de impurezas do hospedeiro

Abstract

The world is on the verge of entering once again a “pre-antibiotic era”, associated with the emergence of antibiotic-resistant bacteria. Bacteriophage therapy poses as one of the most promising tools to combat this threat. However, there is yet an established bacteriophage purification scheme that considers the complete removal of host impurities. Various chromatography modes were tested in this work as this technique should be at the center of a solution. Phenyl Boronate Chromatography (PBC) was successful at adsorbing bacteriophages via hydrophobic interactions, resulting in a yield of 54.5% and a removal of proteins, dsDNA, and endotoxins of 94.9%, 95.8%, and 98.1%, respectively. Based on these optimistic results, Hydrophobic Interaction Chromatography (HIC) was tested. Different ammonium sulfate concentrations in the equilibration phase were tested, with 0.75 M attaining the highest bacteriophage recovery (93.0%) and a removal of proteins, dsDNA, and endotoxins of 98.3%, 88.3%, and 93.3%, respectively. A linear gradient served as a foundation for the development of multi-step gradients more appropriate for an industrial setting. With 0.75 M ammonium sulfate in the equilibration buffer and five elution steps, a bacteriophage recovery of 70.2% was attained, with a removal of proteins, dsDNA, and endotoxins of 96.8%, 92.5%, and 98.8%, respectively. PBC and HIC looked to be innovative tools for the purification of T4 bacteriophages. What is yet to be answered is how these operations would perform with other bacteriophages, along with the further optimization of HIC in terms of ligands and salt selection.

Keywords: Bacteriophage; Antibiotic-resistant bacteria; Phenyl Boronate Chromatography; Hydrophobic Interaction Chromatography; Host impurities removal

Index

List of Figures

List of Tables

List of Abbreviations

ESKAPE *Enterococcus faecium*, *Staphylococcus aureus*, *Klebsiella pneumoniae*, *Acinetobacter baumanii*, *Pseudomonas aeruginosa*, and *Enterobacter* species

ICTV International committee on taxonomy of viruses

MW Molecular weight

pI Isoelectric point

LPS Lipopolysaccharide

VAL Virion-associated lysin

HGT Horizontal gene transfer

Abi Abortive infection

CRISPR Clustered regularly interspaced short palindromic repeats

CF Cystic fibrosis

CFTR Cystic fibrosis transmembrane conductance regulator

IV Intravenous

IND Investigational new drug

FDA Food and drug administration

EDTA Ethylenediamine tetraacetic acid

GMP Good manufacturing practices

USP Upstream processing

DSP Downstream processing

PFU Plaque-forming units

MCB Master cell bank

MFB Master phage bank

PEG Polyethylene glycol

TFF Tangential flow filtration

UF Ultrafiltration

DF Diafiltration

MWCO Molecular weight cut off

SE	Staphylococcal enterotoxins
IEC	Ion-exchange chromatography
SEC	Size-exclusion chromatography
MMC	Multi-modal chromatography
DBC	Dynamic binding capacity
AEC	Anion-exchange chromatography
SDS-PAGE	Sodium dodecyl sulfate–polyacrylamide gel electrophoresis
CIM	Convective interaction media
QA	Quaternary amine
HIC	Hydrophobic interaction chromatography
PBC	Phenyl boronate chromatography
BA	Boronic acid
EU	Endotoxin unit
PMB	Polymyxin B
ECHA	European Chemicals Agency
TSB	Tryptic soy broth
TSA	Tryptic soy agar
PBS	Phosphate buffered saline
qPCR	quantitative-PCR
OD	Optical density
CFU	Colony-forming-unit
SM	Saline-magnesium
DLPA	Double-agar plaque assay
MOI	Multiplicity of infection
CV	Column volume
EFW	Endotoxin-free water
LAL	Lyophilized amebocyte lysate
TE	Tris-EDTA

1. Introduction

Bacteriophages, in a modest manner, are defined as “bacteria eaters”, thus capable of killing bacteria. Currently, bacteriophages are viewed as an alternative to antibiotics against antibiotic-resistant bacteria. Progressively, investment in new antibiotics has been plunging, mainly due to the complexity associated with their discovery, in terms of efficient biological activity and safeness. Moreover, new antibiotics are no longer economically viable.[1] Antibiotic-resistant bacteria may be referred to as ESKAPE (*Enterococcus faecium*, *Staphylococcus aureus*, *Klebsiella pneumoniae*, *Acinetobacter baumanii*, *Pseudomonas aeruginosa*, and *Enterobacter* species) pathogens, containing both Gram-positive and Gram-negative bacteria. These ever-growing bacteria are life-threatening in many situations, primarily in immunocompromised patients.[1–4] Therefore, there is an urgent need to find new therapeutic tools against antibiotic-resistant bacteria. This is where phage therapy looms, as it targets all types of bacteria, including ESKAPE pathogens, while still being specific for each bacterium species, which also contributes to the preservation of the natural human microbiome.[5]

1.1. General historical aspects of bacteriophages

Early evidence of bacteriophage’s existence was reported by Ernest Hanbury Hankin in 1896.[6] Hankin aimed at quantifying the number of *Vibrio cholera* in the river of Ganges, India. In his studies, a reduced number of this bacterium was observed in some parts of the river. This was the first report of what is known nowadays as “bacteriophage”, in the past named “Hankin’s phenomenon”.[5,7] Later on, in 1915, Frederick Twort published the first paper exploring the biological activity of bacteriophages.[8] Twort cultured micrococcus, isolated from vaccinia virus, and observed increasingly transparent areas. Furthermore, he reported that this “transparent material” did not grow on his own. Twort was not able to pinpoint exactly what was killing bacteria, even hypothesizing that a small bacterium could be responsible. Finally, in 1917 the term “bacteriophage” was coined by Felix d’Herelle to the “anti-Shiga microbe”.[9] This microbiologist was investigating an outbreak of *Shigella disenteriae*, which causes bacillary dysentery, that disseminated in French troops. Briefly, D´Herelle incubated various *Shiggela* strains with bacterium-free filtrates, made from stools, and observed bacilli arrest in development and further lysis, based on the appearance of clear zones in agar cultures, later referred to as “plaques”.[7,10,11] Felix d´Herelle’s findings elicited the use of bacteriophages in the therapeutic application, the so-called phage therapy.[7] In the following years, phages were successfully used to treat cholera[12,13] and typhoid fever[14], among other examples. Notwithstanding, in the 1930s, the American Medical Association’s Council on Pharmacy and Chemistry concluded that the use of phages in a clinical environment was not advisable. This was mainly associated with the poor knowledge of phage’s biology and experimental ambiguous results. [10,11,15] Despite this, phage therapy research carried on in the former USSR and Eastern Europe. Unfortunately, much of the work performed during this period was lost or locked in the Kremlin.[16] Regarding the reviewed articles of this era, it was concluded that the clinical criteria used for phage dosages were untrustful and would not meet the pharmaceutical standards present nowadays.[17–19] Other factors contributing to the phage’s use decline in the 1940s was the discovery of penicillin and its easy scale-up and production contrary to phage preparations, which were not optimized, much less ready for large-scale productions.[16,20] It was only around the 1980s that

phage therapy emerged once again, mainly associated with the appearance of antibiotic-resistant bacteria and the complexity behind the development of new antibiotics.[10] This interest has been brought to the modern days, with arising companies specializing in the production and purification of phages, as well as the first clinical trials in humans.[16]

1.2. Bacteriophage biology

1.2.1. Classification and structure

In the early 21st century, bacteriophage structure and classification were innately connected. This is, phage classification was mainly based on its structure. The first bacteriophage classification was performed in 1943, by H.Ruska, employing electron microscopy.[21] Until the early 2000s, phage classification was still mainly based on this tool, but with initial hints at a new taxonomy method for phage organization: genomics.[22] Interestingly, bacteriophages were the first entities to be fully sequenced, specifically phage ΦX174 in 1977.[23] In 2002, Brussow and Hendrix stated that through genome sequencing, complete phage genomes were expected to increase considerably in the following years.[24] Included in the general OMICS area of study, metagenomics was the main contributor to the discovery of a variety of new phages and their organization in different orders, families, and genera.[25] The International Committee on Taxonomy of Viruses (ICTV), organizes viruses, such as phages, in different tiers: phylum, class, order, and family, among others. Comparing the different reports published by ICTV, it is possible to observe exactly the effect of genome sequencing in phage discovery and classification. Considering only tailed phages, the 6th report, released by ICTV in 1995, registered 30 species, divided into 3 families. Data published in October 2020, assessed a much larger number of the same tailed phages, organized into 14 families with 2814 species.[26] For many years, before the mass implementation of genome sequencing, only 3 main tailed phages (*Caudovirales*) families were considered: *Myoviridae*, *Syphoviridae,* and *Podoviridae*.[27] More recently, it is possible to observe new *Caudovirales* families with more species than the original families.[26] For instance, the family *Autographiviridae* has 373 species, compared with the 130 species present in *Podoviridae*. Curiously, *Autographiviridae* originated from a genus within *Podoviridae*, named *Autographivirinae*.[26] In 2019, a proposal was made to ICTV, based on preliminary results from Iranzo *et al*.[28] which placed *Autographivirinae* as a different cluster in the dsDNA viruses, originating its own family within *Caudovirales*. This example portrays how interchangeable phage taxonomy classification is, and that phage organization will continue to branch out, picking up already discovered genera.

Phages are said to be polyphyletic in origin, thus derived from not only one ancestral lineage but more. This means that phages are highly diverse entities, both at structural and biological levels.[22] As a result, it is not an easy task to generalize phage size and few studies have been performed regarding this subject. Notwithstanding, in 1998, Ackermann[27] stated that tailed phages have an average molecular weight (MW) of 100 MDa, with an average head diameter of 66 nm and an average tail length of 154 nm.[27] Moreover, phage's isoelectric point (pI) is between 2.4 and 7.4.[29] In terms of their genome, bacteriophages mainly contain dsDNA, with a few examples containing ssDNA, ssRNA, and dsRNA.[22,30] Phage's genomic material is usually encapsulated in a protein-made structure, named capsid (head), which in some cases may contain lipid layering.[22] In 2006, Ackermann stated that the large majority of

phages belonged to the *Caudovirales* order, hence being tailed. In 2016, about 95% of phages were tailed.[22] Within this order, most phages have icosahedral heads, composed of one or two specific protein copies, organized either in hexamers or pentamers.[31] The main differences within *Caudovirales* are at the level of the tail, which is normally covered with proteins organized with helical symmetry.[32] As an example, *Siphoviridae*, the largest family of tailed phages, has long, non-contractile but flexible tails. On the other hand, *Myoviridae* is characterized by contractile tails, due to the presence of an extra protein sheath surrounding the central protein tube.[22,30,31] Another important aspect that differentiates phages within *Caudovirales* is the geometry in the baseplate of the tail, responsible for the interaction with bacteria. One of the newer families, *Ackermannviridae* has umbrella and prong-like structures in the base plate responsible for adsorption.[30] Regarding another architectural characteristic of phages tails, *Podoviridae*, one of the original *Caudovirales* families, has no connector between the tail and the capsid. Moreover, their tail is short and non-contractible.[22] The main enumerated characteristics of the families *Myoviridae*, *Siphoviridae*, and *Podoviridae* are illustrated in Figure 1. Apart from tailed phages, these viral particles may also be classified regarding their nucleocapsid geometry, which may be polyhedral, filamentous, or pleomorphic.[22,30–32]

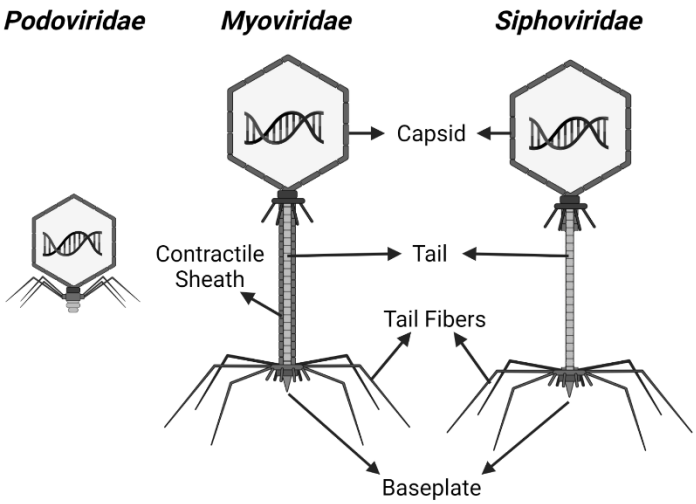

Figure 1- Structure of the three original *Caudovirales* families. All families have in common the presence of an icosahedral capsid containing the phage's nucleic acid, a tail, a baseplate, and tail fibers. Both *Myoviridae* and *Siphoviridae* are characterized by the presence of long tails, with *Myoviridae* having an extra protein sheath surrounding the tail and responsible for its contractile feature. *Siphoviridae* and *Podoviridae* have non-contractile tails, with the latter being recognized by their smaller tails. Adapted from BioRender.com.

1.2.2. Bacteriophage-host interactions

Bacteriophage-bacteria interactions are initiated by the phage's recognition of a specific receptor present on the bacterium's surface.[33–35] These interactions are mainly mediated by terminal adhesins, present in tail fibers, themselves associated with the baseplate of the bacteriophage.[36] In a situation where phages are not infecting bacteria, these fibers assume random movements. When phages recognize bacteria, the same fibers adopt a fixed orientation, pointing toward the host receptor.[34,37] Upon recognition of a specific receptor by the tail fibers' adhesins, a conformational change occurs in the baseplate, which leads to the contraction of the outer protein sheath layer present in tailed phages. This process is named adsorption and is done in two steps. Initially, electrostatic interactions are responsible

for the referred recognition, in a less specific, reversible binding, to a primary receptor. This is immediately followed by the irreversible binding of tail fibers or other baseplate proteins to a secondary receptor, which coincides with sheath contraction. With this, the phage particle is brought closer to the host cell surface.[34,36–38]

The next step in the phage infection process is the penetration of the host envelope, which differs in Gram-positive or Gram-negative bacteria. In the former, the cell's envelope is composed of a thick, functionalized layer of peptidoglycans, that include among other constituents, teichoic and lipoteichoic acids. Both can be used as specific receptors for phage interaction.[36,39] On the other hand, Gram-negative bacteria possess an outer membrane containing LPS (Lipopolysaccharide), a much thinner middle peptidoglycan layer, and an inner membrane. Phage receptors among these bacteria include mainly LPS, but also outer membrane proteins, such as porins, transport-associated proteins with secretion, enzymes, and so forth.[33,36,39] In addition, bacteriophages may also recognize bacterial pili, flagella, and capsular or slime external polysaccharide matrixes.[33] Depending on the type of bacteria targeted by a phage, different challenges emerge upon envelope penetration. Against the thick peptidoglycan wall present in Gram-positive bacteria, phages use murein-degrading enzymes, which are a group within Virion-associated lysins (VALs). Phages infecting Gram-negative bacteria, with the addition of VALs, also possess depolymerases, responsible for the degradation of LPS. In this case, LPS works both as a receptor and a cell entry point, as its degradation leads to the initial penetration of the cell's envelope.[34] Depolymerase activity is also used against the bacterium's capsule, or slime layer, if present. These protective layers are composed of viscous fibers of carbohydrates.[34]

With the cell's envelope successfully invaded, DNA translocation occurs, being the final step in the phage infection process. The energetical and mechanical aspects involved in this process are still not fully understood and are generally considered specific for each phage.[34,37,38] Overall, the phage releases its DNA contained in the capsid through the tail's central tube into the host's cytoplasm. Concerning phage T4, it has been observed that binding to the secondary receptor induces protein rearrangements throughout the tail, as to open space for the DNA to be ejected. [38] More recently, Harada *et al*.[34], in a general approach, suggested that a receptor present in the cytoplasmatic membrane, and not at the cell surface, is responsible for triggering DNA release and tail tube channel opening. Energetically speaking, DNA translocation can be based on ATP, membrane potential, or enzyme activity however, it has been reported that some phages do not require any energy sources, such as phage T5.[36] In response to the presence of intracellular host endonucleases targeting the translocated phage DNA, different protection mechanisms might be triggered. As an example, phage´s T4 genome is methylated in the carbon 5 of the pyrimidine ring in cytosine residues. This virtually conceals the phage DNA from the referred enzymatic action, being recognized as bacterial genetic material.[34]

1.2.3. Type of life cycle

Following phage DNA translocation, two distinct life cycles may transpire, either a lytic or a lysogenic one. In the lytic pathway, pursued by the so-called virulent bacteriophages, the host metabolic machinery is taken hostage. Herewith, the production of new virions is prioritized, which includes the replication of the phage's genome and the transcription and translation of viral proteins, such as the

ones encoding for the capsid and tail. With the mass production of bacteriophages, cell lysis occurs, due to the production of phage-encoded enzymes.[34,40] This process will be further discussed in the next section. Temperate phages initially follow a lysogenic life cycle, without provoking cell lysis. Here, the phage genome is integrated into the host genome, being named prophage. The prophage is replicated along with the host during consecutive bacterial generations, in a dormant state with no major metabolic consequences.[32] While in the lysogenic mode, the phage-integrated bacterium becomes immune to further infection by the same phage species.[41] Upon certain environmental alterations, such as intracellular stress or damage, the prophage may be activated, and switch its life cycle to a lytic one. As a result, mass production of phages is triggered, followed by cell lysis.[32,34,40,42] The lysogenic and the lytic life cycles are illustrated in Figure 2, showcasing how both are innately connected. Remarkably, during the quiescent state of prophages, virulence genes may be transferred, via HGT (Horizontal gene transfer) mechanisms, to other bacteria.[31,42,43] Furthermore, Brüssow and Boyd stated that prophages could contribute to the increase of virulence in the targeted bacteria, with genes encoding for proteins associated with evasion of host immune defense or further damage to host cells.[43,44] Alternative infection modes might also transpire.[45] Filamentous phages follow a chronic infection mode, based on the production of free phages without the consequence of cell lysis. The morphology of filamentous phases allows their extrusion through the bacterial envelope without compromising its stability, thus cell fate.[46,47]

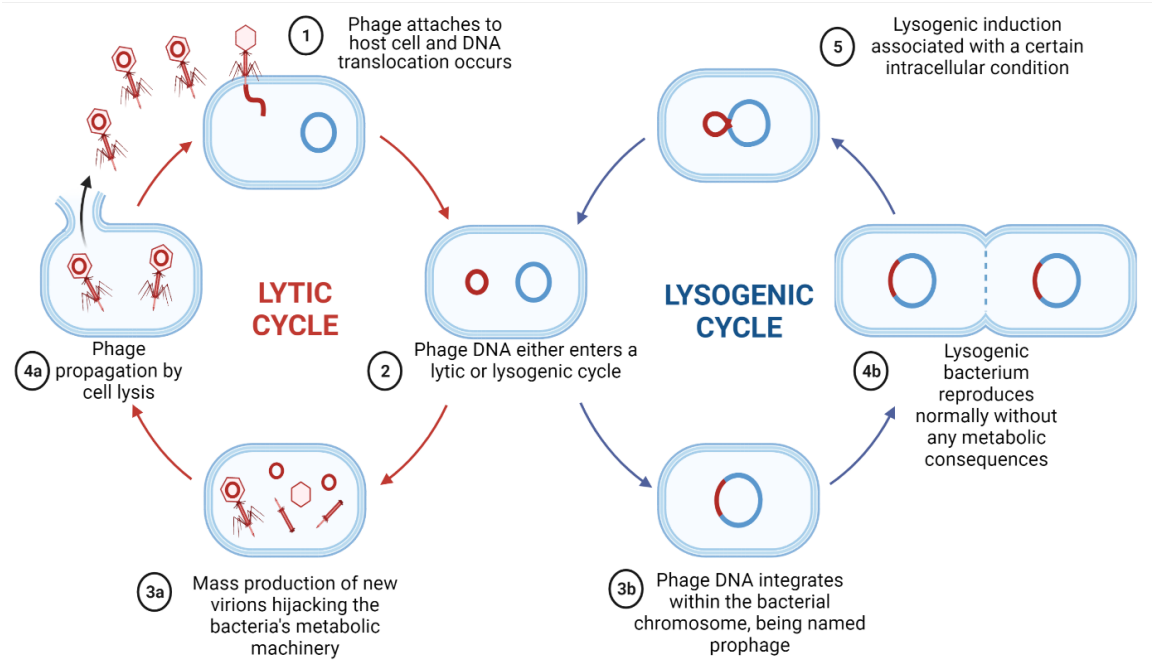

Figure 2- Bacteriophage lytic and lysogenic life cycle description. In the lytic and lysogenic life cycle, infection of a bacteriophage starts with its attachment and DNA injection in the host cell. Following, the phage DNA can enter a lytic or a lysogenic cycle, that involves, respectively, mass production of virions or integration in the host genome. Lysogenic induction may also occur, leading to a switch in the life cycle of temperate phages. The different possible steps in both life cycles are enumerated and briefly overviewed in the illustration. Adapted from BioRender.com.[48]

1.2.3.1. Cell lysis mechanisms

Both virulent and temperate bacteriophage infections culminate in cell lysis, with the latter requiring lysogenic induction. While ssRNA or ssDNA phages have simpler cell lysis mechanisms, mainly based on the action of a single lysis gene, dsDNA phages require additional constituents and processes.[36] The

former phages make use of a single protein to disrupt the host cell wall. This protein, coined “amurin”, targets host enzymes associated with peptidoglycan synthesis, whilst not possessing murein-degrading activity, contrary to dsDNA phages.[36,46]

Double-stranded DNA phages utilize a fine-tuning mechanism composed of two key factors. One of them is the production of endolysins, which are muralytic enzymes capable of degrading the peptidoglycan layer present in either Gram-positive or Gram-negative bacteria.[36,46,47,49] The peptidoglycan layer is composed of repeating units of N-acetylglucosamine and N-acetyl muramic acid, linked by β 1→4 bonds, and cross-linked by peptide bridges.[50] Phage-encoded endolysins act upon these sugar and peptide moieties. Endolysins by themselves have no effect on the cell wall stability and mainly accumulate in the cytoplasm, as they have no secretory signal sequence.[36,46,47] Herewith, an additional component is required, which permeabilizes the cell membrane and enables endolysin secretion to the periplasm. Holins are small transmembranar proteins, encoded by phages, which arrange themselves as homo-oligomers and create small lesions in the cell membrane, allowing for endolysin passage and concomitantly, cell wall degradation.[36,47] As suggested by Wang *et al*.[49], cell lysis is directly controlled by holin production. Additionally, a holin inhibitor might also be produced during the lytic life cycle.[36,46] This “antiholin” is associated with the fine-tunning of the cell lysis process, as it enables the continued accumulation of holin in the cytoplasm until a certain concentration threshold is met and steep holin utilization is done.[36]

1.3. Bacteriophage applications

The possible bacteriophage applications are an ever-growing research field. At the vanguard, phage therapy continues to impress and innovate, branching out to virtually all possible therapeutic grounds. These include gastrointestinal complications, skin and pulmonary infections, dental care, and so forth.[34,35,51–53] Excluding phage therapy, phages have been used in a wide variety of multidisciplinary areas, such as phage display technology, food biopreservation, plant pathogen control, vaccine and gene delivery, and biosensor development.[34,35]

1.3.1. Phage therapy

Antibiotic use is on the verge of becoming idle, as the human population dangerously takes a step closer to a “pre-antibiotic era”. Antibiotic overuse is one of the main contributors to the appearance of antibiotic-resistant bacteria, promoting the appearance of these bacteria when irrationally employed.[34] In the last 30 years, only two new antibiotic classes (lipopeptides and oxazolidinones) were approved for use, both against Gram-positive bacteria.[1] The most exploited antibiotics nowadays were discovered between 1930 and 1962.[54] Pharmaceutical companies are not interested in developing new antibiotics, mainly due to the complexity behind new biological activity against bacteria.[1] Instead, the focus has been directed towards deriving already discovered antibiotics, which is far less efficient against antibiotic-resistant bacteria.[1,51,55]

Theoretically speaking, phage therapy is a simple and efficient alternative to antibiotics. Phage therapy can be divided into two major classes. The lytic-based phage therapy uses the lytic action of bacteriophages to eliminate bacteria by inducing cell lysis from within, bursting out. Recently, attention

has been given to the endolysin-based phage therapy, based on the exogenous use of phage-produced endolysins to eliminate bacteria. These enzymes, associated with the phage infection process, may work as antibiotics, being coined "enzybiotics".[36,46,56]

1.3.1.1. Acute and chronic infections caused by *Pseudomonas aeruginosa*

P. aeruginosa, a Gram-negative bacillus, is classified as an ESKAPE pathogen.[2,57–59] This opportunistic bacterium is mostly known for causing nosocomial infections, either acute or chronic, mainly in immunocompromised, cystic fibrosis (CF), or cancer patients.[58,59] In the considered context, the focus will be turned toward the impact of this pathogen in pulmonary infections, mainly in CF patients. CF is characterized by a deficient secretion capacity in the pulmonary epithelium, associated with the impaired cystic fibrosis transmembrane conductance regulator (CFTR) responsible for chloride transport. This dysregulation leads to the accumulation of mucus in the pili layer, constructing a favorable environment for the growth of *P. aeruginosa*, whose elimination is notoriously arduous due to its wide variety of antibiotic-resistance mechanisms.[57,59] Currently, the most efficient tool to combat *P. aeruginosa* infections is the inhalation of colistin. Alarmingly, Liu *et al*.[60] unveiled the presence of a plasmid containing a colistin-resistance gene in *E. coli*, with its transmissibility being registered *in vivo*.[60] Naturally, it is only a matter of time until this gene is observed in *P. aeruginosa*, further underlining the urgent need to find alternative therapies to eradicate this pathogen.

Phage therapy has been extensively explored as one of these alternatives, in the context of chronic infections in CF patients, either in animal models or in a few clinical trials. In October 2020, a phase I/II clinical trial was launched by Armata Pharmaceutical aimed at studying the efficiency and safety of inhaled AP-PA02, a phage cocktail, in treating chronic lung infections caused by *P. aeruginosa* in CF patients. As of October 2022, recruiting is still undergoing.[61] Interestingly, the basis for this clinical trial is linked to a case report associated with the treatment of a single CF patient with a *P. aeruginosa* lung infection.[62] This study followed the case of a woman with CF which had worsened with a pulmonary exacerbation. Diverse IV (intravenous) antibiotic treatment was not eliciting any positive outcome and she had even developed acute kidney injury. Phage therapy was resorted to as the remaining option, based on an emergency Investigational New Drug (IND) approval by the FDA (Food and Drug Administration). 100 days after AB-PA01 treatment, the renal function returned to normal and *P. aeruginosa* was eradicated, with no recurrence of CF exacerbation.[62] This promising result drove Armata Pharmaceutical to explore the possibility of the now-approved clinical trial involving an optimized version of the AB-PA01 phage cocktail, named AP-PA02.[61]

1.3.2. Antibiotic treatment *versus* phage therapy

Up to this point, phage therapy has been praised as an almost ultimate, flawless, solution against antibiotic-resistant bacteria. This emerging tool has many advantages, while still presenting some limitations when compared with antibiotic treatment. One of the most important characteristics of phage therapy is its specificity, as each phage species is tailored to only infect a specific bacteria species. Herewith, phage's action in the human microbiome is minimal and only targets its respective bacteria, maintaining the remaining commensal bacteria.[5,51] Bruttin and Brüssow[63] experiments are an example

of this preservation, based on a study involving fifteen healthy adults receiving a phage T4 dose in drinking water with no observable effects on the commensal *E. coli* population of the volunteers.[63] On the other hand, antibiotic use many times destabilizes the normal balance of the human flora due to its non-selective nature.[51,52,64] As described by Chhibber and Kumari[51], phages are "intelligent" drugs, as they only multiply if their host is present. When target-bacteria presence ceases, phages are quickly excreted or inactivated by the host's immune system.[51,52,64] The excretion of antibiotics is not connected to the presence of bacteria but rather by the administered dose and requires metabolic action before exiting the system. Herewith, phage toxicity is generally lower when compared with antibiotics.[52]

Despite all said, the hard truth is that phage therapy still presents many limitations. At a first glance, the pharmacokinetic parameters of phage administration are still far from being defined.[5] Phages also greatly vary in virulence and infection mechanisms, contributing to increased pharmacodynamics complexity.[64] The selectivity of phage therapy is both an advantage and a drawback. Assessment of a certain infection to its utmost detail must be done, to determine the exact pathogen infecting the patient. This is arduous and laborious work.[5] One way to go around this issue is the use of phage cocktails, which are a mixture of phages.[5] Phages with different characteristics and specific target bacteria should be used, targeting a broad range of bacteria.[65] Another limitation is associated with the HGT mechanism present in phages, as infection may lead to the horizontal transfer of genes between bacteria that contribute to their pathogenicity, leading to a futile therapeutic use of phages.[5,43] When bacterial lysis is the aim of the employed phage therapy, lytic phage use is mandatory, as lysogenic phages are less predictable regarding their induction and take more time for the intended action. A major consequence of Gram-negative bacteria lysis is the release, among others, of LPS. LPS is an endotoxin known to cause septic shock.[5] One possible way to handle this issue is the use of non-lytic bacteriophages to cause cell death, minimizing endotoxin release into the organism.[65,66]

One of the most important drawbacks of phage therapy coincides with the exact problem it tries to solve: resistant bacteria. Bacteria are not only capable of developing antibiotic resistance but can also develop phage resistance.[5,64] There are different identified phage-resistant bacteria mechanisms. As an example, a bacteria population may evolve in such a way as to insert single point mutations in the gene encoding for the used receptor for phage adsorption, resulting in its impairing or no integration at the cell surface.[5,64,67] Phages, in a similar way to bacteria, also acquire counter-resistance mechanisms through an evolutionary process, based on new adsorption receptors or adapting to the modified receptor.[64,67] Another bacterial defense mechanism is based on the degradation of phage DNA upon translocation.[5,64] This can be done by restrictive endonucleases, despite many phages having counter-mechanisms that "hide" their genome from these enzymes.[31,34] A more robust DNA-degrading system is based on the CRISPR (Clustered Regularly Interspaced Short Palindromic Repeats) system.[5,64] Notwithstanding, reports have found that bacteriophages have successfully developed resistance mechanisms against the CRISPR system, through the presence of anti-CRISPR genes conserved in different *P. aeruginosa* phages.[68] Lastly, bacteria may also possess Abortive Infection, or "Abi", systems, that are triggered upon phage infection and promote immediate cell death, preventing phage propagation.[5,64]

1.4. Bacteriophage manufacturing

Up until this point, the importance of bacteriophages as an alternative to antibiotics against antibiotic-resistant bacteria is quite well understood. Still, the most important aspect regarding the use of bacteriophages is their large-scale manufacturing according to GMP (Good Manufacturing Practices). This aspect has been extensively discussed, going back as far as 1970.[69] Despite this, no definitive purification scheme has been established as "conventional" for the mass production of bacteriophages, mainly due to the biological and structural variability among phages. While designing a bacteriophage purification process, one must take into account the presence of impurities throughout the different stages, originating mainly in the host lysis. Nucleic acids, such as RNA and gDNA, host proteins, and LPS (in Gram-negative bacteria) are the most common impurities found.[70] All impurities are strictly regulated and must obey certain product specifications, considering a range of acceptable values in the final drug substance.

In the upcoming sections, the scope of bacteriophage upstream and downstream processing (USP and DSP, respectively) will be explored, with the intent to compare current production and purification strategies at each step. In Figure 3, the current processes used throughout different DSP stages are represented.

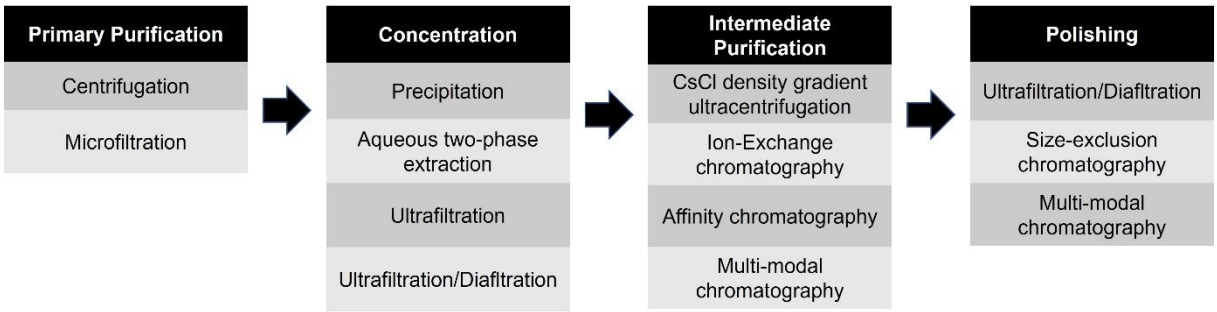

Figure 3- Common processes present in the different stages of bacteriophage DSP. A typical bacteriophage DSP design is initiated by primary purification, followed by a concentration step and intermediate purification. Specific polishing tools, such as size-exclusion chromatography, are not commonly employed. Additionally, some techniques are associated with more than one stage

1.4.1. Upstream processing

The ultimate goal behind phage's USP is to obtain high phage titers, measured in plaque-forming units (PFU), whilst minimizing cell lysis that releases cellular debris, nucleic acids, proteins, and LPS.[70–72] For a successful bacteriophage USP, it is crucial to understand not only the intrinsic biological aspects of bacteriophages but also how they relate to the infected host. As a side note, in any GMP-driven industrial process, the source material should be identical in different batches/runs. To ensure this, master cell banks (MCB) and master phage banks (MFB) ought to be manufactured right from the start. Herewith, reproducibility is attained in every performed process. Moreover, the identity, viability, and purity of both MCB and MFB must be checked regularly.[70,73]

The bioreactor operation modes for bacteriophage production may be divided into fed-batch, continuous (single-stage or multi-stage), and double-stage semi-continuous.[70–72,74–76] Among these operation modes, fed-batch is the most common when it comes to bacteriophage production however, a

continuous approach is of the utmost interest in the biopharmaceutical industry.[70] As main advantages, batch operations are very robust, cheaper than continuous processes, and attain high phage titers (10^{10} – 10^{16} PFU/mL).[70] Still, they present many limitations. Generally, large equipment footprints and volumes are needed in batch, as well as a lot of manpower.[70,72,76] Phage productivity is limited by the maximum tank volume.[70,74] Additionally, before each run, the bioreactor must be cleaned and sterilized, contributing to higher downtime periods and thus less productivity.[70–72,74,75] Batch-to-batch variation is also an issue in this operation mode even if MCB and MFB are employed.[70–72] The main advantage of continuous operations compared to batch ones is the higher phage productivity, mainly due to the possibility of long-term utilization in the pharmaceutical industry.[70,71] Additionally, the ability to change the dilution rate allows the user to regulate bacterial growth, optimizing it for phage infection.[70,74]

1.4.2. Clarification

Regardless of the chosen bioreactor mode of operation, a crude phage lysate is attained, which before entering the downstream processing, needs to be clarified. This stage is typically named clarification and is aimed at removing cellular debris, uninfected bacteria, and other released host components such as large proteins.[70,77–79] Traditionally, a simple combination between a low-speed centrifugation and a microfiltration (0.22 or 0.45 µm membranes) is enough to acquire a clarified phage lysate, ready for further processing and the specific removal of problematic host components.[70,77–79] The use of chloroform as an artificial cell lysis inducer, and concomitant phage releaser, has also been used at this stage however, it has various drawbacks and safety issues. The addition of an organic solvent treatment in the manufacturing of a human-therapeutic product is always unadvisable from a regulatory point of view, also potentially inactivating lipid-containing and filamentous phages.[71,77] An additional nuclease treatment before DSP may also be employed, as phage lysates resultant from a high biomass concentration are viscous solutions, due to the release of nucleic acids.[71,79]

1.4.3. Downstream processing

1.4.3.1. Traditional bacteriophage purification procedure

Viruses, including bacteriophages, purification strategy is historically based on a cesium chloride (CsCl) density gradient ultracentrifugation.[70,77,78,80–82] This technique may be performed after precipitation and chloroform extraction, always finalized with dialysis to remove CsCl.[83] Density gradient ultracentrifugation is divided into rate-zonal separation (particles' buoyant density separation) and isopycnic separation (particles' size and shape separation), reaching centrifugal forces such as 100000 *g* or higher.[84] The result is a limited but highly purified phage fraction, with efficient LPS removal.[78,81] Moreover, density gradient centrifugation approaches are advantageous when compared with the remaining operations as they enable the user to distinguish empty bacteriophages from viable ones.[84] Over the last decade, with the appearance of alternatives for phage purification, CsCl density gradient centrifugation has seen a steep downfall in use and popularity, as its disadvantages became increasingly apparent. This operation is mainly used on a laboratory-scale, due to its limited productivity which only withholds up to 5-10 liters of crude lysate.[77,78] Therefore, for large-scale therapeutic use under batch cGMP conditions, CsCl density gradient ultracentrifugation is not a viable option.[77,78,80,82,85]

Furthermore, this technique is time-consuming and requires expensive equipment, which also needs to be handled by skilled workers.[77] Additionally, some phages may become inactive following this ultracentrifugation due to interaction with CsCl, osmotic shock, or exposure to high shear stress.[78,81] CsCl is also considered a safety risk, being cumbersome when implemented in purification processes for therapeutic products.[86]

1.4.3.2. Primary recovery and concentration

Following clarification, a primary recovery/concentration stage with the main intent of reducing volume and removing impurities is performed. For this step, a wide variety of unit operations may be considered and will be discussed in the following sections. In most cases, the concentration and intermediate purification stages are indistinguishable, as different unit operations may simultaneously reduce volume and remove specific host components.

1.4.3.2.1. Precipitation

Precipitation is an alternative to the use of ultracentrifugation as an initial bacteriophage purification strategy, working as a concentration method that attains similar high yields and exposes phages to milder stress conditions.[70,71] Precipitation is a simple and inexpensive method that, in a nutshell, is based on the addition of one or more components that cause the precipitation of the targeted product.[70,77,87] Several studies have explored the combined use of PEG (polyethylene glycol) and NaCl in bacteriophage precipitation, however, all at a laboratory-scale or for research purposes.[87–89] PEG-precipitation is based on the volume exclusion phenomenon, where proteins are sterically removed from the solvent due to the presence of PEG chains until their solubility threshold is reached and precipitation occurs. The addition of salts such as NaCl and $MgSO_4$ further contributes to this process by sequestering water molecules required for protein solvation.[70,87]

PEG-NaCl precipitation of bacteriophages was first reported by Yamamoto *et al*.[89] in 1970. In more recent years, Branston *et al*.[87,88] studied the precipitation of the filamentous phage M13 using a similar approach to that of Yamamoto *et al*.[89] The authors attained phage recovery rates up to 97% considering different experimental designs: 2 and 4 % (w/v) PEG 6000 supplemented with NaCl or $MgSO_4$.[87] Branston and co-workers registered a 97% DNA recovery in the obtained supernatant, resulting in a purification factor higher than 300.[87] The same research group added endotoxin removal as a goal to bacteriophage purification, all within a precipitation step.[88] A single precipitation round with 2% (w/v) PEG 6000 and 0.5 M NaCl reduced endotoxin content by 88%, while two subsequent rounds reduced the remaining endotoxin content only by 18%. Herewith, only a 2 $\log_{10}$ reduction in endotoxin content was attained, suggesting co-precipitation with bacteriophages. Phage recovery throughout three precipitation rounds was 97%.[88]

1.4.3.2.2. Tangential flow filtration

Tangential flow filtration (TFF) is a greatly versatile operation that can be used to attain different goals simultaneously, and that can be operated in different modes. In a summarized way, TFF may be used to concentrate solutions, thus reducing volume, removing impurities, or performing buffer exchange.[70,71,85] It can be operated either in a concentration mode, most commonly using ultrafiltration

(UF), in a diafiltration (DF) mode, or both in a sequential manner.[70,85] The UF/DF strategy is started by UF as the initial goal is to reduce the volume to, among other reasons, decrease the volume of the new buffer required in the DF step. In UF, bacteriophages are retained in the retentate, while low-molecular-weight molecules pass through the membrane and are collected in the permeate.[70,84] The separation feature of UF is innately connected to the molecular weight cutoff (MWCO) of the chosen membrane. For ultrafiltration operations, this value is between 100 and 1000 kDa.[71,77,79] For a MWCO of 100 kDa, any particle with a lower MW will theoretically pass through the membrane, contrary to particles with a MW higher than 100 kDa. As bacteriophages have molecular weights in the MDa scale, a 100 kDa membrane in UF is sufficient for a successful purification process.[70,77] As referred, UF is usually followed by a DF operation, which aims to exchange the resulting purified phage fraction buffer into a more appropriate one, using membranes with selective pores for the former buffer.[70,77] UF brings to the table the possibility of industrial implementation, in a much easier manner than ultracentrifugation.[70,77,84,85] Furthermore, UF attains high phage productivity, owning to its high-throughput feature, and is versatile, as different membrane pore sizes may be used to separate different components.[84]

In a similar way to precipitation methods, the removal of endotoxins may be a co-objective in UF designs however, the reported results have not been favorable. Bourdin *et al*.[78] applied UF systems as an alternative to ultracentrifugation and observed phage recoveries close to 100% in a much smaller volume when using a 30 kDa MWCO membrane. Notwithstanding, LPS levels were left effectively unchanged in most tested phages after ultrafiltration. The authors suggested the use of membranes with a 100 kDa cut-off to remove endotoxins more efficiently.[78] Hietala *et al*.[83] explored this option by employing a 100 kDa MWCO membrane in a UF mode. While phage recoveries were high, the endotoxin content in the concentrate showed little change when compared with the initial content. The tested phages were specific for *Staphylococcus* strains, which are known to produce staphylococcal enterotoxins (SE), a type of exotoxin.[83] Regarding these SE, a 20-fold removal was observed by Hietala and colleagues, associated with the fact that SE has MW lower than 100 kDa. This displayed the use of UF as a method to remove enterotoxins from lysates.[83]

1.4.3.3. Purification and final polishing

Following primary recovery, bacteriophage purification is aimed. Chromatography is a highly diverse technique that enables the capture of phages or impurities yielding high purification factors, being also easy to scale-up and regulate column parameters.[70,85,90] Herewith, chromatography is used both in the capturing/intermediate purification of bacteriophages and in the final polishing step of DSP. In the intermediate purification, the most used chromatography step is based on the ionic charge of phages (ion-exchange chromatography, or IEC). For the polishing step, separation based on the molecular weight of phages (size-exclusion chromatography, or SEC) or MMC (multi-modal chromatography) is usually employed, as well as a UF/DF system.[70,79,84,85] Chromatography steps used in the capturing stage should be operated in a positive mode, thus using stationary phases that bind bacteriophages and wash impurities.[70,84] Even though little attention has been given to this subject, capture chromatography steps in positive mode for bacteriophages have an important drawback, as binding of these virions to the stationary phase may be irreversible, or denaturing can occur.[91] As a result,

bacteriophage purification in negative mode, where these virions are collected in the flow-through, may be of interest.[91] This type of chromatography is commonly used as a final polishing step.[70,84]

One of the most important aspects of any referred chromatography system is the structural properties of the stationary phase. The packing of chromatographic columns may be done with beads, membranes, or monoliths.[84,85] The classic chromatography stationary phase rests on the use of porous beads, with diameters ranging from 30-100 nm.[70,84,85] Bacteriophages are structurally complex entities, that in addition to being filamentous or tailed, have a size varying from 3-100 × 90-800 nm.[70,84] Herewith, phage penetration in chromatographic beads is very limited and adsorption to these particles is mainly associated with the outer shell, resulting in low dynamic binding capacities (DBC).[70,84,92] Monoliths and membrane stationary phases overcome this problem, allowing a high DBC for phages. The former alternative is a continuous homologous stationary phase, whereas the second is the simple use of membranes previously associated with filtration processes.[84,85] Both structures possess large pores and interconnected channels, which enable higher phage adsorption to the stationary phase.[84] This results in a much higher DBC compared to chromatographic beads.[70,84,85] While this remains true, it should be noted that DBC is highly dependent on the number of impurities present, as these hamper phage binding to the column, in addition to the ionic strength of the used buffer and residence time.[70,85,93] Another major advantage of using monoliths or membranes is that the diffusion of particles is not a critical factor, as these are driven by convective-flow transport, which is independent of the particle diffusion. This allows for an increased flow rate in these structures compared to beads, resulting in lower operating times and higher phage productivity (better economics) without altered resolution.[79,84,85]

1.4.3.3.1. Ion-exchange chromatography

IEC is the most used chromatographic system for viral particle DSP designs.[85] Particles are separated based on their global charge, associated with the working pH. For bacteriophages, the user aims to separate impurities, such as nucleic acids or proteins, in a high-resolution manner. In this case, an anion-exchange chromatography (AEC) is commonly employed, as phage's pI is commonly below 6, thus at a neutral pH, these particles will have a negative charge and are adsorbed to the positively-charged column.[70,85] Nevertheless, at a neutral pH, many impurities, such as endotoxins and nucleic acids, are also negatively charged and may bind to the AEC column under the same conditions as phages. Bacteriophage elution may be accomplished by increasing the ionic strength, or by lowering the pH until phages become positively charged, hence eluting. The latter option is not advisable as it may denature bacteriophages.[70,85] Several studies have employed AEC in bacteriophage purification, using packed-bed columns or small- and larger-scale disk monolithic columns.[90,92–95]

Monjezi *et al*.[90] aimed at purifying the M13 phage using a SepFast™ Super Q packed-bed column, containing a strong anion exchanger. For the elution buffer, a high ionic strength was employed (citrate buffer with 1.5 M NaCl at pH 4), when compared to the equilibration buffer (50 mM Tris-HCl pH 7.5). With these conditions, the researchers registered an average 74% phage recovery, which is a comparable value with the traditional CsCl density gradient ultracentrifugation. Furthermore, productivity was greatly increased, as the operating time is much lower in AEC, with lesser costs and reduced labor work compared with ultracentrifugation.[90] While no protein contaminants were detected via a SDS-

PAGE (sodium dodecyl sulfate-polyacrylamide gel electrophoresis), endotoxin and nucleic acid content were not evaluated in this experiment.

As an alternative to packed-bed columns, monolithic ones may be used. Smrekar *et al*.[92] explored the possibility of implementing convective interaction media (CIM) columns in a T4 phage purification design. For this purpose, QA (quaternary amine) methacrylate-based CIM disk monolithic columns were employed. An initial linear-gradient chromatography (0.3-0.5 M NaCl) was performed, aiming at optimizing a step-gradient system. With the latter elution profile, concentrated bacteriophage fractions may be obtained, with narrower peaks (higher resolution). Step-gradient chromatography adds another benefit as it has been reported that DNA elutes at a NaCl concentration ranging from 0.6-0.8 M, not superimposing the NaCl concentration interval for phage elution. The authors observed a 71% phage recovery at 0.5 M NaCl, with a defined peak, and when ionic strength was further increased to 1.0 M NaCl, another peak was observed, likely containing most DNA.[92] Unfortunately, this hypothesis was not confirmed as nucleic acid quantification was not performed. Additionally, a 99% protein removal rate was attained.[92] Years later, the same research group further explored the CIM implementation for the purification of phages T7, M13, and λ.[93] When eluting phages in a linear-gradient operation mode with 20 mM Tris, 1.0 M NaCl pH 7.5, phage recovery across the board was close to 100%. Impurities such as nucleic acids, proteins, and endotoxins were not evaluated. The work done by Kramberger *et al*.[95] displays the scalability factor of monolithic systems. The authors aimed at purifying phage VDX-10, initially using a 0.34 mL CIM QA disk monolithic column. With a 100 mM phosphate buffer with 0.6 M NaCl concentration at pH 7, 54% phage recovery was attained, in addition to the removal of more than 99% DNA and 90% proteins. When scaling up this process to an 8 mL CIM QA monolithic column, phage recovery was 65%, with similar protein and host DNA removal rates.

1.4.3.3.2. Hydrophobic interaction chromatography

Hydrophobic interaction chromatography (HIC) exploits the interaction between immobilized hydrophobic ligands and hydrophobic surface regions of proteins. From a simple point of view, HIC employs adsorption conditions with high salt concentrations and elution conditions with decreasing salt concentrations.[96–98] The adsorption step of this chromatography is based on the "*salting out*" effect, where the addition of salts to a solution enhances protein-protein hydrophobic interactions and may lead to precipitation.[96,98–100] Briefly, in aqueous solutions, water molecules solvate proteins by interacting with their superficial hydrophilic amino acids, while their hydrophobic residues are hidden at the core. Upon salt addition, water molecules primarily solvate these ions and leave unchecked the proteins. This leads to a decrease in the hydration layer surrounding proteins, exposing hydrophobic amino acids, with subsequent enhancement of protein-protein interactions by hydrophobic interactions.[96,100]

The selection of the stationary phase and the mobile phase in HIC is of the utmost importance. The HIC mobile phase choice is based on the Hofmeister series (Figure 4). Anions such as phosphate and sulfate, and cations such as ammonium and potassium, promote hydrophobic interactions and are called lyotropes (or antichaotropes). Chaotropic ions promote the "*salting in*" effect, which increases protein solubility thus implicating the opposite effect intended in the mobile phase of HIC.[98–100] Generally speaking, ammonium sulfate is the most used solution for HIC adsorption as it is highly soluble and

stable, also offering a high "*salting out*" effect.[101] Ammonium phosphate or sodium chloride are other alternatives. HIC is also affected by the pH of the mobile phase. While there is not a simple answer for the relationship between the pH and the hydrophobicity strength, generally, a pH increase results in a decrease of hydrophobic interactions, while a pH decrease causes the opposite.[98,100] Note that this highly depends on the pI of each protein. The stationary phase of HIC is based on linear chain alkanes ligands or aromatic ligands. The hydrophobicity of the stationary phase increases with the increase of the length of the alkyl-chain, while the adsorption selectivity decreases.[96] Aryl ligands further increase the hydrophobicity of the stationary phase by also promoting aromatic π-π interactions. Note that highly substituted HIC matrices may lead to elution problems, due to overpowering hydrophobic interactions between the ligands and the proteins.[98,99] Elution in HIC may be accomplished in several ways, with a decrease of salt in the elution buffer being the most popular. Alternatively, organic solvents, detergents, and chaotropic salts may be added to the elution buffer. Nonetheless, these alternatives may lead to protein denaturation or inactivation.[98,99] In terms of the operation mode, linear-gradient elution for optimization purposes followed by multi-step-gradient elution in HIC is generally pursued. Note that the sample to be loaded in HIC should be supplemented with a high salt concentration, which must be previously guaranteed that it does not lead to protein precipitation.[98]

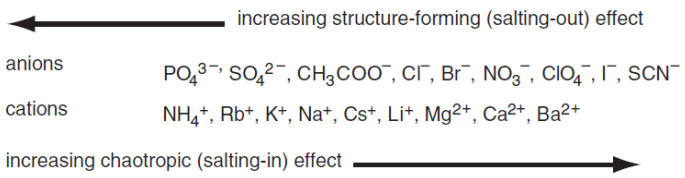

Figure 4- Hofmeister series of anions and cations. Ions promoting either the "*salting out*" or the "*salting in*" effect are displayed.[98]

Little scientific knowledge associating HIC with virus purification is available.[97] Bacteriophage purification with HIC has not been researched as of the date of this thesis (October 2022). HIC has been used at a lab-scale to purify the influenza A and B virus[97], as well as the vaccinia Ankara virus[102]. In both papers, 1 mL columns of the ToyoScreen HIC Mix Pack® were used as the stationary phase, while ammonium sulfate was at the base of the mobile phase. HIC-based processes are usually problematic due to the initially applied high salt concentrations, which may instantly inactivate the virus or lead to its precipitation.[97] Therefore, the optimization phase of HIC is rather complex and looks at combining different stationary phases with different mobile phases, at different salt concentrations, to attain the best possible process conditions for industrial purification.

1.4.3.3.3. Phenyl boronate chromatography

Affinity chromatography for virus purification is based on the specific but reversible adsorption of a viral component to an immobilized ligand in a chromatographic matrix. The interaction virus-ligand is usually associated with a superficial structural component. Although affinity chromatographic results in high purification factors, combined with low costs and operation simplicity, no specific ligands are known for most viruses, including bacteriophages.[84,103] Most studies exploring the use of affinity chromatography

to purify bacteriophages focus on the removal of endotoxins, rather than the recovery of phages. Recently, phenyl boronate chromatography (PBC) was associated with bacteriophage purification.[104]

PBC has been reportedly used for the purification of proteins[105–107], nucleic acids[105,108], and LPS[105], among others. The biological affinity behind PBC is bedded in the reversible esterification between phenyl boronate and 1,2-*cis*-diol groups.[105,107,109] The protonation status of boronic acid (BA) ligands depends on the medium's pH, considering BA's pKa of 8.8.[107] Interestingly, the formation of ester bonds between BA and *cis*-diol groups occurs both in acidic and alkaline environments, with the former being less favorable.[107] As a result, it has been observed that the tetrahedral conformation of BA, associated with its hydroxylation in alkaline conditions (pH > 8.8), is more stable than the trigonal planar conformation present in an acidic medium (pH < 8.8) (Figure 5) .[105,107,109]

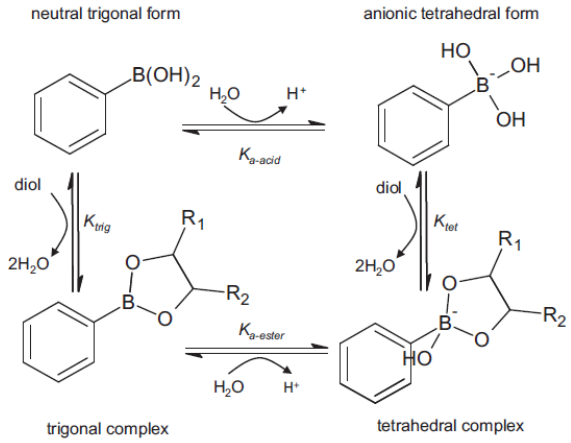

Figure 5- *Cis*-diol esterification reaction with boronic acid ligands in alkaline and acidic environments.

RNA possesses a 1,2-*cis*-diol group in its ribose, whereas LPS has *cis*-diols in the saccharide moiety. Herewith, both components may be captured via adsorption to a PBC matrix. Importantly, through this interaction, DNA is not expected to interact with BA as it possesses a deoxyribose ring.[107] PBC's use in bacteriophage purification is most likely not associated with the referred "primary" interaction in these columns but with secondary, non-specific, interactions. Among these, one can point out charge-transfer interactions, ionic interactions, and hydrophobic interactions.[105,109] The latter are present in phenyl boronic acid ligands and are based on aromatic π-π interactions.[107,109] Additionally, the hydroxyboronate anion, present in the tetrahedral BA conformation, may work as a weak cation-exchanger.[107,109] Charge-transfer interactions are solely associated with the trigonal planar BA conformation. The boron atom works as an electron acceptor due to the existence of an empty orbital. Therefore, electron donors such as unprotonated amines and carboxyl groups, present in proteins, may interact with BA in this state.[109]

Viúla[104] has been the first to integrate PBC in a bacteriophage purification process. Bacteriophage adsorption to the column with selective protein removal and semi-DNA removal was attained when a clarified phage lysate was directly applied. An equilibration buffer composed of 15 mM Tris-HCl pH 7 and an elution buffer of 1.5 M Tris-HCl pH 8.5 were employed. Using a single-step gradient, the author registered a 49% phage recovery rate, with 96% and 47% of proteins and DNA, removed, respectively. LPS nor RNA contents were tested.[104]

1.4.3.3.4. Size-exclusion chromatography

SEC is a size-based separation technique that, due to its low selectivity, is mainly used as a polishing step in purification designs. SEC enables the separation of phages from small impurities depending on the size exclusion limit associated with the used resin.[79,84] Particles with a MW lower than the size exclusion limit will penetrate the resin's pores, while particles with a higher MW will be collected first in the void column volume (negative-mode operation). SEC has a few benefits, as it is operated under mild conditions and enables buffer exchange simultaneously to separation, seeing that it is run in isocratic mode.[79,84,85] It is a better fit for cases where the contaminants have a MW considerably different than the product to be purified.[84] Despite this, this chromatography presents many limitations. The loaded volume in the column is usually minimal, as it represents a reduced percentage (10%) of the column volume. Therefore, SEC use on a large-scale is hindered. Due to the poor pressure resistance of SEC resins, low flow rates must be applied in this operation, further reducing productivity. Virus concentration is also not attained, as product dilution is the most likely outcome.[79,84,85]

Owning to the referred drawbacks, SEC sees little attention when it comes to bacteriophage purification. Zakharova *et al*.[110] employed SEC, using a Sephacryl S-500 resin with a size exclusion limit close to 20 MDa, to purify M13 bacteriophages following a double PEG precipitation. The authors observed that most phages were eluted in the first peak, whereas contaminants and PEG were mainly present in the second peak. Phage recovery was about 90%.[110] Bacteriophage dilution occurred, as the total volume collected for these particles was 4.5 mL, compared to the initial 0.5 mL loaded into the column. In another study, Boratyński *et al*.[111] were set to investigate the effect on T4 and T7 phage titer and endotoxin content of a UF system followed by a SEC, using Sepharose 4B with a size exclusion limit of 20 MDa, and an affinity chromatography with Matrex cellufine sulfate. Regarding the first peak in SEC, the authors observed a phage recovery of 50% and 84% for phages T4 and T7, respectively. Additionally, endotoxin removal by SEC was quite limited, most likely due to the formation of micelle-like structures, up to 0.1 µm, that co-eluted with the bacteriophages.[70,111] All-in-all, SEC-associated phage recovery results are not the lousiest, and endotoxin removal is minimal.[110,111]

1.4.3.3.5. Multi-modal chromatography based on core bead technology

MMC emerges as an alternative for the simultaneous capturing/polishing of bacteriophages, or solely as an intermediate purification system. This type of chromatography combines two or more separation principles. In the specific case of core bead technology, it uses beads with a functionalized porous inner core, possessing affinity, ionic, or hydrophobic ligands, and an unfunctionalized porous outer shell.[79,91] Compared to SEC, MMC presents the additional benefit of better binding small impurities, due to its inner functionalized nature, whilst still excluding bacteriophages. Importantly, while designing the MMC beads, one must be aware of the pore size in the inner core and outer shell. The pore size in the outer shell must be small enough to exclude the product but not to exclude impurities, while the inner core must possess small enough pores to promote impurity binding (high surface area) but not to hamper impurity diffusion.[91]

Capto™ Core 400 and 700 (Cytiva, Marlborough, USA) are core-shell chromatographic resins, commercially available, which compared to SEC resins, present higher flow rates and loading volumes. These resins are based on crosslinked agarose beads with an inner core functionalized with an octyl-amine ligand.[70,91,112] The number in each commercialized resin is an indicator of the size exclusion limit.[91] Regarding the functionalized inner ligand, it has a pKa equal to 10.5 and is highly hydrophobic (Figure 6).[91,112] According to what was researched for this work, Capto™ Core has not been used for bacteriophage purification however, this unexploited potential is present. This resin has been used to purify other viruses, such as influenza A or the human papilloma virus.[112] James *et al*.[112] tested the viability of Capto™ Core 700 to be implemented in purification designs for reoviruses and adenoviruses. The authors opted for an in-slurry purification strategy, which was independent of chromatographic equipment and viable for high-throughput use. This method was based on the simple addition of Capto™ Core 700 resin to a virus lysate, followed by end-to-end rotation for 1 hour and a final centrifugation step to separate the resin from the purified fraction. With three successive extraction rounds, James and co-workers found comparable virus recoveries with a CsCl density gradient ultracentrifugation control experiment. Capto™ Core resins are an interesting alternative bacteriophage purification step due to their multi-separation principle, theoretically being more selective for the product of interest.

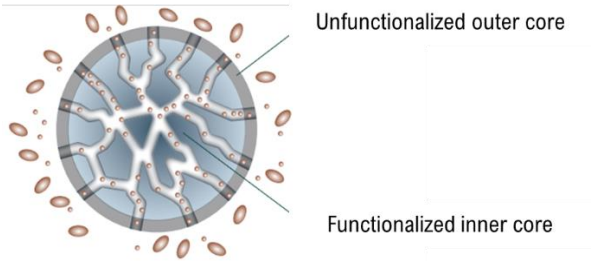

Figure 6- Capto™ Core 700 chromatographic resin composition.

1.4.4. Presence of endotoxins during bacteriophage production

Endotoxins are quite probably the most problematic impurity encountered in phage preparation. LPS is present in the outer membrane of Gram-negative bacteria and is released upon cell lysis.[83,113,114] It is composed of three main moieties: Lipid A, an oligosaccharide core, and a long-chain polysaccharide (*O*-antigen).[113,114] Owning to the presence of Lipid A, LPS is highly immunogenic and induces a pro-inflammatory response, which activates a cytokine-based coagulation cascade, leading to septic shock.[83,113] This calls for an urgent need for endotoxin removal from pharmaceutical preparations, such as phage therapy, according to the acceptable threshold for endotoxin content.[83,113,114] EU (endotoxin unit) is the standard endotoxin quantification measurement, based on the activity of 0.1 ng of *E. coli* LPS.[113] The acceptable endotoxin content for intravenous administration is 5 EU per kg of patient body weight per hour, while for intrathecal applications, this value is 0.2 EU/kg/h.[83,113,114] Generally, these values are increased for lower drug-dose administration, which is the common scenario.[114]

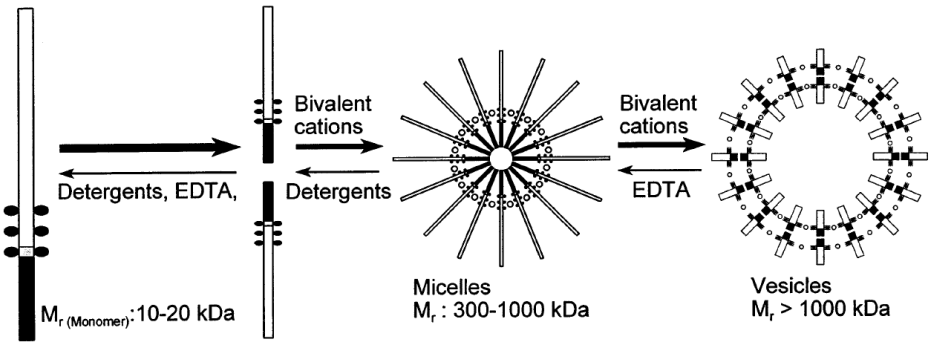

Figure 7- Endotoxin structure polymorphism and dissociation options. Endotoxins in aqueous solutions may present themselves as monomers, micelles, or vesicles, all varying in molecular weight. While bivalent cations stabilize endotoxin aggregates, detergents and EDTA dissociate them. Black sections are associated with lipophilic sites, while white sections represent hydrophilic moieties. Black circles represent charged functional groups, and white circles represent bivalent cations. Adapted from Anspach and Petsch.[114]

Endotoxin monomers have molecular weights ranging from 10-20 kDa.[113,114] Herewith, considering the significantly higher MW of bacteriophages, a 100 kDa UF should suffice for endotoxin removal in the permeate, while recovering phages in the retentate. Unfortunately, endotoxins commonly aggregate in micelles, with sizes ranging from 300-1000 kDa, or vesicles with 0.1 µm.[113,114] Lipid A is responsible for this aggregation status, based on hydrophobic interactions between alkyl adjacent chains. Additionally, bivalent cations contribute to the stabilization of these structures, establishing bridges among adjacent phosphate groups. Herewith, utilizing detergents or chelator agents, such as Tween® and EDTA, respectively, has been implemented in several endotoxin removal designs. These contribute to the dissociation of endotoxin micelles or vesicles, easing the pharmaceutical purification procedure. Endotoxin dissociation is interesting for the separation of endotoxins from phages with a 100 kDa UF. Additionally, it has been suggested that endotoxins can interact with proteins, further complicating their removal process.[114,115] Calcium-based bridges between the protein-bound carboxylic group and the endotoxin-bound phosphate group have been suggested to be at the origin of these interactions.[114] The variety among the discussed endotoxin structures and how they can be dissociated are illustrated in Figure 7.

1.4.4.1. Affinity chromatography

Chromatographic techniques are the most selective for endotoxin removal. Among these, one can point to affinity chromatography as the better suited. Theoretically speaking, AEC is useful to adsorb endotoxins, however, endotoxin removal from acidic proteins with AEC would lead to co-elution between both components.[113,114] This is the case for bacteriophages. Herewith, AEC should only be used to separate basic proteins from endotoxins.[113] Affinity adsorption skips this issue as the employed ligands are specific for endotoxin binding, ideally not interacting with bacteriophages.[113,114] Endotoxins are structurally different in each bacteria species, mainly due to the surface *O*-antigen, thus ligand design must target a conserved region of LPS: Lipid A. Adsorption between affinity ligands and Lipid A is mainly based on hydrophobic and electrostatic interactions.[113] Polymyxin B (PMB), histamine and histidine, and most recently, PolyBall, are some of the examples of affinity ligands used for endotoxin removal.[113,114,116] None of these ligands have been used for endotoxin removal from phage preparations, however, a newly commercialized affinity column named EndoTrap® has had optimistic results.[83,117] This resin has

an affinity ligand derived from a bacteriophage, contributing to its high endotoxin removal rates.[117,118] Lionex, the EndoTrap® manufacturer, reports that the maximum endotoxin binding capacity of this resin is 2-5 × 10^6 EU/mL, together with endotoxin removal rates above 99.9%.[118] Hietala *et al*.[83] explored the use of EndoTrap® for endotoxin removal from an *E. coli* phage preparation. The authors performed a UF on the phage lysate, followed by a AEC and a EndoTrap® step, or only a EndoTrap® step. EndoTrap® was extremely efficient in removing endotoxins. The phage lysate had an endotoxin-to-phage ratio (EU/10^9 PFU) close to 10^4 EU/10^9 PFU and after EndoTrap® use, with or without a prior AEC step, this value was as low as 0.1 EU/10^9 PFU. Additionally, phage recovery in the column was close to 100% in both cases. Merabishvili *et al*.[117] also used a EndoTrap® resin to remove endotoxins present in a *P. aeruginosa* BCF-1 phage lysate. The authors directly applied clarified phage lysate in a EndoTrap® packed column and registered high endotoxin removal rates, without quantifying this process.[117]

1.4.4.2. Other removal strategies

Non-specific endotoxin removal throughout the bacteriophage DSP is usually not an easy task, mainly due to the aggregation state of endotoxins. Hietala *et al*.[83] failed to remove endotoxins from a *Staphylococcus* phage lysate when employing a UF with a 100 kDa membrane, with only a four-fold decrease in endotoxin-to-phage ratio. These results display the UF limitation in removing endotoxin-aggregates from bacteriophage preparations. UF is better suited for endotoxin removal in the retentate from water, salts, and other small-molecular drugs.[113,114] As referred, detergent use should dissociate endotoxin aggregated and result in a more efficient UF. Hashemi *et al*.[119] aimed at removing endotoxins from a T7 phage preparation by applying a detergent step before a 100 kDa UF. The initial endotoxin concentration in the phage lysate was 1.7 × 10^6 EU/mL. After three cycles of 1% DOC (deoxycholate) treatment followed by UF, endotoxin concentration was 0.83 EU/mL, while UF alone only removed 9% of the initial LPS content. As a setback, phage recovery after three treatment cycles was 55%.[119] Precipitation may also be employed as an endotoxin removal tool, as assessed by Hietala *et al*.[83]. The authors performed a PEG 8000 precipitation, observing a twenty-fold decrease in endotoxin-to-phage ratio, accompanied by 51% phage recovery.[83] These results increasingly point to affinity chromatography as the best option for endotoxin removal from bacteriophage preparations.

Triton X-100 and Triton X-114 have also been widely used for endotoxin removal with high reported efficacies. One example involves the work of Branston *et al*.[88], which did not attain high enough endotoxin removal rates employing a PEG-NaCl precipitation process. To improve this process, the authors tested the implementation of 2% (v/v) Triton X-110 addition in their precipitation process and obtained a 5.7 $\log_{10}$ endotoxin content reduction, compared to the one obtained solely with precipitation (2 $\log_{10}$ reduction). Phage recovery was close to 97%.[88] Implementation of treatments with the Triton X series in the manufacturing of therapeutic products is not advisable due to their endocrine-disrupting properties. Recently, these products have entered the “Authorization List” of ECHA (European Chemicals Agency) and are classified as of “very high concern”, requiring prior authorization for use.[120] Therefore, safer alternatives for endotoxin dissociation must be used, such as the polysorbates Tween® detergents.[70]

1.4.5. Aim of studies

Antibiotic-resistant bacteria are an emerging crisis that few are prepared for, with the world being on the verge of entering once again a “pre-antibiotic era”. With few alternatives available, bacteriophage therapy poses as one of the most promising tools to combat antibiotic-resistant bacteria. There is yet a standardized bacteriophage manufacturing process at a large-scale, with optimistic recovery rates and high host impurity removal. Several reports have optimized single stages of bacteriophage purification, but there is little advance in constructing a complete industrial design. The traditional CsCl density gradient ultracentrifugation design is not capable of being implemented at large-scale and lacks phage productivity, whilst being costly.

This work aims to design an integrated purification process for bacteriophages that can be scaled up to industrial use. One aspect lacking in the various examples discussed up to this point is the absence of complete quantification of host impurities at each purification stage. For this purpose, this work intends to quantify proteins, total dsDNA, genomic dsDNA, and endotoxins in every considered downstream processing stage. Chromatography must be at the center of a scalable, efficient, and reproducible purification process for bacteriophages. Viúla[104] proposed PBC as a novel alternative chromatography mode for the purification of bacteriophages. What remained to be answered was to what extent PBC removes endotoxins and how bacteriophages adsorb to this column. Both questions were answered in this work. The findings in PBC motivated the use of HIC for the purification of bacteriophages. Three operation modes were tested: single-step gradient, linear gradient, and multi-step gradient. For optimization purposes, various ammonium sulfate concentrations in the equilibration buffer were tested. To eliminate the salt from the final bacteriophage solution, SEC was employed. Capto™ Core 700 chromatography was the final mode handled in this work due to its theoretical effectiveness and lack of experimental evidence involving bacteriophages. Optimization stages in terms of the equilibration buffer were performed, as well as the conjugation with PBC to eliminate the need for a DNA digestion enzymatic step before loading. The thesis work was finished with the analysis of the best chromatography processes if they were to be used in a hypothetical bacteriophage therapy treatment. This evaluation was done based on available acceptance criteria and data regarding bacteriophage dosage from other works.

2. Materials and methods

2.1. Materials

Escherichia coli DSM 613 and T4 bacteriophage DSM 4505 were acquired from DSMZ (Braunschweig, Germany). Tryptic Soy Broth (TSB) and Tryptic Soy Agar (TSA) were purchased from Biokar Diagnostics (Pantin, France). Glycerol (99% w/v), Tris-HCl, NaOH, and phosphate buffer saline (PBS) 10X (1.37 NaCl M, 0.027 M KCl, 0.119 phosphates) were bought from Fischer Scientific (Pittsburgh, USA). The impurity quantification kits were purchased from Thermo Fischer (Massachusetts, USA). In the qPCR, DNA extraction was done with the Wizard® Genomic DNA purification kit (Promega, Madison, USA), while the qPCR reactions were performed with the Luna ® Universal qPCR Master Mix (New Englands Biolabs, Massachusetts, USA). CHES, Sorbitol, and EDTA were purchased from Sigma Aldrich (Missouri, USA). $MgCl_2$, $(NH_4)_2SO_4^-$, and Tween 20 were acquired from Panreac Quimica (Barcelona, Spain). Denarase® was acquired from c-LEcta (Leipzig, Germany). All chromatography resins (expect aminophenylboronate P6XL) were purchased from Cytiva (Uppsala, Sweden). The aminophenylboronate P6XL resin was acquired from ProMetic Biosciences (Montreal, Canada).

Bacteria or bacteriophage handling were performed under sterile conditions in a laminar flow chamber (Alpina, Zakładowa, Poland). Bacteria growth and bacteriophage amplification were done in an incubator from Biotech (Madrid, Spain). Optical densities (OD) were measured in the Hitachi U2000 spectrophotometer from Hitachi (Tokyo, Japan). Solid medium revitalization/amplification was done in the Incubator 1000 from Heidolph (Schwabach, Germany). Bacteriophage-bacteria adsorption was done in an incubator from MMM Medcenter Einrichtungen GmbH (Semmelweisstraβe 6, Germany). Top agar was thermostatized in an incubator from Memmret (Büchenbach, Germany). Centrifugation of the crude phage lysate was done in an Eppendorf Centrifuge 5810 R from Eppendorf (Hamburg, Germany). Filtration of the crude phage lysate was either done with a Whatman® Puradisc 0.2 µm syringe filter acquired from GE Healthcare (Uppsala, Sweden) or a 0.22 µm pore-sized falcon top filter from Labbox (Barcelona, Spain) in conjugation with a vacuum pump from KNF (Trenton, USA). All chromatography experiments used an ÄKTA start system, associated with the UNICORN 1.1 start software and the Frac30 fraction collector, acquired from GE Healthcare (Uppsala, Sweden). Diafiltration was done with Vivaspin® 6 100 kDa MWCO centrifuge filters purchased from GE Healthcare (Uppsala, Sweden). The impurity quantification assays utilized both a SpectraMax 340PC spectrophotometer from Molecular Devices (San Jose, USA) and a POLARstar OPTIMA spectrofluorometer from BMG Labtech (Allmendgrün, Germany). In the qPCR, total extract genomic DNA was quantified with the NanoDrop One, acquired from Thermo Fischer (Massachusetts, USA, while the reactions were made with the aid of the LightCycler® 2.0 from Roche (Basel, Switzerland).

2.2. Host cell preparation

2.2.1. Rehydration of dried *E. coli* 613 cell culture

The first step in the constructed project is the handling of the selected bacteria for T4 bacteriophage propagation. *E. coli* DSM 613 was opted as the most appropriate host for the T4 bacteriophage. *E. coli* 613 rehydration was performed following the DSMZ recommended guidelines. Freeze-dried bacteria in

a double-vial glass ampoule were first handled by heating the tip of the ampoule and cracking it by adding a few drops of water (thermic shock). With a gentle strike, the tip of the ampoule was broken off and the secondary packaging material was taken out, which included the insulation material and the cotton plug. With the *E. coli* freeze-dried bed successively reached in the inner vial, 500 µL of 2.5% w/v TSB medium was added. The bacteria pellet was allowed to rehydrate for 30 minutes. Subsequently, the *E. coli* suspension was gently mixed to fully assure that all bacteria are dissolved.

2.2.2. Master cell banks

The production of MCB for *E. coli* 613 and *E. coli* K-12 was kicked off by the preparation of the correspondent pre-inoculums. Each pre-inoculum included 5 mL of TSB medium. For *E. coli* 613, 75 µL of the rehydrated bacteria (see section 2.2.1) was added, while for *E. coli* K-12 an available MCB vial was used. The pre-inoculums were grown overnight at 37ºC and under agitation (250 rpm) in the incubator. On the following day (16-18h), two 5 mL TSB medium inoculums were prepared with the correspondent overnight bacteria culture. OD at 600 nm was measured in the spectrophotometer. Knowing that a final $OD_{600\ nm}$ of 0.1 was intended to attain in the inoculum (5 mL of TSB medium), the following equation was employed to determine the volume of pre-inoculum needed: $V_i = (Cf_{\times}Vf)/C_i$, where V_i and C_i are the bacteria volume and concentration in the pre-inoculum, respectively, and V_f and C_f are the bacteria volume and concentration in the inoculum, respectively. Following, the inoculums were grown at 37ºC and under agitation, at 250 rpm until an $OD_{600\ nm}$ of 1.0 was attained. At this stage, incubation was stopped and the MCB for each bacterium was generated by adding 70 µL of the cell suspension to 30 µL of glycerol (50%, w/v). 30 MCB vials for *E. coli* 613 and *E. coli* K-12 were made, each with a total volume of 100 µL and a final concentration of glycerol close to 15 % (w/v).

2.2.3. Bacteria growth curves

The generation of the *E. coli* 613 and *E. coli* K-12 growth curves started with the preparation of a pre-inoculum of bacteria, in 5 mL of TSB medium, grown overnight at 37ºC and under agitation (250 rpm). On the next day (16-18 h), 200 mL of TSB medium was inoculated with the previously prepared pre-inoculum, knowing that a final OD of 0.1 was intended to attain in the inoculum (200 mL of TSB medium). Next, the inoculum was grown at 37ºC and under agitation, at 250 rpm. $OD_{600\ nm}$ was measured throughout 310 min and 360 min for *E. coli* 613 and *E. coli* K-12 respectively, with various time points. In each, four 100 µL samples were taken from the cell culture. Duplicates of $OD_{600\ nm}$ were performed, as well as duplicates of colony-forming-units (CFU). The CFU method is based on successive 1:10 dilutions in 15 mM Tris-HCL pH 7.0 diluent and Saline-Magnesium (SM) diluent (50 mM Tris-HCl pH 7.5, 100 mM NaCl, 8.1 mM $MgSO_4.7H_2O$, 0.01% w/v gelatine) [121] for *E. coli* 613 and *E. coli* K-12, respectively. For the selected dilutions, 100 µL of diluted bacteria sample was plated and spread in TSA plates. TSA plates were prepared by the addition of 10 mL of TSA medium (4% w/v TSA) to each petri dish. The TSA plates, each associated with a bacteria sample dilution, were incubated overnight at 37ºC without agitation in the incubator. On the next day, CFU was counted. Only plates with 30-300 bacteria were considered acceptable. The concentration (CFU/mL) for each bacteria sample may be determined with the following equation:

$$C_{E.coli}\ (CFU/mL) = N_b \times 10^d \times 10$$

N_b represents the number of bacteria, while *d* represents the reciprocal of the counted dilution. The 10x factor is associated with the volume of the bacteria sample plated (0.1 mL).

2.3. Revitalization of vacuum-dried T4 bacteriophages

T4 bacteriophage DSM 4505 revitalization was performed following the DSMZ guidelines. The vacuum-dried T4 bacteriophages were confined in the same double-vial glass ampoule described in section 2.2.1. Inside the inner vial, a filter paper coated with T4 bacteriophages was present. With sterile scissors and forceps, the filter paper was cut into two pieces. Revitalization of T4 bacteriophages in solid and liquid mediums were performed in parallel. The liquid medium bacteriophage revitalization was done as a backup, in the event of any issue emerging in the solid medium bacteriophage revitalization. According to DSMZ, higher phage titers and a reduced appearance of phage-resistant bacteria occurs in the solid medium amplification. Therefore, this method was preferably selected over the liquid medium revitalization and used in further bacteriophage amplification procedures. The revitalization of the vacuum-dried T4 bacteriophage was done with *E. coli* 613 as the host bacterium. The protocols for the solid and liquid medium revitalization of the T4 bacteriophage are represented in the Appendix (A.1) The simplified revitalization/amplification scheme for the T4 bacteriophage is represented in Figure 8.

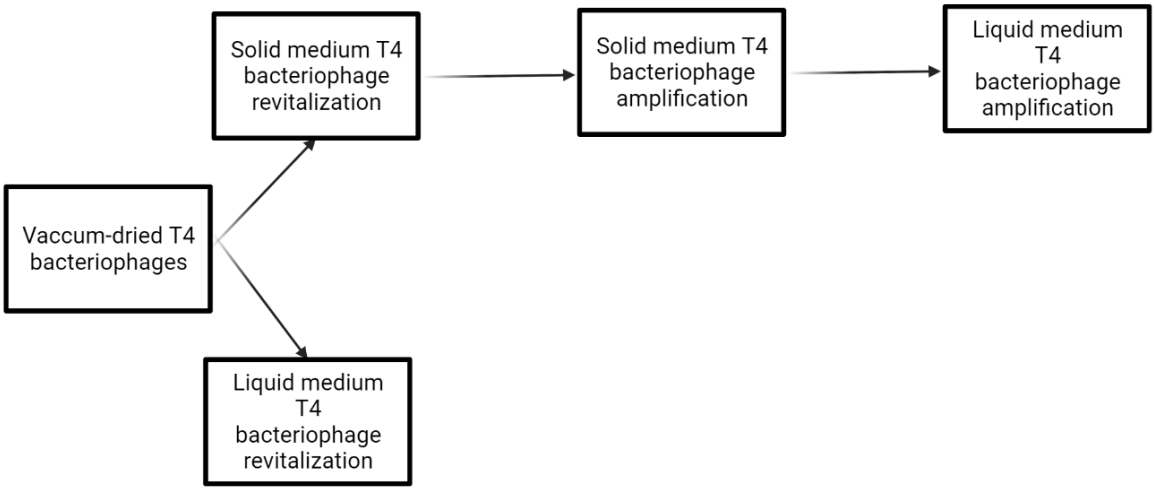

Figure 8- General devised revitalization and amplification scheme for the vacuum-dried T4 bacteriophages.

2.4. Double-agar plaque assay

Bacteriophage quantification was performed by the double-agar plaque assay (DLPA). Initially, an *E. coli* pre-inoculum in 5 mL of TSB medium was grown overnight, at 37ºC and under agitation (250 rpm). On the following day (16-18 h), 5 mL of TSB medium was inoculated with the previously prepared pre-inoculum, knowing that a final $OD_{600\ nm}$ = 0.1 was intended to attain. The inoculum was grown at 37ºC and under agitation, at 250 rpm. Meanwhile, successive 1:10 dilutions of the T4 bacteriophage samples were performed in SM diluent. To 15 mL falcons, 100 µL of the respective diluted T4 phage was added to 200 µL of the inoculum grown until the beginning of the exponential phase. A pre-adsorption step between bacteriophages and bacteria, before top agar addition, was performed by incubating the samples for 15 minutes, at 37ºC, without agitation. [122]

In parallel, top agar must be fully melted and thermostatized at 64ºC in the incubator. Top agar was prepared with 0.7% w/v agar-agar in a TSB medium. Following its removal from the incubator, the top agar was supplemented with 10 mM $MgCl_2$.[121] After the incubation of the 15 mL falcons is finished, 3 mL of the top agar was added to each sample, which was then gently mixed and poured onto TSA plates. The TSA plates, each associated with a T4 bacteriophage dilution, were incubated overnight at 37ºC without agitation in the incubator. On the next day, PFU was counted. Only plates with 30-300 plaques were considered acceptable. The concentration (PFU/mL) for each phage sample may be determined with the following equation:[121]

$$C_{Phage}\ (PFU/mL) = N_P \times 10^d \times 10$$

N_p represents the number of plaques, while *d* represents the reciprocal of the counted dilution. The 10x factor is associated with the volume of the T4 phage sample plated (0.1 mL). Throughout the experimental work, control tests were implemented in each performed DLPA, based on the sole presence of top agar, $MgCl_2$, T4 bacteriophages, and *E. coli*. An illustration summarizing the steps included in the DLPA is represented in Figure 9.

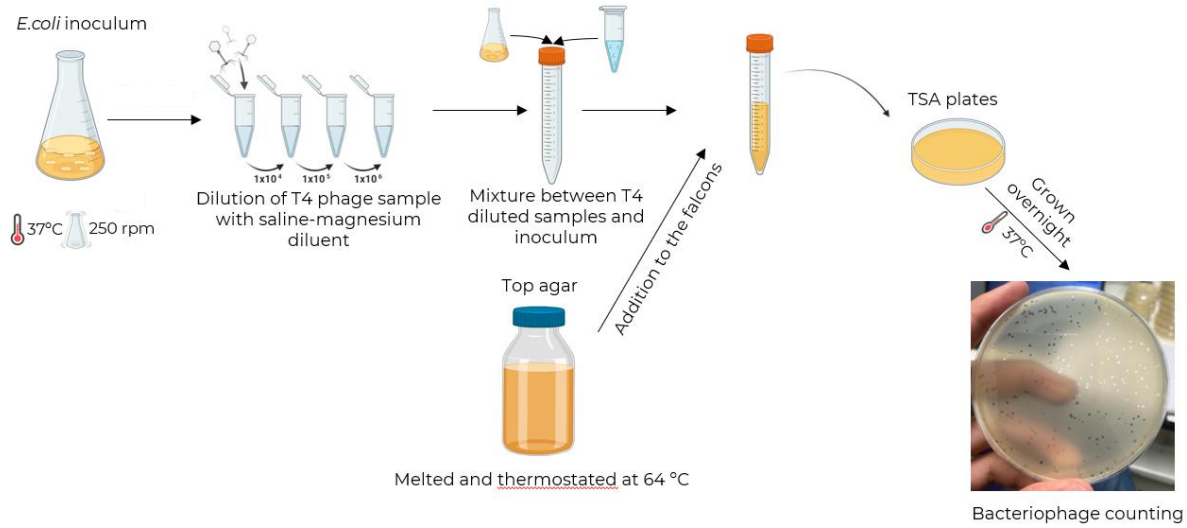

Figure 9- Double-agar plaque assay experimental procedure. Bacteriophage counting was done based on the forementioned equation in this section. N_p corresponds to each lytic zone caused by bacteriophages bursting out of the bacteria. Created with BioRender.com.[48]

2.5. Amplification of T4 bacteriophages

The end-goal of a bacteriophage amplification procedure is to attain a bacteriophage lysate volume high enough to generate a stock solution easily accessible and that can be stored at 4 ºC. This eliminates the necessity of always using MFB for each purification strategy employed. Therefore, a liquid medium amplification, regardless of any previous revitalization/amplification procedures, should be performed as a final step in the amplification of bacteriophages.

As referred, the solid medium revitalization of vacuum-dried T4 bacteriophages was used for further amplification procedures. Nonetheless, its low volume (< 100 µL) was not enough to perform a liquid medium amplification. Herewith, a second solid medium amplification, originating from the solid medium

revitalization lysate, was performed (Figure 8). Subsequently, with a higher volume of clarified T4 bacteriophage lysate, a final liquid medium amplification was done.

2.5.1. Solid medium amplification

In this case, the same protocol present in the DLPA (2.4) is applied. Dilutions of the clarified bacteriophage lysate, originating in the solid medium revitalization, were performed in SM buffer, until 10^{-5}. After the addition of the diluted T4 phage samples with the *E.* coli inoculum, together with the melted top agar, this content was poured onto TSA plates. The TSA plates, each associated with a T4 phage dilution, were incubated overnight at 37ºC without agitation.

On the next day, all plates presented almost total bacteria elimination, as no bacteria lawn was present. Therefore, the number of bacteriophages in each plated dilution was uncountable and easily harvestable via a similar protocol to the solid medium revitalization of bacteriophages (Appendix, A.1). To the plates corresponding to dilutions 10^{-2} to 10^{-5}, 4 mL of SM buffer was added. These plates were then slowly agitated at room temperature for 4 hours. The harvested crude phage lysate was clarified using centrifugation followed by microfiltration. Centrifugation was done at 8000 x *g*, with a temperature of 4ºC and lasting 20 min. The recovered supernatant was filtered with a syringe filter. A final volume of about 4 mL was attained.

2.5.2. Liquid medium amplification

The production of the final T4 bacteriophage lysate was initiated by the overnight pre-inoculation of *E. coli* in 30 mL of TSB medium, at 37 ºC and under agitation (250 rpm). On the next day, 200 mL of TSB medium was inoculated with the previously prepared pre-inoculum, knowing that a final OD of 0.1 was intended to attain in the inoculum (200 mL of TSB medium). Next, the inoculum was grown at 37ºC and under agitation, at 250 rpm. $OD_{600\ nm}$ was measured until the beginning of the exponential phase, correspondent to an $OD_{600\ nm}$ = 0.25-0.30, according to the analyzed bacteria growth curve in section 3.1. At this stage, T4 bacteriophage infection was performed, considering a Multiplicity of Infection (MOI) of 0.1. MOI represents the ratio between the number of bacteriophages and bacteria. Infection was performed with the clarified T4 bacteriophage lysate obtained from the previous solid medium amplification. The determination of the infection volume is discussed later in the Results and is demonstrated in section A.2.1.1 (Appendix). To improve bacteriophage attachment and intracellular replication in *E. coli*, divalent cations should be added to the bacteria culture.[121] Therefore, simultaneously with the T4 bacteriophage infection, 10 mM $MgCl_2$ was added to the bacteria culture. The same incubation conditions were resumed until a final $OD_{600\ nm}$ lower than 0.1 was obtained. The resultant crude T4 bacteriophage lysate was clarified using centrifugation followed by microfiltration. Centrifugation was done at 8000 x g, with a temperature of 4ºC for 20 min. The recovered supernatant was microfiltered through a falcon top filter, using a vacuum pump. A small volume was excluded from the final clarified T4 bacteriophage lysate to construct MFB, while the remaining was stored at 4ºC. An illustration summarizing the steps included in the liquid medium amplification is represented in Figure 10. Note that the first time this procedure was done, *E. coli* 613 the host was used. However, other amplifications done throughout the thesis work used *E. coli* K-12 as the host.

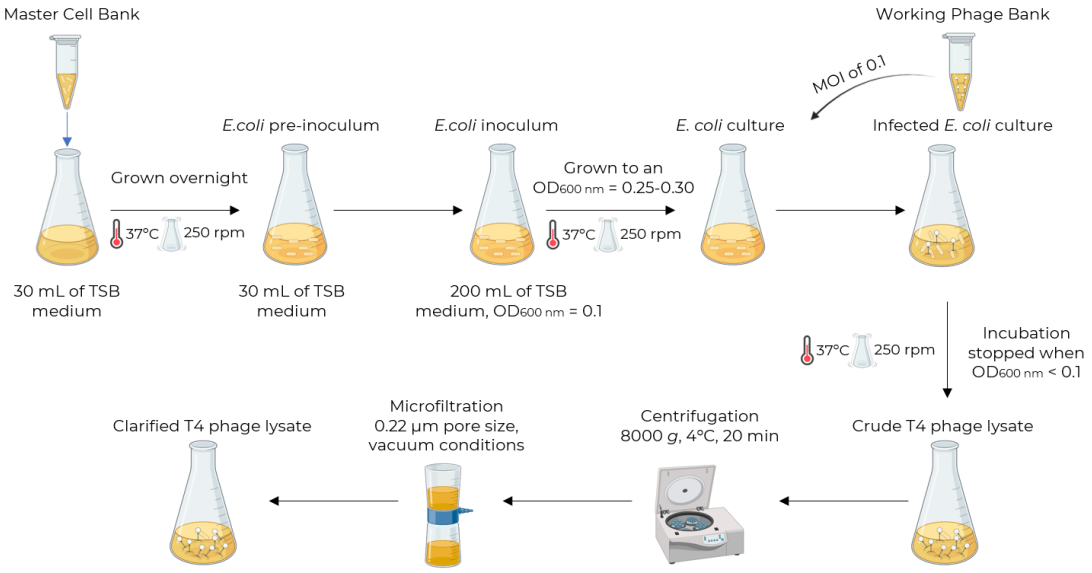

Figure 10- Liquid medium T4 bacteriophage amplification experimental procedure from a *E. coli* pre-inoculum to a clarified phage lysate. Created with BioRender.com.[48]

2.6. Chromatography

2.6.1. Phenyl boronate chromatography

Chromatography experiments were carried out in an ÄKTA start system associated with the UNICORN 1.1 start software. Absorbance (mAU) at 280 nm and conductivity (mS/cm^2) were continuously monitored in the outlet stream of the column. The used column was packed with 1 mL of Aminophenylboronate P6XL resin. A constant flow rate of 1 mL/min and an injection volume of 5 mL were employed in all chromatographic runs. The sample loop was pre-cleared with Mili-Q water and with washing buffer before sample loading.

Throughout all chromatography runs, equilibration was done with 6 column volumes (CV). The described Viúla[104] conditions used an equilibration buffer composed of 15 mM Tris-HCl pH 7.0. Column washing was done with 6 CV of equilibration buffer, while column elution was done with 10 CV of 1.5 M Tris-HCl pH 8.5. To assess which secondary interactions in PBC were responsible for T4 bacteriophage adsorption to the column, other chromatographic conditions were devised:

- To enhance hydrophobic interactions, the equilibration buffer employed was 15 mM Tris-HCl, 1.5 M $(NH_4)_2SO_4$ pH 7.0. Column washing was done with 5 CV of equilibration buffer, while column elution was done with 12 CV of 15 mM Tris-HCl pH 7.0. Sample conditioning before loading with 1.5 M $(NH_4)_2SO_4$ was performed.
- To hamper charge-transfer interactions, the equilibration buffer employed was 15 mM CHES pH 9.5. Column washing was done with 5 CV of equilibration buffer, while column elution was done with 10 CV of 1.5 M Tris-HCl pH 8.5. Sample diafiltration before loading with centrifuge filters was performed (see sections 2.6.1.1 and 2.6.1.2).

- *Cis*-diol esterification was investigated with an equilibration buffer composed of 15 mM Tris-HCl pH 7.0. Column washing was done with 8 CV of equilibration buffer, while column elution was done with 8 CV of 15 mM Tris-HCl, 150 mM Sorbitol pH 7.0

Fractions of 1 mL were collected with the Frac30 fraction collector and pooled together when indicated. Bacteriophage titer in each fraction pool was determined with the DLPA. Additionally, the protein, dsDNA, and endotoxin content were assessed (see section 2.7). Cleaning-in-place (CIP) was done with 10 CV of Milli-Q water, followed by 5 CV of 1.0 M NaOH, and 10 CV of Milli-Q water. Column cleaning and storage were performed at the end of each chromatographic run with 10 CV of Milli-Q water, followed by 5 CV of 20% (v/v) ethanol.

2.6.1.1. Bacteriophage pH endurance

The ability of bacteriophages to withstand alkaline environments was investigated to unveil the appropriate pH of the equilibration buffer used in hampering the charge-transfer interactions in PBC. The pH of the bacteriophage sample was altered via serial dilutions in modified SM buffers. SM buffers with different pH (8.5, 9.0, and 9.5) were prepared and within the DLPA, serial dilutions 1:10 of the bacteriophage sample were done with each new SM buffer. The pH of the diluted bacteriophage sample to be plated matched the corresponding SM buffer pH, following dilutions up to 10^{-7}. Afterward, the normal DLPA was carried out and the bacteriophage titer was evaluated.

2.6.1.2. Diafiltration

Diafiltration of the bacteriophage lysate was carried out with centrifuge filters. Centrifuge cycles at 4400 rpm, 4ºC, for 5-10 min were performed. The selected diafiltration buffer was composed of 15 mM CHES pH 9.5. Initially, the centrifuge filter was washed with its total volume of Milli-Q water, followed by the diafiltration buffer. 5 mL of bacteriophage sample was added to the centrifuge filter and a concentration step was performed, resulting in a final volume of 500 µL. Subsequently, diafiltration with four volumes of buffer (2 mL) was done. When 500 µL of the sample was once again reached, the original volume was restored (5 mL) by adding the diafiltration buffer.

2.6.2. Phenyl Sepharose FF chromatography

All Phenyl Sepharose FF chromatography experiments were carried out with the same system configurations, including flow-rate and loading volume, as described for the PBC. A HiTrap™ Phenyl Sepharose 6 Fast Flow (High sub) pre-packed 1 mL column was selected. The equilibration/washing buffer was composed of 15 mM Tris-HCl, 1.5 M $(NH_4)_2SO_4$ pH 7.0 (except when stated otherwise), while the elution buffer was composed of 15 mM Tris-HCl pH 7.0. Column equilibration was done with 6 CV, followed by a loading phase of 5 CV and a washing phase of 5 CV. Three elution operation modes were tested: linear-gradient elution, single-step-gradient elution, and multi-step-gradient elution. In the linear-gradient operation mode, elution was done with 20 CV (0-100% elution buffer). For the single-step-gradient operation mode, elution was done with 7 CV and different ammonium sulfate concentrations (1.5, 1.0, 0.75, and 0.50 M) were tested. The same operation mode was also used before a SEC for buffer exchange. Three multi-step-gradient elution schemes were devised: Processes 1, 2, and 3. Process 1 employed a two-step-gradient elution operation mode (80% and 100% elution buffer), while

Process 2 used a five-step-gradient elution operation mode (70%, 75%, 80%, 85%, and 100% elution buffer). Process 3 implemented a five-step-gradient elution operation mode (35%, 50%, 65%, 80%, and 100%) with an equilibration/washing buffer composed of 15 mM Tris-HCl, 0.75 M $(NH_4)_2SO_4$ pH 7.0. All processes used elution steps of 5 CV. Fractioning and content analysis of each defined pool was done as described for the PBC. CIP and column cleaning and storage followed the same procedure as the PBC.

2.6.3. Size exclusion chromatography

All size exclusion chromatography experiments were carried out with the same system configurations, including flow-rate, as described for the PBC. The used column was packed with 24 mL of Superdex 200 Increase 10/300 GL resin. An injection volume of 500 µL was employed in all chromatographic runs. This chromatography was used for buffer exchange following a single-step-gradient elution Phenyl Sepharose FF chromatography. The presence or absence of a Tween 20 pre-treatment step was tested. Sample conditioning was done with 0.05 % (v/v) Tween 20 and 20 mM EDTA. Both reagents were simultaneously added to the sample and an incubation time, at room temperature, for 30 minutes followed. PBS was used as the running buffer in an isocratic elution operation mode. In both conditions, an equilibration phase of 1 CV, followed by a washing phase of 1.2 CV, was employed. Column cleaning was done with 1 CV of Milli-Q water. Fractioning and content analysis of each defined pool was performed as described for the PBC.

2.6.4. Capto™ Core 700 chromatography

All Capto™ Core 700 chromatography experiments were carried out with the same system configurations, including flow-rate and loading volume, as described for the PBC. A HiTrap™ Capto™ Core 700 pre-packed 1 mL column was selected. Throughout all chromatography runs, equilibration, washing, and elution were done with 6 CV. The initially tested chromatography conditions included an equilibration/washing phase with 15 mM Tris-HCl, 150 mM NaCl pH 7.5, while elution was performed with 15 mM Tris-HCl, 1 M NaCl pH 7.5. Subsequently, the removal of salt from the equilibration buffer was tested. Here, an equilibration/washing phase with 15 mM Tris-HCl pH 7.5 and an elution phase with 15 mM Tris-HCl, 1 M NaCl pH 7.5 were employed. The loaded bacteriophage lysate was pre-treated with Tween 20 and Denarase®, as described in section (2.6.4.1). Fractioning and content analysis of each defined pool was done as described for the PBC. CIP and column cleaning and storage followed the same procedure as the PBC.

2.6.4.1. Sample pre-treatment with Tween 20 and Denarase®

Bacteriophage lysate pre-treatment before Capto™ Core 700 chromatography loading was done with 0.05% (v/v) Tween 20 and 250 U/µL Denarase®. The Denarase® stock had an enzyme activity of 2.50E+05 U/mL. No $MgCl_2$ supplementation was done as the bacteriophage lysate already contained Mg^{2+} in its composition. Following the addition of Tween 20 and Denarase®, the bacteriophage sample was incubated for 2 h at 37ºC and under agitation (250 rpm). The enzymatic reaction was stopped by the addition of 20 mM EDTA, which also worked together with Tween 20 to promote the dissociation of endotoxin aggregates.

2.7. Impurities quantification assays

2.7.1. Pierce™ BCA protein assay

The Pierce™ BCA protein assay was performed according to the manufacturer's instructions. PBS 1X solution was used as the diluent. The initial BSA stock solution had a volume of 1 mL and a concentration of 2 mg/mL. The diluted BSA standards were prepared with the BSA stock solution, according to Table A.1 (Appendix), and stored at -20ºC. A concentration working range of 400-5 µg/mL was employed. Standard curves with the diluted BSA standards were prepared each time a new BCA protein assay was performed. The BCA working reagent was prepared by mixing 50 parts of Reagent A with 1 part of Reagent B (50:1), provided by the manufacturer.

In a 96-well microplate, 25 µL of each diluted BSA standard was added, as well as 25 µL of each tested sample, to their respective wells. Serial dilutions 1:2 of the samples were performed in PBS 1X (25 µL per well). In the last well of each sample-associated row, 25 µL was discarded, maintaining a constant volume of 25 µL. Following, 200 µL of BCA working reagent was added to each well. The microplate was then covered with foil and incubated for 30 min at 37 ºC. With the time elapsed, absorbance at 562 nm was read in a spectrophotometer. The $OD_{562\ nm}$ of the blank standard was subtracted from each diluted BSA standard and the analyzed samples. The standard curve was prepared by plotting the blank-corrected $OD_{562\ nm}$ of each BSA standard against its corresponding concentration (µg/mL). With the average $OD_{562\ nm}$ of the tested samples, considering the most appropriate dilutions, their protein concentration (µg/mL) values were determined.

2.7.2. Quant-iT™ PicoGreen™ dsDNA assay

The Quant-iT™ PicoGreen™ dsDNA assay was performed according to the manufacturer's instructions. TE 1X (200 mM Tris-HCl, 20 mM EDTA pH 7.5) solution was used as the diluent. The initial lambda DNA standard, with a concentration of 100 µg/mL, was diluted 100-fold in TE 1X, to a final concentration of 1 µg/mL. PicoGreen™ dsDNA standard solutions were prepared with the 1 µg/mL working stock solution of dsDNA, as indicated in Table A.2 (Appendix), and stored at 4ºC. A concentration working range of 1000-1 ng/mL was employed. Standard curves with the dsDNA standards were prepared each time a new dsDNA assay was performed. Quant-It™ PicoGreen™ reagent was prepared by making a 200-fold dilution of the initial stock solution. The PicoGreen™ reagent is sensible to photodegradation thus its protection from light was assured by covering it with foil throughout this assay.

In a 96-well microplate, 100 µL of each dsDNA standard solution was added, as well as 100 µL of each tested sample, to their respective wells. Serial dilutions 1:2 of the samples were performed in TE 1X (100 µL per well). In the last well of each sample-associated row, 100 µL was discarded, maintaining a constant volume of 100 µL. Following, 100 µL of the diluted PicoGreen™ reagent was added to each well. The microplate was then incubated for 5 minutes at room temperature, and covered with foil to protect it from photodegradation. With the time elapsed, the samples were excited at 480 nm and the fluorescence emission intensity was measured at 520 nm using a spectrofluorometer. To plot the standard curve and determine the dsDNA concentration (µg /mL) in each sample, the same procedure of the BCA protein assay was conducted.

2.7.3. Pierce™ chromogenic endotoxin assay

The Pierce™ chromogenic endotoxin assay was performed according to the manufacturer's instructions. To maintain the best possible endotoxin-free environment, all described procedures took place inside the laminar flow chamber. Pyrogenic-free materials, such as 15 mL falcon tubes, pipette tips, and 96-well microplates were used throughout the assay to avoid endotoxin contamination.

Several materials must be prepared before the undertaking of this assay. Firstly, endotoxin stock solutions were reconstituted by adding endotoxin-free water (EFW) to a final concentration of 10 EU/mL. The endotoxin stock solutions were then vortexed for 15 min. Endotoxin standard solutions were prepared with the initial stock solution, as described in Table A.3 (Appendix). Similarly to the BSA standards, the endotoxin standards were stored at 4ºC and new standard curves were prepared each time a new endotoxin quantification assay was performed. The lyophilized amebocyte lysate (LAL) was reconstituted by adding 1.7 mL of EFW to each vial. Its powdered content was dissolved by gently swirling the vessel. Pooling between different LAL vials was done when a higher lysate volume was required. Importantly, the reconstituted LAL is only stable for a week at -20ºC and must not be frozen again when thawed. Finally, the chromogenic substrate was reconstituted by adding 3.4 mL of EFW to each vial. Its stability is the same as the endotoxin standard solutions however, the substate must be heated to 37ºC for no more than 5-10 min before its use.

Throughout the assay, the 96-well microplate should have been maintained at 37ºC ± 1ºC. However, due to the lack of appropriate equipment, this was not possible to achieve. Therefore, the microplate was kept at room temperature whenever solutions were added to it. 50 µL of each endotoxin standard solution or sample was added to its respective well. Serial dilutions 1:10 with EFW of the samples were done separately from the microplate, in sterilized but not pyrogenic-free eppendorfs. Following, 50 µL of reconstituted LAL was added per well. After the addition of LAL to all wells, the microplate was incubated at 37 ºC for T1. T1 is indicated in the label of the LAL manufacturer's vial and is between 10-12 min. Once T1 elapsed, the microplate was removed from the incubator and 100 µL of the pre-heated reconstituted chromogenic substrate was added per well. Following the addition of the substrate to all wells, the microplate was incubated at 37ºC for T2 = 6 min. Subsequently, 50 µL of 25% acetic acid (stop solution) was added to each well. After gently tapping the microplate, absorbance at 405 nm was read in a spectrophotometer. To plot the standard curve and determine the endotoxin concentration (EU/mL) in each sample, the same procedure of the BCA protein assay was conducted.

2.7.4. *E. coli* K-12 genomic DNA extraction

The *E. coli* K-12 genomic DNA extraction was performed with the Wizard® Genomic DNA Purification Kit following its guidelines. *E. coli* K-12 was grown overnight in 5 mL of TSB medium, at 37ºC and under agitation (250 rpm). On the following day, 1 mL of overnight culture was centrifuged at 14 000 x *g* for 2 min. While the supernatant was removed, the sedimented cells were resuspended with 600 µL of Nuclei Lysis Solution. The cells were lysed by incubating them at 80ºC for 5 min. After the cell lysate had cooled to room temperature, 3 µL of RNase Solution was added. The tube's sample was then gently inverted and incubated at 37ºC for 60 min. After being cooled to room temperature, 200 µL of Protein Precipitation

Solution was added to the sample. Importantly, mixing by high-speed vortex was performed to assure the contents were homogenous. The sample was then incubated in ice for 5 min. Following, centrifugation at 14 000 x *g* for 3 min was done. The supernatant containing the DNA was transferred to a new tube with 600 µL of isopropanol, while the protein-containing pellet was discarded. Following, the sample was mixed until the formation of thread-like DNA strands, incorporated in a mass, were visible. Subsequently, the sample was centrifuged at 14 000 x *g* for 2 min. While carefully discarding the supernatant, the DNA pellet was resuspended with 600 µL of 70% (v/v) ethanol. Another centrifugation cycle was done, with the same characteristics as the previous one, to wash the DNA pellet. Following, the DNA pellet was air-dried. The genomic DNA was rehydrated by the addition of 100 µL of PCR H_2O and stored at 4ºC. PCR H_2O was produced by autoclaving and filtrating, through a 0.22 µm pore membrane, Milli-Q water.

2.7.4.1. qPCR assay

The qPCR assay was performed according to the employed Luna® Universal qPCR Master Mix kit. The forward and reverse primers targeting the genomic DNA of *E. coli* K-12 were the same as the ones used by Longin *et al.*[123] and their sequences are represented in Table A.4 (Appendix). Initially, the primers were diluted to 10 mM using PCR H_2O and stored, alongside the stocks, at -20ºC. Each qPCR reaction was prepared with a final volume of 20 µL, using sterilized eppendorfs and pipette tips. To each reaction, 10 µL of Luna Universal qPCR Master Mix and 0.5 µL of each primer were added. In the case of the samples to be tested, 9 µL of their volume was added to the correspondent reaction. Note that samples were previously prepared according to the appropriate dilution, which most of the time was 1:5 and 1:10. The previously extracted genomic DNA was quantified using a NanoDrop One, and serial dilutions 1:10 with PCR H_2O were performed. The DNA standards were generated by the addition of 0.98 µL of each serial dilution to the correspondent reaction, with the volume being completed with 8.02 µL of PCR H_2O. This resulted in the following genomic DNA standards: 1000, 100, 10, 1, 0.1, and 0.01 ng. Each sample was transferred to its correspondent capillary and placed on the LightCycler® 2.0. The defined qPCR cycling conditions are represented in Table A.5 (Appendix). Absolute quantification and melting temperature curves for each qPCR assay were generated. The former was used for the quantification of the genomic dsDNA (ng/mL) while the latter indicated the quality of the performed qPCR reaction, by the detection of secondary products.

3. Results and discussion

3.1. T4 bacteriophage amplification

The T4 bacteriophage amplification process was kicked off by an initial screening of the employed bacteria growth behavior. Bacteriophage infection is performed at the beginning of the host exponential phase. Therefore, to understand when this event takes place, growth curves for both *E. coli* K-12 and *E.* coli 613 were performed and represented in Figure 11 and Figure A.1 (Appendix), respectively. The parallel study concerning bacteria concentration (CFU/mL) is represented in Table A.6 and Table A.7 (Appendix). It is not only important to determine the appropriate $OD_{600\ nm}$ value for bacteriophage infection but to also understand what the concentration of host cells at this point is, needed for the determination of the MOI.

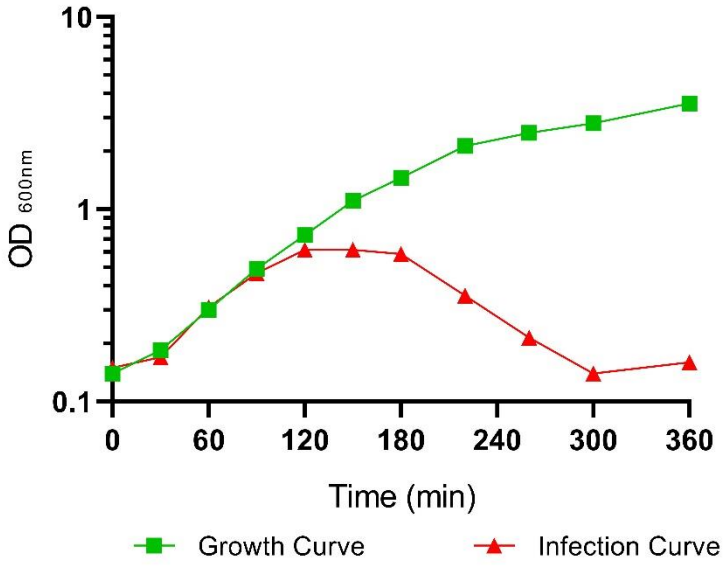

Figure 11- Growth curve for *E. coli* K-12 and T4 bacteriophage infection curve using the host *E. coli* K-12. Bacteria were grown at 37ºC in 200 mL of TSB medium. The $OD_{600\ nm}$ is represented in a logarithmic scale, over a time course of 360 min. The growth curve is represented with green squares, while the infection curve is represented with red triangles. The initial host density was 0.14. Bacteriophage infection was performed with a MOI of 0.1 and occurred at 60 minutes with an $OD_{600\ nm}$ = 0.31. The bacteriophage amplification process was halted when cell growth abruptly decreased and $OD_{600\ nm}$ was below 0.2.

Figure 11 showcases a well-defined bacteria growth curve, composed of an initial lag phase (0-30 min), followed by an exponential phase (30-220 min), and reaching the stationary phase (> 220 min). Note that the death phase is not perceivable. The bacteria growth rate determined was 3.80 h^{-1}, considering a linear regression between 220 and 30 min. More importantly, the early beginning of the exponential phase for *E. coli* K-12 was pinpointed to an $OD_{600\ nm}$ = 0.3, around 60 minutes of growth. According to Bourdin *et al.*[78] and Smrekar *et al.*[92], bacteriophage infection should be done at the beginning of the exponential phase of *E. coli* cells. Infection done later in the bacteria life cycle requires a larger MOI, due to the higher host concentration. High MOI can lead to "lysis from without", where bacteria are eliminated due to the high number of simultaneous infecting phages, and not by their interior replication.[124] Therefore, bacteriophage infection was performed around 60 minutes.

From this point onwards, all data necessary for the T4 bacteriophage amplification process was gathered. All calculations regarding this process are represented in section A.2.1.1 (Appendix). The T4 bacteriophage amplification curve for the host *E. coli* K-12 is also represented in Figure 11, while the same curve associated with *E. coli* 613 is present in Figure A.2 (Appendix). According to Figure 11, host cell propagation is maintained, although at a lower growth rate, after bacteriophage infection, until around 120 minutes. At this point, the cell growth rate becomes identical to the bacteriophage infection rate, as no increase nor decrease in $OD_{600\ nm}$ is observed. A decrease in this parameter occurs after 160 minutes, where phage propagation rules over the growth rate. The amplification process was halted when $OD_{600\ nm}$ was below 0.2, indicating that most host cells were dead, thus the maximum phage titer was most likely achieved.

After the clarification procedures were undertaken, the bacteriophage concentration of the final clarified T4 bacteriophage lysate was determined via the DLPA. It should be noted that this value was determined every week of experiments, and not only one T4 bacteriophage stock lysate was used throughout this thesis.

Two host bacteria were used throughout this work: *E. coli* 613 and *E. coli* K-12. Initially, *E. coli* 613 was the appropriate host for the T4 bacteriophage, according to the supplier. However, due to unknown problems either in the preparation of the MCB or in the amplification procedure, *E. coli* 613 had to be discarded shortly after the beginning of the thesis work, despite initial successful results. From chapter 3.2.1.2 point onwards, *E. coli* K-12 was used as the host bacterium, after being successfully infected by T4 bacteriophages and generating reproducible bacteriophage stock lysates. Until chapter 3.2.1.1, associated with the *cis*-diol esterification, *E. coli* 613 was used as the host bacterium.

3.2. Chromatography

This thesis project looked at exploring the different alternatives for the downstream processing of bacteriophages, in search of novel and improved processes that could be looked further into the future. Amongst these, Phenyl Boronate Chromatography, Hydrophobic Interaction Chromatography, and Capto™ Core 700 Chromatography were investigated. A summary of each explored chromatography and its correspondent tested conditions is represented in Figure 12. This illustration allows the reader to take a glance at the general organization behind this thesis.

3.2.1. Phenyl boronate chromatography

PBC was the first chromatography operation mode to be tested in this thesis. Its successfulness in purifying bacteriophages, with efficient protein and DNA removal rates, was observed by Viúla[104] who managed to attain a bacteriophage yield of 49%, with 96% and 47% of proteins and DNA removed, respectively. Despite the promising results, no endotoxin quantification was done, nor was any attempt to explain the interactions involved in the adsorption of these viral particles to the chromatographic column. The beginning point of this thesis was thus to try to answer these questions.

The first PBC run performed in triplicate employed the optimized buffer conditions determined by Viúla[104], where column equilibration and washing were performed with 15 mM Tris-HCl pH 7.0, while

elution was performed with 1.5 M Tris-HCl pH 8.5. As the analysis for each of the three independent chromatography runs is the same, replica two was selected for this section as a successful endotoxin quantification procedure was conducted. Its respective chromatogram is represented in Figure 13. The chromatograms for the first and third replicas are represented in Figure A.3 and Figure A.4 (Appendix), respectively.

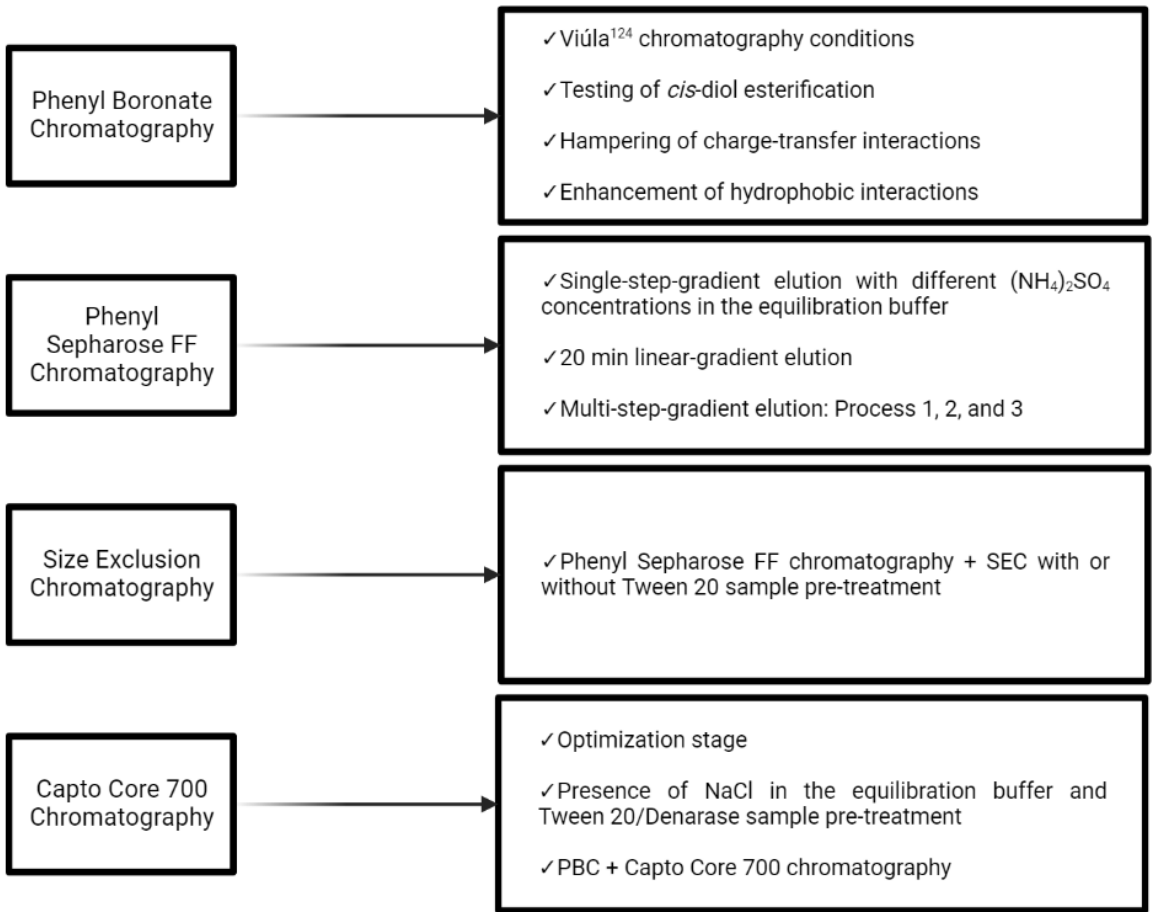

Figure 12- Thesis experimental planning. Different types of chromatography, each with specific conditions, were tested throughout the performed experimental work.

According to Figure 13, two distinct absorbance peaks are observed. The first one is the flow-through which is associated with the column loading and washing and contains all the components that did not interact with the PBC column. The second peak coincides with the elution, triggered by increasing the ionic strength, which contains the components that were adsorbed and eluted under the working conditions. At this initial phase, the whole run was analyzed in terms of bacteriophage recovery and impurity removal. To ease this process, pools of fractions were devised and identified in Figure 13. Importantly, the flow-through peak was divided into pools 1 and 2, while the elution peak is pool 4. Pool 3 corresponds to column washing, performed between the loading and the elution steps. In Table 1, both bacteriophage and impurities contents for each pool collected in replica 2 are represented. The correspondent analysis for the first and third replicas is represented in Table A.8 and Table A.9 (Appendix), respectively.

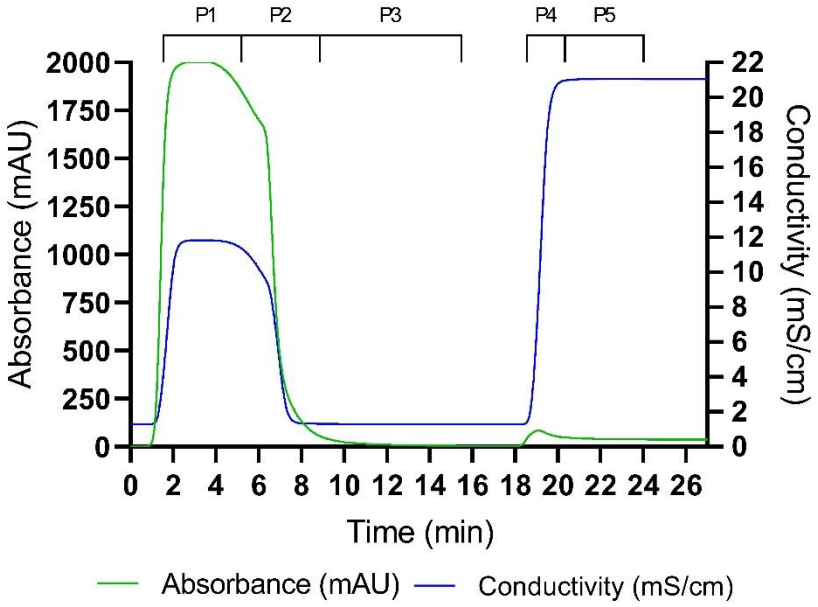

Figure 13- PBC chromatogram of replica 2 using the previously optimized chromatography conditions. Absorbance (mAU) at 280 nm and conductivity (mS/cm) were measured throughout time (min) at 1 mL/min on the outlet stream of the chromatography column. The equilibration/washing buffer was 15 mM Tris-HCl pH 7.0 and the elution buffer was 1.5 M Tris-HCl pH 8.5. Fractions of 1 mL were collected and various pools of fractions were considered for further analysis, which are represented in the upper section of the chromatogram by **PX** (with **X** being the pool number). The following pool composition was devised: **Pool 1** (Fraction 2 to 6), **Pool 2** (Fraction 7 to 12), **Pool 3** (Fraction 13 to 16), **Pool 4** (Fraction 21 to 24), and **Pool 5** (Fraction 25 to 27). The flow-through peak was divided into Pools 1 and 2, while the elution peak is Pool 4.

Table 1- Content composition for the feed lysate and pools 1-5 of replica 2 of the previously optimized chromatography conditions in PBC. For each defined pool and the lysate, its respective volume (mL), and bacteriophage (PFU/mL), protein (µg/mL), dsDNA (ng/mL), and endotoxin (EU/mL) concentration are represented.

Pools	Volume (mL)	[Bacteriophage] (PFU/mL)	[Protein] (µg/mL)	[dsDNA] (ng/mL)	[Endotoxin] (EU/mL)
Lysate	5	(2.58 ± 0.03)E+09	3926 ± 435	10443 ± 2259	(8.87 ± 0.78)E+04
1	5	(2.86 ± 0.21)E+08	2711 ± 129	6874 ± 1240	-
2	4.78	(8.33 ± 0.05)E+07	966 ± 77		
3	4	(3.00 ± 0.37)E+05	38.3 ± 12.5	-	-
4	4	(1.22 ± 0.13)E+09	44.4 ± 7.5	492 ± 9	(1.06 ± 0.56)E+04
5	3	(2.95 ± 0.18)E+07	42.2 ± 0.8	-	-

When analyzing Table 1, most bacteriophages (37.8%) were collected in the elution step (Pool 4), while a significant amount was lost in the flow-through (14.2%). Additionally, pools 3 and 5 show little interest as only a small fraction, lower than 1%, of the injected bacteriophages was collected.

The next step in the analysis of this chromatography run is the determination of the average bacteriophage recovery, as well as the respective impurities removals, in the elution pool, considering all three replicas. The results are represented in Table 2.

Table 2- Bacteriophage recovery and impurities removals for the elution pool of all three independent replicas of the previously optimized chromatography conditions in PBC.

	Bacteriophage recovery rate (%)	Protein removal rate (%)	dsDNA removal rate (%)	Endotoxin removal rate (%)
Elution Pool (Pool 4)	41.0 ± 7.4	99.4 ± 0.2	96.3 ± 0.4	85.1 ± 5.4

Likewise the work from Viúla[104], a high protein removal was registered, likely due to the absence of *cis*-diol moieties in these molecules. Secondary interactions appear to also not contribute to the column adsorption of proteins, despite the presence of amine and carboxyl groups in the side chains of amino acids that could allow adsorption by charge-transfer interactions. Interestingly, Gomes *et al*.[105] observed high protein binding rates (84-91%) in PBC, attributed to charge-transfer interactions, when injecting a plasmid-containing *E. coli* lysate. The fact that the lysate used by the authors was the result of an alkaline lysis, thus having a high ionic force that could promote hydrophobic interactions between proteins and the ligand, may explain the different results stated. DNA removal was much higher in this work compared to that of Viúla[104]. Charge-transfer interactions between the nitrogen atoms of adenine, guanine, and cytosine with the boron receptor in BA ligands could contribute to dsDNA column adsorption. Available π electrons in pyrimidine and purine heterocyclic aromatic rings may also contribute to the establishment of the same interactions.[125] Nonetheless, this effect was not apparent in the developed work, which was beneficial as the necessity of a DNA digestion step before PBC loading was abolished. Endotoxins can bear *cis*-diol groups in their polysaccharide group, thus their binding to PBC was expected to occur at a larger extent than the one observed, where only 15% of endotoxins remained adsorbed to the PBC column. Despite the high endotoxin removal, the final absolute value (10^4 EU/mL) was far beyond the needed endotoxin concentration for therapeutic use. To illustrate this point better, Rhoads *et al*.[126] characterized their bacteriophage therapy product, indicated for the treatment of venous leg ulcers, with an endotoxin content below 10^3 EU/mL.

3.2.1.1. *Cis*-diol esterification

Bacteriophage adsorption in PBC is most likely associated with secondary interactions with the immobilized ligand, the aminophenyl boronic acid. Among these, charge-transfer and hydrophobic interactions are thought as the most likely to be at the core of this adsorption. *Cis*-diol esterification is the primary interaction present in PBC however, bacteriophages do not contain moieties capable of establishing this type of interaction. To prove that bacteriophages do not adsorb to PBC through this interaction, a specific elution condition was devised, based on the addition of sorbitol to the elution buffer, which hampers *cis*-diol esterification bonds by competitive binding. The chromatogram associated with the described chromatography condition is represented in Figure 14.

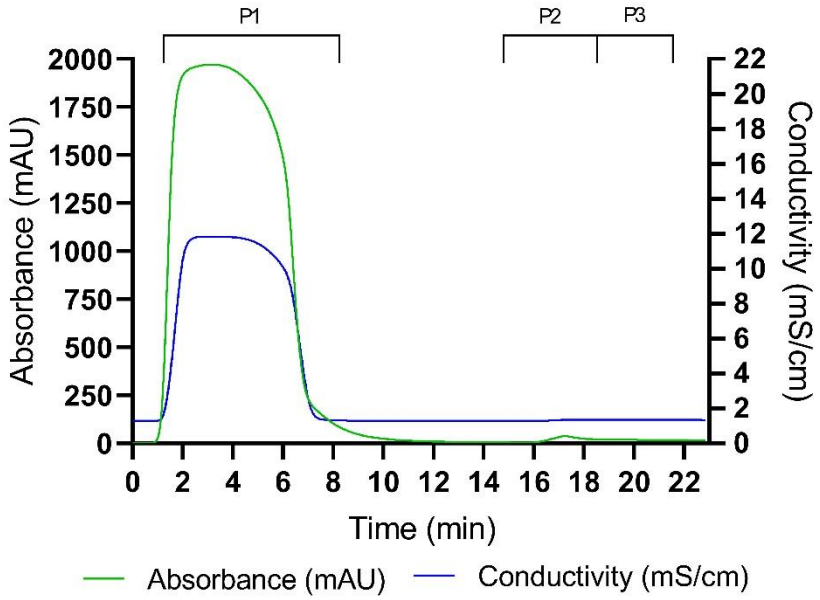

Figure 14- PBC chromatogram exploring the *cis*-diol esterification interaction. Absorbance (mAU) at 280 nm and conductivity (mS/cm) were measured throughout time (min) at 1 mL/min on the outlet stream of the chromatography column. The equilibration/washing buffer was 15 mM Tris-HCl pH 7.0 and the elution buffer was 15 mM Tris-HCl, 150 mM Sorbitol pH 7.0. Fractions of 1 mL were collected and various pools of fractions were considered for further analysis, which are represented in the upper section of the chromatogram by **PX** (with **X** being the pool number). The following pool composition was devised: **Pool 1** (Fraction 2 to 12), **Pool 2** (Fraction 19 to 22), and **Pool 3** (Fraction 23 to 25).

When analyzing Figure 14, upon elution triggering by the addition of sorbitol to the system, an absorbance peak is visualized (Pool 2). To assess if a large fraction of bacteriophages was collected within this pool, the bacteriophage content within each peak was analyzed and is represented in Table 3.

Table 3- Content composition for the feed lysate and pools 1-3 of the *cis*-diol esterification in PBC. For each defined pool and the lysate, its respective volume (mL), bacteriophage concentration (PFU/mL), and bacteriophage recovery (%) are represented. No protein, dsDNA, and endotoxin quantification were performed due to this PBC condition being written off as of no interest in the conducted studies.

Pools	Volume (mL)	[Bacteriophage] (PFU/mL)	Bacteriophage recovery (%)
Lysate	5.00	(2.36 ± 0.37)E+09	-
1	5.00	(1.28 ± 0.07)E+08	11.0
2	4.6	(7.84 ± 4.83)E+05	0.0266
3	4.00	(4.55 ± 0.45)E+05	0.0115

Bacteriophage collection in pool 2 was insignificant compared to the injected sample (0.027%), therefore no bacteriophage elution occurred in these chromatography conditions as most viruses were still

adsorbed to the column via secondary interactions. *Cis*-diol esterification was confirmed not to be at the center of bacteriophage adsorption in PBC.

3.2.1.2. Charge-transfer interactions

The possibility of charge-transfer interactions between the boron atom of phenyl boronate ligand and the surface proteins of bacteriophages was the first to be explored in assessing which secondary interactions were responsible for phage adsorption to PBC. To hamper charge-transfer interactions in PBC, its ligand conformation had to be altered, from the trigonal planar structure to the tetrahedral one. To engineer this conformation change, the working pH of the chromatography equilibration/washing buffer had to be increased above 8.8, which is the pKa of phenyl boronate. Nonetheless, it was first important to understand if a pH increase could compromise the phage titer (see section 2.6.1.1). For this purpose, three parallel DLPA were performed, each with increasing diluent pH (8.5, 9.0, and 9.5). It was observed, even at the most basic condition (pH = 9.5) the affect phage titer was not affected, when compared with the original phage lysate (data not shown). It should be noted that the conformation change could have been also engineered by the addition of a Lewis base at pH 7.0 that could coordinate with the boron atom.

In the previous PBC runs, sample loading was done with the original phage lysate, without any buffer exchange or conditioning. The pH of the original phage lysate was around 7.0, thus, the direct phage lysate loading onto the column would not match the desired equilibration conditions (pH = 9.5). To alter the bacteriophage lysate pH, a buffer exchange against the PBC equilibration buffer was performed. Diafiltration was done using Vivaspin® 6 100 kDa MWCO centrifuge filters. Tailed bacteriophages, such as the T4, have an average MW of 100 MDa.[27] Therefore, a diafiltration with a 100 kDa membrane should suffice in exchanging the buffer, while minimizing the loss of bacteriophages to the permeate. The respective bacteriophage recovery, as well as the impurities removals associated with this operation, are represented in Table 4. The detailed content composition of the bacteriophage lysate before and after the diafiltration is represented in the Table A.10 (Appendix).

Table 4- Bacteriophage recovery and impurities removal after a diafiltration using Vivaspin® 6 100 kDa MWCO centrifuge filters with the original bacteriophage lysate.

Bacteriophage recovery (%)	Protein removal (%)	dsDNA removal (%)	Endotoxin removal (%)
34.4	89.8	33.6	80.5

The operated diafiltration resulted in a great loss of bacteriophages (65.6%) while removing most proteins (89.8%) and endotoxins (80.5%). The problem at this stage did not seem to relate to the bacteriophage size, as it should not penetrate the membrane's pores. The fact that the bacteriophage yield in the permeate was below 1% (data not shown) indicated that bacteriophages were not passing through the pores. Most likely, a high degree of bacteriophage inactivation occurred in this operation, either by irreversible adsorption to the membrane or damage to the virus' components. Similar bacteriophage yield results were observed by Bourdin *et al*.[78] in three T4-like test phages when performing an ultrafiltration using a 30 kDa cutoff with an initial volume of 800 µL. Interestingly, the same

bacteriophages were recovered with a 100% yield when processing volumes up to 65 L. Possibly, buffer exchange with a large-scale filtration equipment could minimize bacteriophage infectivity loss.

Following the diafiltration, the phage lysate now at the desired pH for PBC loading was attained. The chromatogram associated with the described chromatography condition is represented in Figure 15.

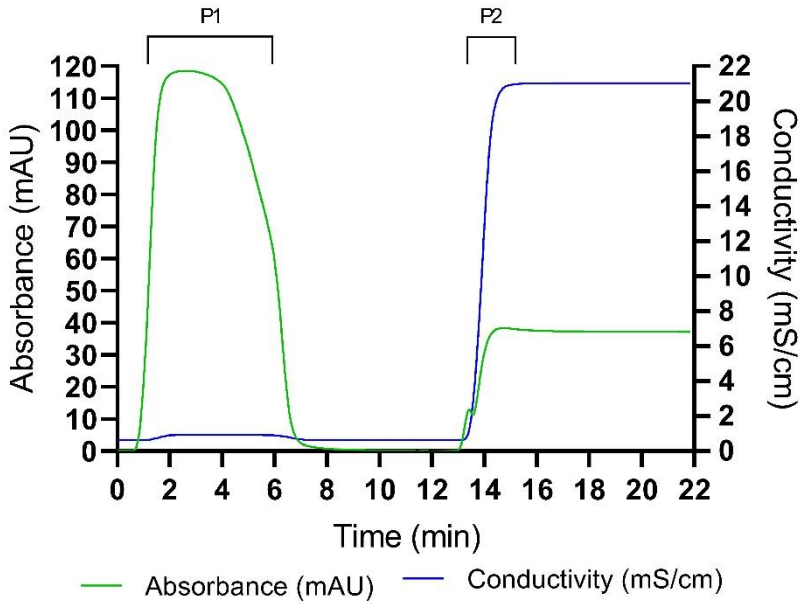

Figure 15- PBC chromatogram hampering the charge-transfer interactions. Absorbance (mAU) at 280 nm and conductivity (mS/cm) were measured throughout time (min) at 1 mL/min on the outlet stream of the chromatography column. The equilibration/washing buffer was 15 mM CHES pH 9.5 and the elution buffer was 1.5M Tris-HCl pH 8.5. Fractions of 1 mL were collected and various pools of fractions were considered for further analysis, which are represented in the upper section of the chromatogram by **PX** (with **X** being the pool number). The following pool composition was devised: **Pool 1** (Fraction 2 to 10) and **Pool 2** (Fraction 16 to 17). The flow-through and elution peaks are associated, respectively, with Pools 1 and 2.

Absorbance values throughout the chromatogram in Figure 15 are considerably lower than previous PBC experiments, likely associated with the previous removal of proteins and small metabolites in the diafiltration process. When the elution phase was initiated, a small absorbance peak, immediately overshadowed by the baseline absorbance of the elution buffer, is observed. To understand if bacteriophages were being collected in the flow-through or only upon elution triggering, the composition of the two defined peaks was determined and is represented in Table 5.

Table 5- Content composition for pools 1 and 2 of the charge-transfer interactions in PBC. For each defined pool, its respective volume (mL), and bacteriophage (PFU/mL), protein (µg/mL), dsDNA (ng/mL), and endotoxin (EU/mL) concentrations are represented.

Pools	Volume (mL)	[Bacteriophage] (PFU/mL)	[Protein] (µg/mL)	[dsDNA] (ng/mL)	[Endotoxin] (EU/mL)
1	7.50	(1.07 ± 0.02)E+08	238 ± 60	2156 ± 479	-
2	2.00	1.30E+09	-	50.1 ± 9.5	(1.11 ± 0.28)E+03

If bacteriophages were adsorbed to a PBC column via charge-transfer interactions, they should be collected in the washing phase of the performed chromatography. This occurs due to the tetrahedral conformation of the BA ligands in the equilibration phase, which does not allow this type of interaction. If in this conformation, bacteriophages remained adsorbed during the washing phase and were only collected in the elution phase, charge-transfer interactions were not responsible for phage adsorption in PBC. According to the registered results in Table 5, most (48.8%) of the injected bacteriophages in this chromatography were collected in the elution phase, while a reduced fraction (15.1%) was collected in the flow-through peak (Pool 1). This indicates that most bacteriophages were still able to adsorb to the column under the set conditions. Therefore, the elimination of charge-transfer interactions during the loading phase, by the ligand conformation change, did not prevent the binding of bacteriophages to the column. The combined yield of buffer exchange and PBC was 16.8%, which also turns this approach not viable.

3.2.1.3. Hydrophobic interactions

Bacteriophages are protein-based viral particles and, as such, are susceptible to column binding due to surface hydrophobic and aromatic π-π interactions with the phenyl ring within BA ligands. To study if hydrophobic interactions between viral protein residues and the BA ligands were responsible for bacteriophage adsorption to PBC, an enhancement of these interactions was promoted. Hydrophobic interactions enhancement was attained by pre-equilibrating the PBC column with a high ammonium sulfate concentration. The addition of ammonium sulfate to the equilibration/washing phase of PBC also required the conditioning of the sample with the same salt concentration. It was important to assure that upon ammonium sulfate addition to the bacteriophage lysate, no precipitation occurred, as this would greatly hamper phage titer before column loading. Three ammonium sulfate concentrations were tested: 0.5, 1.0, and 1.5 M. No visible precipitation occurred in any of these values. Therefore, the highest ammonium sulfate concentration was selected for further chromatography studies. Hydrophobic interactions were then reduced by the complete removal of ammonium sulfate in the elution phase. Here, molecules are eluted in increasing order of hydrophobicity. The chromatogram associated with the described chromatography condition is represented in Figure 16.

Figure 16 showcases the existence of different levels of hydrophobicity among the content loaded onto this PBC. In the elution phase, various absorbance peaks are observed, where pool 2 contains the least hydrophobic particles and pool 4 contain the most hydrophobic molecules. A more detailed analysis of the content composition in each pool is performed in Table 6.

According to Table 6, most bacteriophages are collected at the beginning of the elution phase (Pools 2+3), while the absorbance peak attributed to pool 4 is not associated with the elution of bacteriophages but with other impurities, mainly endotoxins and DNA. Additionally, pools 2 and 3 contained lower impurity levels compared to pool 4, indicating that among the molecules bound to the column during the loading phase, bacteriophages were the least hydrophobic and were immediately collected upon elution triggering. This showed a certain ability to selectively remove impurities from the bacteriophage fraction based on different levels of hydrophobicity. To better illustrate these results, the bacteriophage recovery,

as well as the impurities removals for pools 2 and 3, as well as the combination of both, are represented in Table 7.

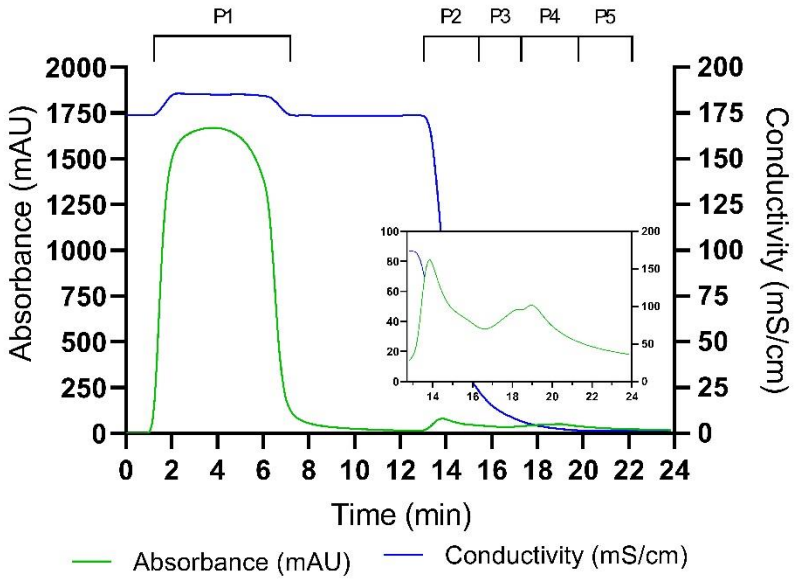

Figure 16- PBC chromatogram exploring the enhanced hydrophobic interactions. Absorbance (mAU) at 280 nm and conductivity (mS/cm) were measured throughout time (min) at 1 mL/min on the outlet stream of the chromatography column The equilibration/washing buffer was 1.5 M $(NH4)_2SO_4$, 15 mM Tris-HCl pH 7.0 and the elution buffer was 15 mM Tris-HCl pH 7.0. Fractions of 1 mL were collected and various pools of fractions were considered for further analysis, which are represented in the upper section of the chromatogram by **PX** (**X** being the pool number). The following pool composition was devised: **Pool 1** (Fraction 3 to 12), **Pool 2** (Fraction 16 to 18), **Pool 3** (Fraction 19 to 20), **Pool 4** (Fraction 21 to 23), and **Pool 5** (Fraction 24 to 26). The flow-through and elution peaks are associated, respectively, with Pools 1 and Pools 2 and 4.

Table 6- Content composition for the feed lysate and pools 1-5 of the enhanced hydrophobic interactions in PBC. For each defined pool and the lysate, its respective volume (mL), and bacteriophage (PFU/mL), protein (µg/mL), dsDNA (ng/mL), and endotoxin (EU/mL) concentrations are represented. Due to the low bacteriophage concentration in pool 5, no further impurity quantification was performed.

Pools	Volume (mL)	[Bacteriophage] (PFU/mL)	[Protein] (µg/mL)	[dsDNA] (ng/mL)	[Endotoxin] (EU/mL)
Lysate	5.00	(2.63 ± 0.20)E+09	4189 ± 394	6194 ± 343	(6.13 ± 3.45)E+04
1	8.56	(2.32 ± 0.04)E+06	1179 ± 23	976 ± 252	1.71E+04
2	3.00	(1.58 ± 0.15)E+09	71.2 ± 12.0	300 ± 75	(7.05 ± 2.27)E+02
3	2.00	(1.22 ± 0.19)E+09	140	206 ± 33	1.79E+03
4	3.00	(1.24 ± 0.26)E+08	35.1 ± 8.4	722 ± 169	(2.77 ± 1.12)E+03
5	3.00	(1.74 ± 0.38)E+07	-	-	-

Table 7- Bacteriophage recovery and impurities removals of the enhanced hydrophobic interactions in PBC.

Pools	Bacteriophage recovery (%)	Protein removal (%)	dsDNA removal (%)	Endotoxin removal (%)
P2	36.0	97.0	97.1	99.3
P3	18.6	98.0	98.7	98.8
P2+P3	54.5	94.9	95.8	98.1

The results displayed in Table 7 showed improvement when compared to the ones of Viúla[104], mainly in terms of bacteriophages and endotoxins. Although the combination of pools 2 and 3 is detrimental to the removal of impurities, a significant increase in bacteriophage yield is observed. Nonetheless, pool 2, may be analyzed by itself due to the high removal of endotoxins, alongside proteins and dsDNA. More importantly, hydrophobic interactions were found to be responsible for the bacteriophage adsorption to a PBC column, either via conventional hydrophobic interactions or via aromatic π-π interactions with the phenyl ring of BA ligands. The T4 bacteriophage presents a few protein complexes that could explain these interactions. The cell-puncturing device is present at the distal end of the bacteriophage tail tube, in the baseplate hub, and works as a needle that penetrates the periplasmic space of the host for phage DNA translocation.[127] This structure is composed of 6 copies of the gp (gene product) 5-gp27 complex with hydrophobic external surfaces.[128,129] Surrounding the tail tube, the contractile outer sheath is composed of 138 copies of the tail sheath protein (gp18). Contemplating all three states the outer sheath presents (extended, intermediate, and contracted), between 35% and 42% of surface amino acids are hydrophobic, while only 21-24% are hydrophilic.[130] Finally, the gpwac protein (6 copies), or fibritin, represents the bacteriophage “whisker” fibers, located at the neck of the virion.[127,131] The central domain of this protein is abundant in hydrophobic residues. These “whiskers” work as environment sensors and stimulate the assembly of the long tail fibers and their attachment to the tail baseplate.[131]

3.2.2. Phenyl Sepharose FF chromatography

Until this point, the use of hydrophobic interactions to simultaneously wash away impurities and bind bacteriophages to a column seems to be the most interesting path. However, HIC has little to no information regarding its use for bacteriophage purification.

PBC is a type of affinity chromatography however, the most interesting part of this chromatography appears to be its phenyl ring, which was able to efficiently interact with hydrophobic moieties among the bacteriophage’s coat proteins. With this in mind, the next hypothesis put forward in this thesis was the use of Phenyl Sepharose for the purification of the T4 bacteriophages. The same chromatography conditions employed in the enhancement of hydrophobic interactions in PBC were initially used in Phenyl Sepharose FF chromatography. Two different operation modes were tested: a single-step-gradient elution and a 20 min linear-gradient elution. The second operation mode was employed to

explore the different levels of hydrophobicity among the column-bound molecules and as a starting point for future multi-step gradient chromatography schemes.

The chromatograms associated with the single-step-gradient elution and linear-gradient elution are represented in Figure 17, respectively. The chromatogram showcasing the absorbance (mAU) and the percentage of elution buffer (%) along the time for the linear-gradient elution is represented in Figure A.5 (Appendix).

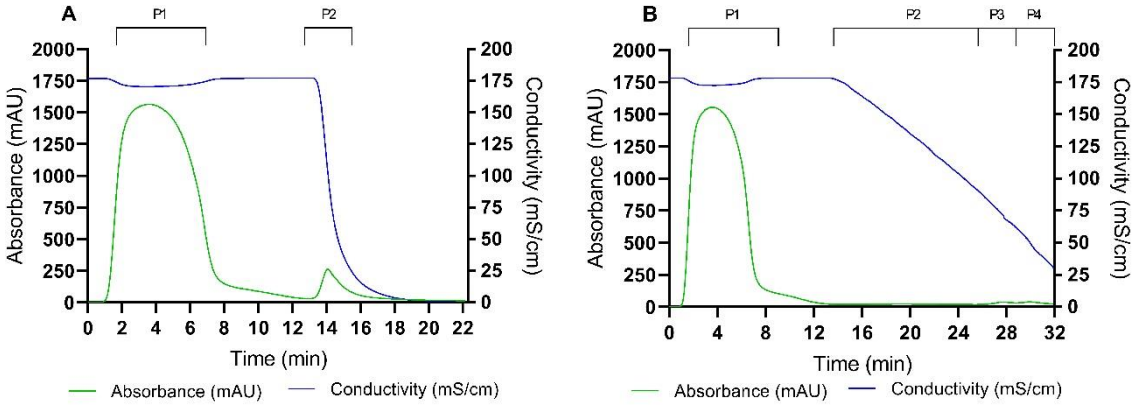

Figure 17- Phenyl Sepharose FF chromatogram with a single-step-gradient elution (A) and a 20 min linear-gradient elution (B). Absorbance (mAU) at 280 nm and conductivity (mS/cm) were measured throughout time (min) at 1 mL/min on the outlet stream of the chromatography column. The equilibration/washing buffer was 1.5 M $(NH4)_2SO_4$, 15 mM Tris-HCl pH 7.0 and the elution buffer was 15 mM Tris-HCl pH 7.0. Fractions of 1 mL were collected and various pools of fractions were considered for further analysis, which are represented in the upper section of the chromatogram by **PX** (with **X** being the pool number). The following pool composition was devised: **(A) Pool 1** (Fraction 3 to 11), and **Pool 2** (Fraction 16 to 19); **(B) Pool 1** (Fraction 3 to 11), **Pool 2** (Fraction 18 to 29), **Pool 3** (Fraction 30 to 31), and **Pool 4** (Fraction 33 to 34). Pool 2 corresponds to the elution pool in the single-step-gradient elution, while pools 3 and 4 correspond to the elution pools in the linear-gradient elution.

When analyzing Figure 17A, it is possible to observe a large UV peak upon the removal of salt, with no following absorbance fluctuations. The linear-gradient elution depicted in Figure 17B tells a different story, as, over 20 minutes, two small absorbance peaks are detected. Pools 3 and 4 in this operation mode are associated with two groups of products that required a significant reduction in ionic strength to elute from the column, likely indicating a different degree of hydrophobicity among the species present in each peak. Pool 2 was devised based on small oscillations in the absorbance signal. The detailed content composition of both operation modes is represented in Table 8. It is worth mentioning that from this stage onwards, additional genomic dsDNA quantification in each experiment was performed, resorting to qPCR.

According to Table 8, in the single-step-gradient elution, most bacteriophages are collected upon triggering elution (90.7%), with the particularity of displaying a low protein concentration but a high dsDNA concentration, when compared to the original bacteriophage lysate. In the linear-gradient elution, most bacteriophages are collected in the second elution peak (27.0%), alongside a minimal protein recovery. Generally speaking, the genomic dsDNA concentration greatly decreased in the elution pools from both operation modes. The bacteriophage recovery and impurities removals for both operation modes are represented in Table 9.

Table 8- Content composition for the feed lysate and the single-step and linear-gradient elution in Phenyl Sepharose FF chromatography. For each defined pool and the lysate, its respective volume (mL), and bacteriophage (PFU/mL), protein (µg/mL), dsDNA (ng/mL), genomic dsDNA (ng/mL), and endotoxin (EU/mL) concentrations are represented. ***** The genomic dsDNA concentration for pool 2 of the single-step-gradient elution considers the lowest possible threshold of the qPCR assay, according to a crossing point (CP) value > 35.00. ****** The bacteriophage concentration for pool 2 of the linear-gradient elution considers the lower threshold of the performed DLPA. ******* The genomic dsDNA concentration for pool 3 of the linear-gradient elution considers the lowest possible threshold of the qPCR assay, according to a CP value > 35.00.

Pools	Volume (mL)	[Bacteriophage] (PFU/mL)	[Protein] (µg/mL)	[dsDNA] (ng/mL)	[Genomic dsDNA] (ng/mL)	[Endotoxin] (EU/mL)
Lysate	5.00	(3.23 ± 0.25)E+09	3114 ± 131	6083 ± 890	308 ± 5	(6.14 ± 3.05)E+04
Single-step gradient elution						
1	8.00	(4.17 ± 0.21)E+07	1918 ± 238	1355 ± 130	-	1.30E+04
2	4.00	(3.67 ± 0.19)E+09	23.4 ± 8.6	1157 ± 362	< 11.1*****	(2.61 ± 0.20)+03
Linear gradient elution						
1	7.50	1.41E+08	1918 ± 223	1121 ± 180	-	-
2	12.0	< 3.00E+08******	13.5	61.6 ± 29.6	-	-
3	2.00	(6.10 ± 0.30)E+08	32.0	778 ± 183	< 11.1*******	(3.28 ± 0.72)E+02
4	2.00	(2.18 ± 0.07)E+09	6.77	853 ± 159	41.1	(5.79 ± 0.12)E+02

Table 9- Bacteriophage recovery and impurities removals of the single-step-gradient and linear-gradient elution in the Phenyl Sepharose FF chromatography. * The genomic dsDNA removal for the linear-gradient elution considers the lowest possible threshold of the PCR assay, according to a CP value > 35.00.

Chromatography elution pool	Bacteriophage recovery (%)	Protein removal (%)	dsDNA removal (%)	Genomic dsDNA removal (%)	Endotoxin removal (%)
Single-step-gradient elution (Pool 2)	90.7	99.4	85.9	> 97.1*****	96.6
Linear-gradient elution (Pool 4)	27.0	99.9	94.8	94.7	99.6

With the registered data in Table 9, it is possible to observe the pros and cons of the single-step-gradient elution versus the linear-gradient elution. While the former offers a high bacteriophage recovery, it fails

at efficiently removing dsDNA. The latter offers high impurities removals, but with a significant sacrifice in the bacteriophage yield. With a linear-gradient elution operation mode, the injected contents are more distributed during the elution phase compared to the single-step-gradient elution. This works better in terms of impurities, as the same content as in the single-step-gradient elution is distributed throughout more fractions during the elution phase period (20 min). However, this is counterproductive for the product to be recovered, which also appears to suffer from the same effect, resulting in a low yield.

Looking at the different interactions observed in the performed HIC, it is possible to conclude that bacteriophages appear to strongly beneficiate from the aforementioned hydrophobic surface regions for their efficient adsorption and subsequent elution from the chromatography column. In terms of protein impurities, these do not appear to interact strongly with the ligand likely because their hydrophobic residues are buried. Endotoxins are amphiphilic molecules with a hydrophobic region represented by the lipid A, and a long hydrophilic region that contains the core and the *o*-antigen oligosaccharide.[132] Therefore, their binding to a HIC column was of no surprise, although it occurred at a shorter extent than expected. The results present in the linear-gradient elution are highly optimistic, with a high endotoxin removal and a final concentration below 1000 EU/mL for the first time.

dsDNA molecules are characterized by their polar phosphate backbone that shields the inner hydrophobic core attributed to the aromatic bases. Intact dsDNA molecules are hydrophilic, thus should not strongly interact with the HIC ligand. Interestingly, about 14% of dsDNA was able to adsorb to the chromatography column in the single-step-gradient elution. Single-stranded nucleic acids, such as RNA and denatured dsDNA, were not quantified, these molecules should interact with the phenyl ring via their exposed hydrophobic aromatic bases. Either total dsDNA quantification with the PicoGreen™ kit, or genomic dsDNA quantification with the qPCR assay, does not include these molecules. With the introduction of the quantification of genomic dsDNA, it is important to notice that the PicoGreen™ method quantifies the total dsDNA present in a sample. This implies the quantification of the genomic dsDNA, but also of the T4 bacteriophage dsDNA. The initial values present in the loaded lysate indicate that most DNA quantified by the PicoGreen™ method is of viral nature, as the genomic dsDNA concentration is much lower. With this, the reduced dsDNA removal observed in the single-step-gradient elution is mainly associated with the bacteriophage genomic material, as the genomic dsDNA removal is much higher. This brings forth an interesting subject related to the therapeutic toxicity of the bacteriophage DNA compared to the host DNA. With the addition that few ongoing pre-clinical trials or clinical trials with bacteriophage products give out information regarding its impurities contents, when it does occur, no differentiation between host DNA or bacteriophage DNA is done. For instance, Rhoads *et al*.[126] indicated that their bacteriophage therapy product had a DNA concentration below 100 ng/mL. From what was gathered for this thesis work, there is only a therapeutic specification for the host DNA, not the viral DNA. Nonetheless, and in the case of the T4 bacteriophage that is composed of dsDNA, no real differentiation was thought to be appropriate for therapeutic use. What is interesting regarding the impurities removals of total dsDNA and genomic dsDNA displayed in Table 9, is that the latter is much higher. The *E. coli* K-12 genome size is about 4.6 Mb, whereas the T4 bacteriophage genome size is close to 170 kb.[133,134] While the higher genome size could lead to believe that more hydrophobic

interactions can be established with the column ligand, the opposite occurred. Possibly, the genomic dsDNA could have suffered degradation throughout the chromatography process that hampered the recognized regions by the qPCR primers, thus resulting in a reduced amount of amplified material and, consequently, virtually higher removal of genomic dsDNA. Another possibility for the observed results is the disruption that high salt concentrations may have in the performed quantification assays or the sensitivity and accuracy of said assays.[84]

3.2.2.1. Influence of ammonium sulfate concentration in HIC

The amount of ammonium sulfate in the equilibration buffer of a HIC is of utmost importance. For optimization purposes, it is critical to explore the lowest possible ammonium sulfate concentration one must use, without sacrificing product yield. This becomes increasingly important at an industrial scale, where cost saving associated with reagents and wastewater treatment is taken into consideration.[70,132] The disposal of ammonium sulfate into the environment is of serious risk, due to its high eutrophication potential.[132] Equipment corrosion at an industrial level associated with the use of high concentrations of this salt may also occur.[70] From the point of view of product viability, high salt concentrations may affect virus integrity, reducing virus infectivity and/or leading to their precipitation.[84,97] All of the above reasons contribute to the reduced use of HIC at an industrial scale and its optimization complexity at different stages. Generally speaking, ammonium sulfate should not be challenging to remove in the polishing steps of DSP, primarily through diafiltration/ultrafiltration processes. Nonetheless, it has been observed within this work how diafiltration operations negatively impact bacteriophage yield, which is one more reason for the optimization of the equilibration buffer included in Phenyl Sepharose FF chromatography.

Three different ammonium sulfate concentrations were tested in the equilibration buffer, namely 1.0, 0.75, and 0.50 M. All chromatography runs were operated with a single-step-gradient elution. The characterization of the injected bacteriophage lysate is represented in Table A.11 (Appendix). The chromatograms associated with each ammonium sulfate (1.0, 0.75, and 0.50 M) are respectively represented in Figure 18.

According to Figure 18, the impact of the different ammonium sulfate concentrations in the equilibration phases slightly affects the UV absorbance intensity of the elution peak (Pool 1). A clear decrease in absorbance is observed in Figure 18C, compared to the remaining ammonium sulfate concentrations. This is reflected in the smaller number of fractions englobed in the respective elution pool. A detailed comparison of content composition between all salt concentrations may be observed in Table 10.

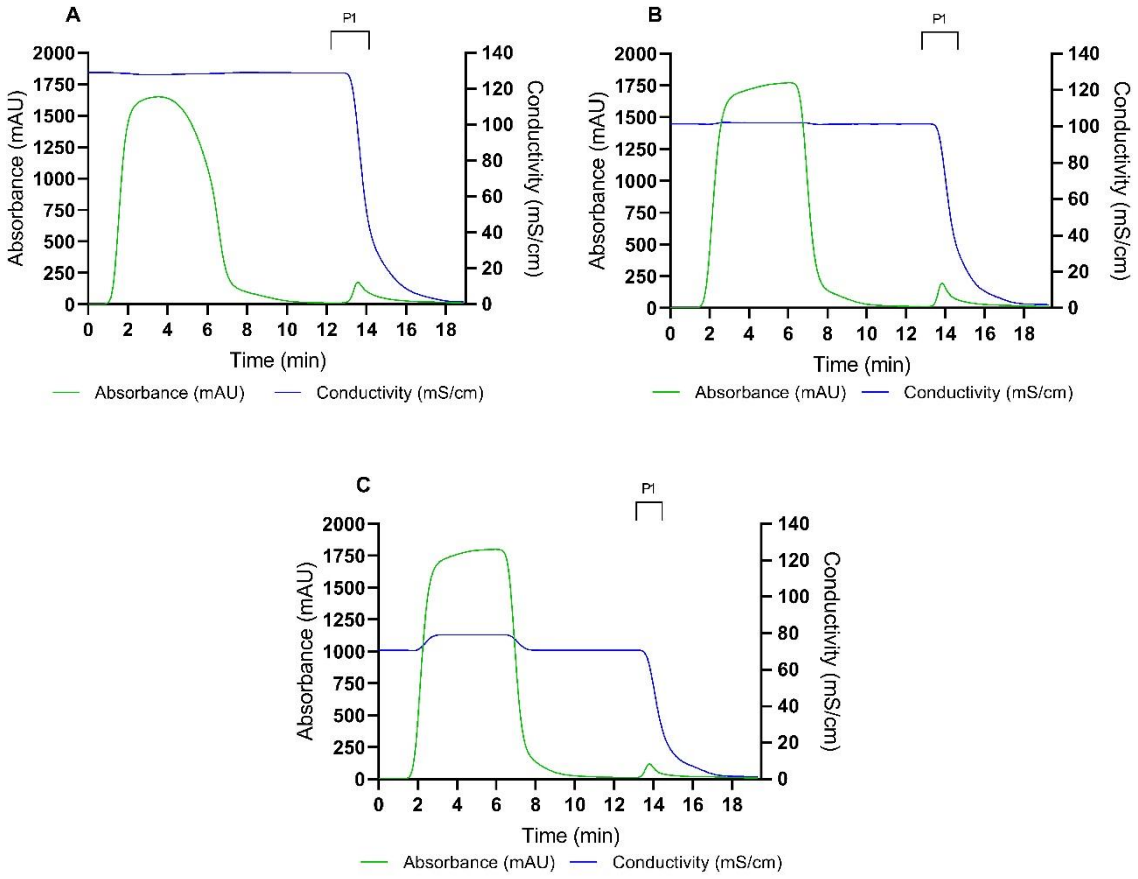

Figure 18- Phenyl Sepharose FF chromatogram with various ammonium sulfate concentrations: 1.0 M (A); 0.75 M (B); 0.50 M (C). Absorbance (mAU) at 280 nm and conductivity (mS/cm) and were measured throughout time (min) at 1 mL/min on the outlet stream of the chromatography column. The equilibration/washing buffer was 1.0 **(A)**, 0.75 **(B)**, and 0.50 **(C)** M $(NH4)_2SO_4$, 15 mM Tris-HCl pH 7.0 and the elution buffer was 15 mM Tris-HCl pH 7.0. Fractions of 1 mL were collected and the pools of the elution fractions were considered for further analysis, which are represented in the upper section of the chromatogram by **P1**. The following pool composition was devised: **(A, B) Pool 1** (Fraction 16 to 18); **(C) Pool 1** (Fraction 16 to 17).

Table 10- Content composition for the different ammonium sulfate concentrations (1.0, 0.75, and 0.50 M) in the equilibration buffer of a Phenyl Sepharose FF chromatography. For each indicated ammonium sulfate concentration conditions, regarding the respective elution pool, its respective volume (mL), and bacteriophage (PFU/mL), protein (µg/mL), dsDNA (ng/mL), genomic dsDNA (ng/mL), and endotoxin (EU/mL) concentrations are represented. *****The genomic dsDNA concentration for 1.0 M ammonium sulfate considers the lowest possible threshold of the qPCR assay, according to a CP value > 35.00.

Ammonium sulfate concentration (M)	Pool volume (mL)	[Bacteriophage] (PFU/mL)	[Protein] (µg/mL)	[dsDNA] (ng/mL)	[Genomic dsDNA] (ng/mL)	[Endotoxin] (EU/mL)
1.00	3.00	(4.43 ± 0.99)E+09	201 ± 31	984 ± 271	< 11.1*****	(3.48 ± 0.31)E+03
0.75	3.00	(5.73 ± 0.62)E+09	141 ± 25	1587 ± 598	82.6	(9.10 ± 0.18)E+03
0.50	2.00	(6.67 ± 0.45)E+09	101 ± 11	1039 ± 348	148	(4.20 ± 0.03)E+03

Considering the data registered in Table 10, the 0.75 M ammonium sulfate concentration in the equilibration buffer appears to be the best choice in terms of bacteriophage concentration. Nevertheless, it also presents the highest dsDNA and endotoxin concentration. With the lower salt concentration, lower hydrophobic forces should be at play during equilibration, leading to a lower concentration of impurities in the elution phase. However, this was not the case in terms of dsDNA, genomic dsDNA, and endotoxins compared to the ammonium sulfate concentration of 1.0 M. A more general comparison between the three chromatography conditions, in terms of the bacteriophage recovery and impurities removals, is represented in Table 11.

Table 11- Bacteriophage recovery and impurities removals for the different ammonium sulfate concentrations (1.5, 1.0, 0.75, and 0.50 M) in the equilibration buffer of a Phenyl Sepharose FF chromatography. * The genomic dsDNA removal for 1.0 M ammonium sulfate considers the lowest possible threshold of the qPCR assay, according to a CP value > 35.00.

Ammonium sulfate concentration (M)	Bacteriophage recovery (%)	Protein removal (%)	dsDNA removal (%)	Genomic dsDNA removal (%)	Endotoxin removal (%)
1.5	90.7	99.4	85.9	> 97.1	96.6
1.0	85.8	97.4	91.6	> 99.4*****	97.4
0.75	93.0	98.3	88.3	99.4	93.3
0.50	72.0	99.2	94.9	99.3	97.9

When analyzing Table 11, it becomes once again clear that there is no ideal ammonium sulfate concentration selection for the equilibration buffer. While 0.75 M salt concentration leads to the highest bacteriophage yield, it also presents the lowest dsDNA and endotoxin removals. These are the highest when the lower salt concentration is initially employed.

It is important to understand that by varying the concentration of ammonium sulfate in the equilibration buffer, the strength at which hydrophobic interactions are enhanced varies. The lower the concentration of salt during the equilibration phase, the lower will hydrophobic interactions be promoted, resulting in reduced binding of particles during the loading phase.[98] This results in higher removals and lower yields with reduced salt concentration. When excluding the chromatography condition with 0.75 M ammonium sulfate, this exact effect is observed throughout concentrations 0.50, 1.0, and 1.5 M considering bacteriophage yield, and dsDNA and endotoxin removals. Highly hydrophobic molecules should be adsorbed to the column at low salt concentrations, but weaker hydrophobic molecules might not bind under the same conditions. The lowest salt concentration in the equilibration buffer resulted in the lowest bacteriophage yield, but the highest removal of endotoxins and dsDNA. This indicates that by reducing the strength of hydrophobic interactions during the equilibration phase, weakly-bound impurities that previously adsorbed to the column no longer did. dsDNA removal saw the biggest change between 0.50 M and 1.5 M ammonium sulfate in the equilibration phase (Table 11), while the remaining impurities saw

little change. The dsDNA binding to a HIC column should be minimal and if it were to occur, weakly established hydrophobic interactions were at play. Therefore, it comes as no surprise that by reducing the salt concentration, these weak hydrophobic interactions no longer occurred.

What was interesting in Table 11 is that the intermediate ammonium sulfate concentration (0.75 M) resulted in the highest bacteriophage yield out of all tested salt concentrations. Compared to 1.5 M ammonium sulfate, the protein and endotoxin removals were lower, but the total dsDNA and genomic dsDNA removals were higher. As stated, by decreasing the salt concentration, fewer particles are expected to bind during the equilibration phase. This leads to an increased number of available ligands for binding. On the other hand, the same decreasing salt concentration reduces the enhancement of hydrophobic interactions and may prevent these available ligands to be occupied. A certain balance is at play. A decrease in salt concentration in the equilibration phase leads to a decrease in competition for the ligands, which may increase bacteriophage binding and yield in the elution phase. However, bacteriophages may not be able to establish hydrophobic interactions due to the reduced hydrophobicity strength. What appears to occur with the salt concentration of 0.75 M, is that the former effect imposes itself compared to the latter. This means that the vacancy of ligands compensates for the reduced hydrophobicity enhancement, leading to a higher bacteriophage yield. Furthermore, when decreasing the salt concentration to 0.50 M, although more ligands are made available, it seems that more bacteriophages are not able to establish hydrophobic interactions, resulting in the lowest yield observed. Therefore, the same aforementioned compensation is not seen.

3.2.2.2. Multi-step-gradient elution

The first chromatography conditions tested with Phenyl Sepharose FF compared a single-step-gradient elution with a 20 min linear-gradient elution (Figure 17). Linear gradients may be considered as preliminary experiments for the identification of optimal buffer composition and at which salt concentration bacteriophages or impurities elute. The identified salt concentrations may then be converted into a multi-step-gradient elution scheme, with a better resolution between peaks when compared to a linear-gradient elution.[98,99] Additionally, high-resolution peaks result in more concentrated and pure samples. Step gradients are also preferable for the industrial purification of biological products due to their simplicity and reproducibility.[98] The next section of this thesis is dedicated to the translation of the linear gradient into a multi-step gradient that could increase the bacteriophage yield whilst maintaining, across the board, the high impurities removals. Three processes were devised, each built upon the information retrieved from the previous one.

3.2.2.2.1. Process 1

The first process carried out consisted of a simple two-step-gradient elution, at 80% (0.3 M $(NH_4)_2SO_4$) and 100% elution buffer. The equilibration buffer employed contained 1.5 M ammonium sulfate. The chromatogram illustrating the absorbance (mAU) and the percentage of elution buffer (%) along the time is represented in the Figure 19A, while the one showcasing the absorbance (mAU) and the conductivity (mS/cm) along the time is represented in Figure 19B.

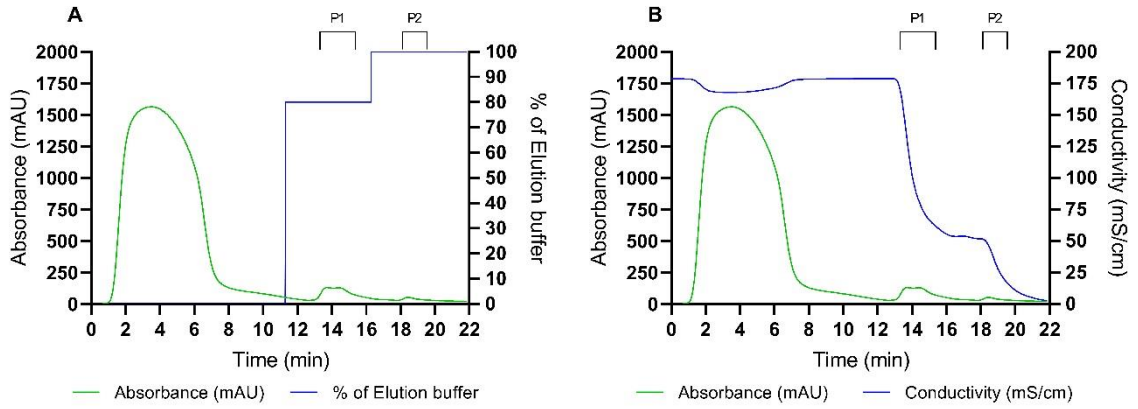

Figure 19- Two-step-gradient elution Phenyl Sepharose FF chromatogram of Process 1. Absorbance (mAU) at 280 nm and % of elution buffer **(A)** or conductivity (mS/cm) **(B)** were measured throughout time (min) at 1 mL/min on the outlet stream of the chromatography column. The equilibration/washing buffer was 1.5 M $(NH4)_2SO_4$, 15 mM Tris-HCl pH 7.0 and the elution buffer was 15 mM Tris-HCl pH 7.0. Fractions of 1 mL were collected and various pools of fractions were considered for further analysis, which are represented in the upper section of the chromatogram by **PX** (with **X** being the pool number). The following pool composition was devised: **Pool 1** (Fraction 16 to 19), and **Pool 2** (Fraction 21 to 22).

According to Figure 19, when 80% of the elution buffer runs through the system, a double UV absorbance peak is detected (Pool 1). Due to the proximity of the two peaks, their separation in different fractions was not possible to achieve. When 100% of the elution buffer is triggered, an additional UV absorbance response is detected (Pool 2), associated with a group of products with a higher hydrophobicity compared to the previous double peak. To understand which of these pools corresponds to the bacteriophage fraction, the detailed composition of each is represented in Table 12.

Table 12- Content composition for the feed lysate and the two-step-gradient elution Phenyl Sepharose FF chromatography of Process 1. For each defined pool and the lysate, its respective volume (mL), % of the elution buffer, and bacteriophage (PFU/mL), protein (µg/mL), dsDNA (ng/mL), genomic dsDNA (ng/mL), and endotoxin (EU/mL) concentrations are represented.

Pools	Volume (mL)	Elution buffer (%)	[Bacteriophage] (PFU/mL)	[Protein] (µg/mL)	[dsDNA] (ng/mL)	[Genomic dsDNA] (ng/mL)	[Endotoxin] (EU/mL)
Lysate	5.00	-	(3.50 ± 0.37)E+09	4348 ± 479	6695 ± 326	1199 ± 134	(8.17 ± 4.45)E+04
1	4.00	80	(1.68 ± 0.22)E+09	170 ± 55	848 ± 278	-	(1.70 ± 0.28)E+03
2	2.00	100	(1.21 ± 0.16)E+09	25.6	405 ± 95	50.9	(2.25 0.39)E+03

Table 12 depicts a more-or-less uniform distribution of bacteriophages in the two defined pools, with the first containing a higher viral concentration. The protein and dsDNA concentrations are also higher in pool 1, as the opposite occurs with the endotoxin concentration. Note that the endotoxin and total dsDNA concentrations are higher than 1000 EU/mL and 100 ng/mL in both pools, respectively.[126] The detailed bacteriophage recovery and impurities removals for both pools are represented in Table 13.

Table 13- Bacteriophage recovery and impurities removals for the two-step-gradient elution Phenyl Sepharose FF chromatography of Process 1. * The genomic dsDNA removal in pool 1 was not able to be determined due to the formation of secondary products.

Pools	Elution buffer (%)	Bacteriophage recovery (%)	Protein removal (%)	dsDNA removal (%)	Genomic dsDNA removal (%)	Endotoxin removal (%)
1	80	38.3	96.9	89.9	-*	98.3
2	100	13.8	99.8	97.6	98.3	98.9

According to Table 13, pool 1 has the best bacteriophage yield, with still high endotoxin and protein removals, but fails when it comes to the dsDNA removal. The latter is much higher in pool 2, alongside the protein and endotoxin removals. Nevertheless, pool 2 presents a minimal bacteriophage recovery that is not optimal for future processes.

3.2.2.2.2. Process 2

Process 2 aimed at taking a more complex approach to the previous process, implementing five elution steps into one chromatography run. Here, the main idea was to separate the double peak observed in pool 1 of the previous chromatography. Additionally, the increase in elution steps results in a more robust chromatogram with each step, with single high-resolution peaks. The aim was the same as before thus to increase bacteriophage yield without sacrificing the remaining parameters. For this purpose, the multi-step-gradient process devised consisted of five elution steps, at 70%, 75%, 80%, 85%, and 100% elution buffer (0.45 M, 0.375 M, 0.3 M, 0.225 M, and 0.0 M of $(NH_4)_2SO_4$, correspondently). As pool 1 of the previous chromatography corresponded to 80% elution buffer, the goal was to increase the number of steps in this zone. The equilibration buffer employed contained 1.5 M ammonium sulfate.

The chromatogram illustrating the absorbance (mAU) and the percentage of elution buffer (%) along the time is represented in the Figure 20A, while the one showcasing the absorbance (mAU) and the conductivity (mS/cm) along the time is represented in Figure 20B.

In Figure 20, it appears that the previous chromatography's pool 1 has been split into at least two UV absorbance peaks. With 70% of elution buffer, a UV response was already detected. In each following 5% elution buffer interval, smaller signals are observed. For each elution step, despite the absorbance fluctuation being minimal, a pool was defined, as some host impurities, such as endotoxins, do not contain moieties that absorb at 280 nm. The content composition for each defined pool is represented in Table 14.

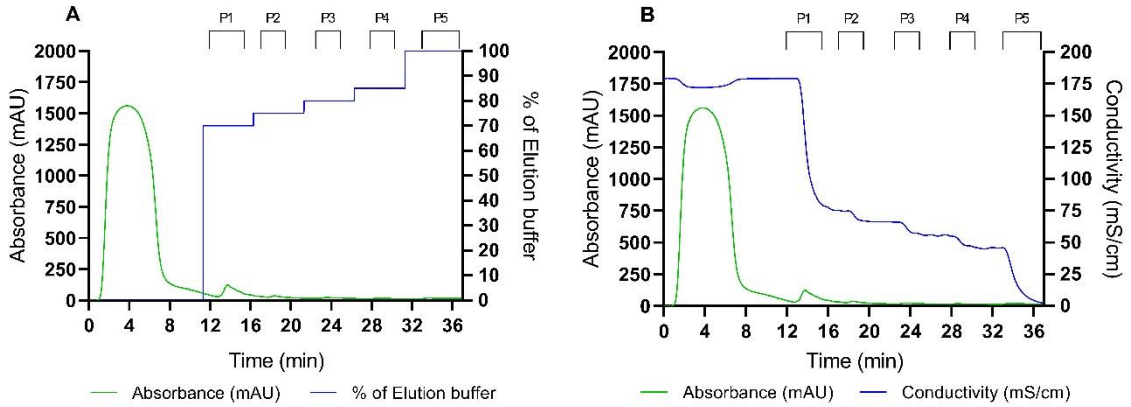

Figure 20- Multi-step-gradient elution Phenyl Sepharose FF chromatogram of Process 2. Absorbance (mAU) at 280 nm and % of elution buffer **(A)** or conductivity (mS/cm) **(B)** were measured throughout time (min) at 1 mL/min on the outlet stream of the chromatography column. The equilibration/washing buffer was 1.5 M $(NH4)_2SO_4$, 15 mM Tris-HCl pH 7.0 and the elution buffer was 15 mM Tris-HCl pH 7.0. Fractions of 1 mL were collected and various pools of fractions were considered for further analysis, which are represented in the upper section of the chromatogram by **PX** (with **X** being the pool number). The following pool composition was devised: **Pool 1** (Fraction 16 to 19), **Pool 2** (Fraction 21 to 22), **Pool 3** (Fraction 26 to 27), **Pool 4** (Fraction 31 to 32), and **Pool 5** (Fraction 36 to 39).

Table 14- Content composition for the multi-step-gradient elution Phenyl Sepharose FF chromatography of Process 2. For each defined pool, its respective volume (mL), % of the elution buffer, and bacteriophage (PFU/mL), protein (µg/mL), dsDNA (ng/mL), genomic dsDNA (ng/mL), and endotoxin (EU/mL) concentrations are represented. *****The genomic dsDNA concentration for pool 4 considers the lower threshold of the qPCR assay, according to a CP value > 35.00.

Pools	Volume (mL)	Elution buffer (%)	[Bacteriophage] (PFU/mL)	[Protein] (µg/mL)	[dsDNA] (ng/mL)	[Genomic dsDNA] (ng/mL)	[Endotoxin] (EU/mL)
Lysate	5.00	-	(3.10 ± 0.30)E+09	4687 ± 646	6998 ± 278	1199 ± 134	(8.17 ± 4.45)E+04
1	4.00	70	(7.57 ± 1.19)E+08	227 ± 31	420 ± 156	-	(4.92 ± 0.40)E+02
2	2.00	75	(3.80 ± 0.20)E+08	144 ± 21	554 ± 118	-	(2.22 ± 0.12)E+02
3	2.00	80	(6.80 ± 0.80)E+08	127 ± 24	322 ± 41	-	1.98E+02
4	2.00	85	(4.85 ± 0.55)E+08	101 ± 11	192 ± 21	< 11.1*****	1.83E+02
5	4.00	100	(3.45 ± 0.75)E+08	94.0 ± 18.0	30.8 ± 1.1	30.8 ± 26.4	1.05E+02

Table 14 unveils some interesting insight into the relationship between the presence of bacteriophages and the UV absorbance signal. The bacteriophage content appears to be distributed uniformly throughout the defined pools, suggesting that bacteriophages interact through different hydrophobic forces with the column. Moreover, the high-intensity absorbance peak detected in the first elution step

(Pool 1) is not associated with a high bacteriophage concentration, when compared to the remaining steps. Additionally, even in elution steps with little to no absorbance signal, the bacteriophage concentration appears to be similar to steps with higher UV signals. Bacteriophages might not result in high UV absorbance responses, also as a result of their very low concentration in the pM range. The impurities content is also evenly distributed throughout all pools, with special attention to the overall low endotoxin levels (< 1000 EU/mL). The bacteriophage yield and impurities removals are represented in Table 15.

Table 15- Bacteriophage recovery and impurities removals for the multi-step-gradient elution Phenyl Sepharose FF chromatography of Process 2. * The genomic dsDNA removal in pools 1, 2, and 3 was not able to be determined due to the formation of secondary products. **** The genomic dsDNA removal in pool 4 considers the lowest possible threshold of the qPCR assay, according to a CP value > 35.00.

Pools	Elution buffer (%)	Bacteriophage recovery (%)	Protein removal (%)	dsDNA removal (%)	Genomic dsDNA removal (%)	Endotoxin removal (%)
1	70	19.5	96.1	95.2	-*	99.5
2	75	4.90	98.8	96.8		99.9
3	80	8.77	98.9	96.3		99.9
4	85	6.26	99.1	97.8	> 99.6**	99.9
5	100	8.90	98.4	99.6	98.2 ± 0.5	99.0

According to Table 15, the highest bacteriophage yield is present in pool 1, associated with the elution triggered at 70% of the elution buffer. Despite being the highest, it is still low compared to the single-step-gradient elution (90.7%). Across the board, impurities removals are efficient, as once again the endotoxin removal stands out as being optimal, even in the pool containing most bacteriophages. Total dsDNA and genomic dsDNA removals range from 95-100% which is much better than the single-step-gradient elution (85.9% and < 97.1%, respectively). Throughout pools 2-5, the bacteriophage yield is the lowest seen until now and is somewhat distributed evenly, as indicated in Table 14. A certain heterogenicity in the way T4 bacteriophages interact with the phenyl ring is present. For example, by interacting with the column via their tail or head, different hydrophobic strengths are at play, which affects the way these viral particles are eluted. As an alternative, some bacteriophages' tails could be stuck in the column's bead pores, which would result in different times of retention not associated with the presence or not of different hydrophobic strengths. To evaluate if the bulkiness of bacteriophages explains their uniform distribution observed in Table 15, monolith or membrane stationary phases could be used, with much higher pore sizes and a convective-flow transport not dependent on particle diffusion.

3.2.2.2.3. Process 3

The final process devised for this section looked to consolidate what was learned with the Phenyl Sepharose FF chromatography. As previously observed, the multi-step gradient approach results in high impurities removal rates, still with the bacteriophage yield left to be optimized. Processes 1 and 2 used 1.5 M ammonium sulfate in the equilibration buffer, which as stated previously, may be reduced up to 0.75 M maintaining the removal of impurities and even increasing the bacteriophage yield. Process 3 implements the referred reduced ammonium sulfate concentration with a downscaled five-step-gradient approach based on the previous one.

In Process 2, bacteriophages started to be collected at 70% of elution buffer. Afterward, 5% elution buffer steps were taken. Considering the new equilibration conditions present in Process 3, these percentages required tweaking. 70% of elution buffer indicates that 30% of equilibration buffer is running through the system. Considering the initial ammonium sulfate concentration, this percentage coincided with 0.45 M of the same salt. If the concentration of ammonium sulfate is reduced to 0.75 M in the equilibration buffer, the equivalent elution is obtained at 40% elution buffer (60% equilibration buffer). Therefore, to maintain the same mindset behind the described elution steps in Process 2, the initial % of elution buffer should be 40%. Overall, Process 3 includes an initial % of elution buffer of 35%, with subsequent elution steps of 50%, 65%, 80%, and 100% (0.488 M, 0.375 M, 0.263 M, 0.15 M, and 0.0 M of $(NH_4)_2SO_4$, correspondently). The lower initial % of elution buffer covered the possibility of bacteriophages eluting sooner than observed in Process 2, while the broad-interval subsequent elution buffer (%) steps aim at painting a complete-picture chromatogram.

The chromatogram illustrating the absorbance (mAU) and the percentage of elution buffer (%) along the time is represented in the Figure 21A, while the one showcasing the absorbance (mAU) and the conductivity (mS/cm) along the time is represented in Figure 21B.

The elution phase present in Figure 21 paints a similar picture when compared with Figure 20 of Process 2. Nonetheless, the intensity of the UV absorbance response in each elution step is smaller than the previous process, with pool 1 representing again the most intense signal from the remaining. Additionally, the downscaled Process 3 did not register the formation of any double absorbance peak. The detailed analysis in terms of content composition for the defined pools is represented in Table 16.

According to Table 16, pool 1, associated with the beginning of the elution phase, did not contain the greatest number of bacteriophages, despite presenting the highest UV absorbance response. Therefore, the detected UV signal is most likely associated with the dsDNA and proteins, which are highest concentrated in pool 1. Pools 2 and 3 appear to contain most bacteriophages, showcasing that the distribution of this product throughout all pools was not uniform as it occurred in Process 2. Additionally, the UV response appears to once again not be proportionate to the concentration of bacteriophages. dsDNA and protein concentrations are similar between both pools, with the latter containing a significantly higher endotoxin concentration, which is still low compared to other experiments. Positively, genomic dsDNA concentration is below the threshold detection in pools 2 and 3. Although not discussed so far, in other experiments, the Pierce™ chromogenic endotoxin assay had

presented results with high standard deviations, often in the same number magnitude. The multi-step-gradient elution schemes devised generally presented low standard deviations, and pools 2 and 3 of Process 3 were no exception, which is positive for reproducibility purposes. The bacteriophage yield and impurities removals for pools 2 and 3, as well as the combination of both, is displayed in Table 17.

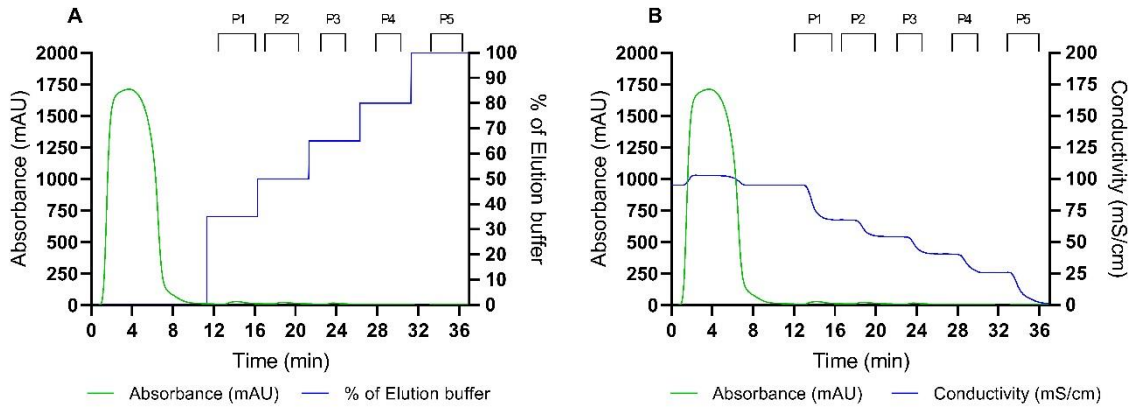

Figure 21- Multi-step-gradient elution Phenyl Sepharose FF chromatogram of Process 3. Absorbance (mAU) at 280 nm and % of elution buffer **(A)** or conductivity (mS/cm) **(B)** were measured throughout time (min) at 1 mL/min on the outlet stream of the chromatography column. The equilibration/washing buffer was 1.5 M $(NH4)_2SO_4$, 15 mM Tris-HCl pH 7.0 and the elution buffer was 15 mM Tris-HCl pH 7.0. Fractions of 1 mL were collected and various pools of fractions were considered for further analysis, which are represented in the upper section of the chromatogram by **PX** (with **X** being the pool number). The following pool composition was devised: **Pool 1** (Fraction 16 to 19), **Pool 2** (Fraction 21 to 24), **Pool 3** (Fraction 26 to 28), **Pool 4** (Fraction 31 to 32), and **Pool 5** (Fraction 36 to 38).

Table 16- Content composition for the multi-step-gradient elution Phenyl Sepharose FF chromatography of Process 3. For each defined pool, its respective volume (mL), % of the elution buffer, and bacteriophage (PFU/mL), protein (µg/mL), dsDNA (ng/mL), genomic dsDNA (ng/mL), and endotoxin (EU/mL) concentrations are represented. *****The genomic dsDNA concentration for pools 2 and 3 considers the lower threshold of the qPCR assay, according to a CP value > 35.00.

Pools	Volume (mL)	Elution buffer (%)	[Bacteriophage] (PFU/mL)	[Protein] (µg/mL)	[dsDNA] (ng/mL)	[Genomic dsDNA] (ng/mL)	[Endotoxin] (EU/mL)
Lysate	5.00	-	(3.70 ± 0.16)E+09	5077 ± 929	8117 ± 440	1199 ± 134	(8.17 ± 4.45)E+04
1	4.00	35	(6.75 ± 0.55)E+08	154 ± 38	475 ± 143	-	(1.68 ± 0.04)E+02
2	4.00	50	(2.15 ± 0.09)E+09	117 ± 21	454 ± 99	< 11.1*****	(4.71 ± 0.02)E+02
3	3.00	65	(1.47 ± 0.11)E+09	111 ± 15	411 ± 51		(1.03 ± 0.07)E+03
4	2.00	80	(4.30 ± 0.60)E+08	104 ± 21	126 ± 18	20.0	1.33E+03
5	3.00	100	7.40E+07	87.3 ± 11.3	37.0 ± 6.2	29.9 ± 8.2	9.42E+01

Table 17- Bacteriophage recovery and impurities removals for the multi-step-gradient elution Phenyl Sepharose FF chromatography of Process 3. * The genomic dsDNA removal considers the lowest possible threshold of the qPCR assay, according to a CP value > 35.00. The elution buffer (%) represented for the combination of pools 2 and 3 is an average considering the volume of each pool.

Pools	Elution buffer (%)	Bacteriophage recovery (%)	Protein removal (%)	dsDNA removal (%)	Genomic dsDNA removal (%)	Endotoxin removal (%)
2	50	46.4	98.2	95.5	> 99.3*****	99.5
3	65	23.8	98.7	97.0	> 99.4*****	99.2
2+3	56	70.2	96.8	92.5	> 98.7*****	98.8

The results represented in Table 17 come much closer to the initial goal set for this thesis section. When considering pool 2 alone, the removal of impurities, mainly endotoxins, and proteins, are high. dsDNA removal is much higher compared to the initial single-step-gradient elution (85.9%). Importantly, bacteriophage yield is the highest across all multi-step and linear gradient experiments, although still close to half of the single-step-gradient elution (90.7%). While pool 3 presents comparable impurities removals, it contains less bacteriophages and should not be considered alone. Overall, the combination of pools 2 and 3 results in a bacteriophage yield closer to the values observed in the single-step-gradient elution, with much higher impurities removals, mainly in terms of dsDNA (total and genomic) and endotoxins. Furthermore, the total endotoxin content is below 1000 EU/mL. The optimization stage performed in section 3.2.2.1 was beneficial for the development of Process 3. The decrease in ammonium sulfate concentration in the equilibration phase, combined with the tweaked elution steps, resulted in a purification process capable of improving the host impurities removals whilst maximizing bacteriophage yield.

3.2.2.3. SEC for buffer exchange

The final step in the DSP of biological products consists of a buffer exchange for formulation/storage, transportation purposes, or to stabilize the final product. Moreover, the high amount of salt used during the previously depicted chromatography stages mandates a final buffer exchange. Buffer exchange is usually performed via a diafiltration, as filtration processes attain high productivity and are easy to implement at a large scale. Nevertheless, the diafiltration of bacteriophage solutions with the use of small-scale centrifuge filters resulted in a reduced bacteriophage yield, not compatible with the industrial standards. To overcome this issue, SEC using a Superdex 200 Increase 10/300 GL resin was investigated for buffer exchange.

To test the efficiency of the Superdex 200 for buffer exchange, an initial single-step-gradient elution Phenyl Sepharose FF chromatography with 1.5 M ammonium sulfate in the equilibration buffer was performed. The resulting chromatogram and detailed content composition of the elution pool are represented in Figure A.6 and Table A.12 (Appendix). The bacteriophage yield, as well as the impurities removals for this chromatography step, are represented in Table 19, with results quite similar to those

previously observed in the initially tested conditions with this chromatography, except for a slightly lower bacteriophage yield (Table 9).

The use of SEC at this stage may also be interesting for the further removal of host impurities, primarily endotoxins. In their natural form, endotoxins aggregate into micelles that will not penetrate chromatography beads. Nonetheless, their dissociation into monomers could be attained by a sample pre-treatment with a surfactant, such as Tween 20, and EDTA. The combined use of Tween 20 with EDTA has the added edge of dissociating possible interactions of the endotoxins with bacteriophages through calcium-based bridges between surface proteins and the LPS phosphate group. Endotoxin monomers should penetrate more easily into the agarose beads, effectively resulting in a higher endotoxin removal.[114,115]

To evaluate the usefulness of Tween 20 and EDTA for these purposes, the presence or absence of this pre-treatment was tested in independent SEC runs. The associated chromatogram without or with the presence of a Tween 20 pre-treatment is represented in Figure 22.

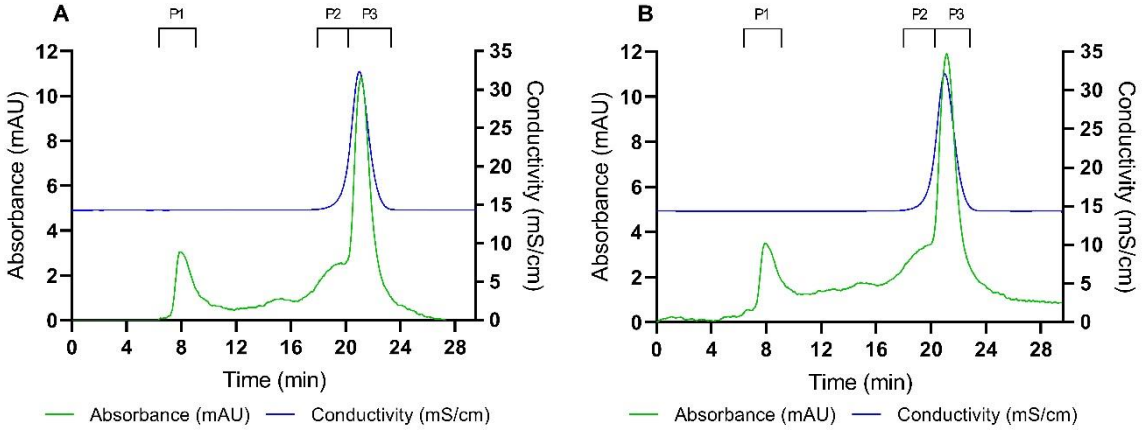

Figure 22- Chromatogram of the SEC without a Tween 20 pre-treatment (A) or with a Tween 20 pre-treatment (B). Conductivity (mS/cm^2) and absorbance (mAU) at 280 nm were measured throughout time (min) at 1 mL/min on the outlet stream of the chromatography column. The equilibration/washing buffer was PBS. Fractions of 1 mL were collected and various pools of fractions were considered for further analysis, which are represented in the upper section of the chromatogram by **PX** (with **X** being the pool number). The following pool composition was devised: **(A, B) Pool 1** (Fraction 9 to 11), **Pool 2** (Fraction 20 to 21), and **Pool 3** (**(A)** Fraction 22 to 25; **(B)** Fraction 22 to 24).

SEC differentiates itself from the remaining chromatography modes due to the absence of an elution step. Therefore, products are collected according to their ability to penetrate the chromatography beads. Bacteriophages, due to their large size when compared to the host impurities, are expected to be excluded from the beads and collected in the void volume with the lowest retention time. According to Figure 22, pool 1 is most likely associated with the bacteriophage fraction. In pools 2 and 3, an increase in conductivity, alongside absorbance, is observed. This might correspond to the detection of the host impurities and salts, e.g. These molecules penetrated the SEC beads and took longer to be collected (higher retention time) when compared to the bacteriophages which were excluded from the pores. Note that no apparent different stands out when comparing the presence or absence of a Tween 20 pre-treatment. The detailed content composition for the performed SEC runs is represented in Table 18.

Table 18- Content composition of the SEC without a Tween 20 pre-treatment and with a Tween 20 pre-treatment. For each defined pool, its respective volume (mL), and bacteriophage (PFU/mL), protein (µg/mL), dsDNA (ng/mL), genomic dsDNA (ng/mL), and endotoxin (EU/mL) concentrations are represented. ***** The bacteriophage concentration for pools 2 and 3 considers the lower threshold of performed DLPA. ****** The protein concentration for pool 1 considers the lower threshold of the performed BCA assay.

Pools	Volume (mL)	Bacteriophage concentration (PFU/mL)	Protein concentration (µg/mL)	dsDNA concentration (ng/mL)	Genomic dsDNA concentration (ng/mL)	Endotoxin concentration (EU/mL)
SEC without a Tween 20 pre-treatment						
1	3	(4.23 ± 0.69)E+08	< 0.100******	85.4 ± 5.0	35.3	(1.10 ± 0.07)E+03
2	2	< 3.00E+05*****	4.20	2.57 ± 0.67	-	-
3	4		10.5 ± 1.4	3.52	-	-
SEC with a Tween 20 pre-treatment						
1	3	(4.50 ± 0.90)E+08	< 0.100******	84.9 ± 9.0	43.6	(9.44 ± 1.30)E+02
2	2	< 3.00E+05*****	4.30 ± 3.90	1.57	-	(1.97 ± 0.009)E+03
3	3		24.3 ± 11.9	2.73 ± 0.91	-	(1.14 ± 0.15)E+02

Table 18 showcases what was previously predicted to occur with this type of chromatography. Pool 1 corresponds to the bacteriophage fraction, whereas pools 2 and 3 each contain a minimal bacteriophage concentration. The dsDNA concentration in pool 1 exceeds the one in pools 2 and 3, likely due to the large size of dsDNA molecules that prevents their penetration in the agarose beads. The opposite occurs with the protein concentration. In addition to most proteins being removed in the first chromatography step, the remaining ones are small enough to penetrate the agarose beads. A major setback in SEC is confirmed by the results in Table 18. Contrarily to the Phenyl Sepharose FF chromatography where most conditions maintained the initial bacteriophage concentration, or even increased it, SEC presents a high degree of product dilution. The bacteriophage concentration in pool 1 for both chromatography conditions is almost an order of magnitude below what was injected (3.63E+09 PFU/mL). Final concentrated bacteriophage samples are more beneficial for therapeutic use. Bacteriophage therapy is based on the administration of a dose with a defined number of viral particles (PFU). This corresponds to a certain volume of the final purified bacteriophage sample. More concentrated samples require the administration of lower volumes or allow for sample dilution before administration. Both routes lead to a reduced delivering of host impurities. The UF/DF use for final buffer exchange and storage is much more used than a SEC exactly because while it does not attain product dilution, it can even concentrate the final sample before diafiltration.

The detailed bacteriophage recovery and impurities removals for both chromatography conditions are represented in Table 19.

Table 19- Bacteriophage recovery and impurities removals for the initial HIC step, and for the SEC (Pool 1) without or with the presence of a Tween 20 pre-treatment, as well as the overall process. * The genomic dsDNA removal in HIC was not able to be determined due to the formation of secondary products. **** The SEC and overall genomic dsDNA removal were not calculated as the removal for the first chromatography step was not able to be determined due to the formation of secondary products. ***** The endotoxin content in SEC exceeded what was loaded onto this chromatography. ****** The overall endotoxin removal was considered equal to the removal during the initial HIC step.

Presence of a pre-treatment	Bacteriophage recovery (%)	Protein removal (%)	dsDNA removal (%)	Genomic dsDNA removal (%)	Endotoxin removal (%)
HIC					
-	83.0	97.7	87.6	-*	97.3
SEC					
No	69.9	94.9	50.5	-**	< 0%***
Yes	74.3	94.9	50.8		
Overall process					
No	58.1	99.9	93.9	-**	97.3****
Yes	61.7	99.9	93.9		97.3****

According to Table 19, a higher bacteriophage yield is attained when Tween 20 is applied before sample loading. The protein and dsDNA removals are equal or very similar between both conditions. Peculiarly, the endotoxin content in pool 1 for both SEC conditions exceeded what was loaded into the column, which should not be possible. The low reproducibility inherent to the endotoxin quantification kit (under the set experimental conditions) may be at the core of this issue. The use of SEC combined with Tween 20 and EDTA for the complete removal of endotoxins, after a previous high-removal step, was not able to be studied.

Note that the determined removals for SEC are associated only with the injected sample. This represents a small fraction of what was recovered with the Phenyl Sepharose FF chromatography. To fully evaluate the efficiency of SEC, the determination of the same percentages must be done considering that the entirety of the elution pool of the previous chromatography is loaded onto this SEC. The need to perform separate runs to process such a small volume as the one obtained in the first chromatography step (4 mL) represents another major setback of SEC. According to the volume injected in the SEC column, 8 SEC runs would be needed to process all the volume obtained in the HIC elution pool. It should be noted that the reduced volume of loading used in SEC (2% of the column volume) was used according to the manufacturer's instructions. The reduced productivity in SEC is incompatible

with the modern industrial needs for the purification of biological products. UF/DF operations once again come on top when it comes to this parameter due to their versatility and high productivity. The overall process analysis in Table 19 corresponds to the SEC processing of the total volume obtained in the first chromatography step. Here, the pre-treatment with Tween 20 appears to be the best choice in terms of bacteriophage recovery, although it is similar to the one obtained in the absence of the same treatment. It is important to notice that the endotoxin removal was considered equal to the first chromatography step. All-in-all, the main purpose of the use of SEC was attained, which was appropriate buffer exchange and removal of salt derived from the HIC. The registered bacteriophage dilution was expected to occur, while the additional removal of impurities was efficient, mainly in terms of proteins and dsDNA.

3.2.3. Capto™ Core 700 chromatography

Capto™ Core 700 represents a type of multi-modal chromatography based on core bead technology. Its functionalized inner ligand allows the user to explore the binding of small impurities by hydrophobic and ionic interactions while excluding products with a size higher than 700 kDa. The versatility this chromatography offers is based on the user's choice of either exploring hydrophobic or ionic interactions between its product and the ligand. Little to no information has been reported regarding the use of Capto™ Core 700 for bacteriophage purification. This thesis section will be aimed at exploring this chromatography and assessing if its theoretical effectiveness proves to be true.

An initial optimization stage regarding equilibration/elution chromatography conditions was performed, based on the work of Trabelsi *et al*.[135]. Octyl-amine is the ligand used in this chromatography and can allow both hydrophobic and ionic interactions with the molecules. Nonetheless, typically established chromatography conditions for each type of interaction contradict each other. To enhance hydrophobic interactions, one must increase the amount of salt present in the equilibration/washing buffer. However, this increase in ionic strength displaces any molecule bound to the column through ionic interactions, due to the competition between the salt and the product to the charged group of the ligand. Overall, the selection of the equilibration buffer for Capto™ Core 700 required optimization for the target product, which in this case are the impurities present in the lysate. For the assumed initial chromatography conditions (section 2.6.4, Methods), octyl-amine is positively charged, and thus may bind negatively-charged impurities, while still promoting hydrophobic interactions with the addition of salt. The chromatogram associated with the described chromatography condition is represented in Figure 23.

Figure 23 depicts a chromatogram alike what has been seen in PBC or HIC, with a small absorbance peak upon elution triggering, most likely associated with the detachment of the bound molecules in the inner core of the agarose beads. While the increase of ionic strength in the elution phase leads do the desorption of molecules bound by ionic interactions, it may further strengthen hydrophobic interactions between the remaining molecules. This call for the critical necessity of thoroughly washing the column at the end of each run. As bacteriophages are expected to be excluded from the beads, they would be collected in the flow-through peak (Pools 1+2). To investigate if this was the case, an analysis of the content composition of each defined pool was performed and represented in Table 20.

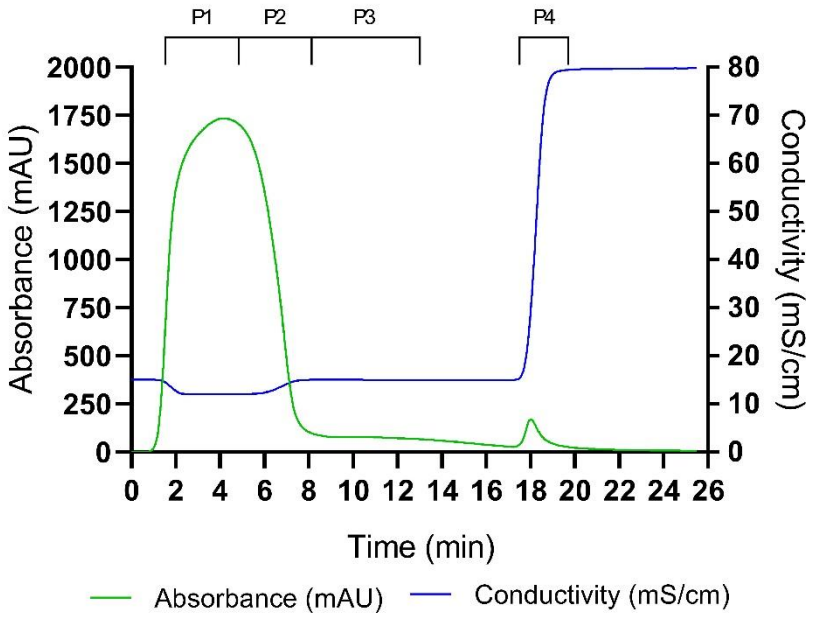

Figure 23- Capto™ Core 700 chromatogram using the initial chromatography conditions. Absorbance (mAU) at 280 nm and conductivity (mS/cm) were measured throughout time (min) at 1 mL/min on the outlet stream of the chromatography column. The equilibration/washing buffer was 15 mM Tris-HCl, 150 mM NaCl pH 7.5, and the elution buffer was 15 mM Tris-HCl, 1 M NaCl pH 7.5. Fractions of 1 mL were collected and various pools of fractions were considered for further analysis, which are represented in the upper section of the chromatogram by **PX** (with **X** being the pool number). The following pool composition was devised: **Pool 1** (Fraction 3 to 6), **Pool 2** (Fraction 7 to 10), **Pool 3** (Fraction 11 to 16), and **Pool 4** (Fraction 19 to 20). The flow-through peak was divided into Pools 1 and 2, while the elution peak is Pool 4.

Table 20- Content composition for pools 1-4 of the initial condition in Capto™ Core 700 chromatography. For each defined pool, its respective volume (mL), and bacteriophage (PFU/mL), protein (µg/mL), dsDNA (ng/mL), genomic dsDNA (ng/mL), and endotoxin (EU/mL) concentrations are represented.

Pools	Volume (mL)	Bacteriophage concentration (PFU/mL)	Protein concentration (µg/mL)	dsDNA concentration (ng/mL)	Genomic dsDNA concentration (ng/mL)	Endotoxin concentration (EU/mL)
Lysate	5	(4.03 ± 0.37)E+09	4189 ± 394	6194 ± 343	308 ± 5	(6.13 ± 3.45)E+04
1	4	(3.25 ± 0.45)E+09	3164 ± 271	4974 ± 352	381 ± 57	8.24E+03
2	4	(3.80 ± 0.85)E+08	1357 ± 154	1525 ± 70	93.2	1.56E+04
3	6	(2.07 ± 0.09)E+06	80.5 ± 5.1	16.5 ± 1.5	-	-
4	2	(1.83 ± 0.04)E+06	408 ± 35	648 ± 50	32.9	3.13E+03

According to Table 20, most bacteriophages were collected in the first part of the flow-through (Pool 1), while a minimal fraction was detected upon elution. Nonetheless, a large number of impurities were collected alongside the bacteriophages. In SEC, it has been seen that dsDNA molecules were able to

not penetrate the agarose beads and co-elute with the bacteriophages in the void volume. As the Capto™ Core 700 chromatography has a considerably lower size exclusion limit, it comes as no surprise that even more dsDNA molecules are excluded from the beads. Contrarily to SEC, proteins also appear to heavily not penetrate the agarose beads and are instead immediately collected upon sample loading. Endotoxins follow the same mindset, indicating that most of these molecules are aggregated into structures with a MW higher than 1000 kDa. Interestingly, most endotoxins are collected in the second half of the flow-through peak, indicating a higher retention time compared to the first half of the same peak. Endotoxin molecules that penetrate the agarose beads should interact via ionic and hydrophobic interactions with the column ligand and be collected in the elution phase. The same applies to dsDNA molecules or proteins that penetrate the resin matrix.

The detailed bacteriophage recovery and impurity removals were represented in Table 21.

Table 21- Bacteriophage recovery and impurities removal of the initial condition in Capto™ Core 700 chromatography.

	Bacteriophage recovery (%)	Protein removal (%)	dsDNA removal (%)	Genomic dsDNA removal (%)	Endotoxin removal (%)
Flowthrough Pool (P1)	64.5	37.4	35.8	1.18	89.2

The results displayed in Table 21 represent the poor performance already predicted in Table 20 regarding the Capto™ Core 700 chromatography. It should be noted that there was no previous purification step as performed with the SEC polishing step. In this case, the sample loaded into the column was the lysate and not a HIC elution pool. The Capto™ Core 700 resins were designed for polishing application and not for the initial recovery as used in this experiment, explaining the weak performance of this resin. Indeed, impurities failed to be removed, primarily proteins and dsDNA. The endotoxin removal, although seemingly high, still results in a final endotoxin content higher than 1000 EU/mL. The genomic dsDNA removal was minimal compared to the total dsDNA. This indicates that most dsDNA removed is viral, while the genomic material heavily co-eluted with the bacteriophages. Considering that most dsDNA molecules are intact, the depicted disparity may be associated with the much larger size of the genomic dsDNA compared to the viral dsDNA. The latter more easily penetrates the agarose pores, while the former is immediately collected.

3.2.3.1. Presence of salt in the equilibration buffer and Denarase® treatment

With the previously gathered results in Capto™ Core 700 chromatography, a few optimization steps were carried out, looking mainly to improve impurity removal without any previous chromatography step. Firstly, the influence of salt in the relationship between hydrophobic and ionic interactions was tested, by including or not NaCl in the equilibration buffer. Beforehand, the bacteriophage lysate was both treated with Denarase® and Tween 20. The enzymatic treatment was aimed at digesting the large dsDNA molecule into smaller duplexes not concerning for therapeutic use. Tween 20 was again used

to dissociate endotoxin aggregates into monomers that can penetrate the resin matrix and attach to the column ligand.

The treatment with Denarase® led to a 97.0% total dsDNA removal in the bacteriophage lysate. The chromatograms associated with the presence or absence of salt in the equilibration buffer, considering the previously treated bacteriophage lysate with Denarase® and Tween 20, are represented in Figure 24.

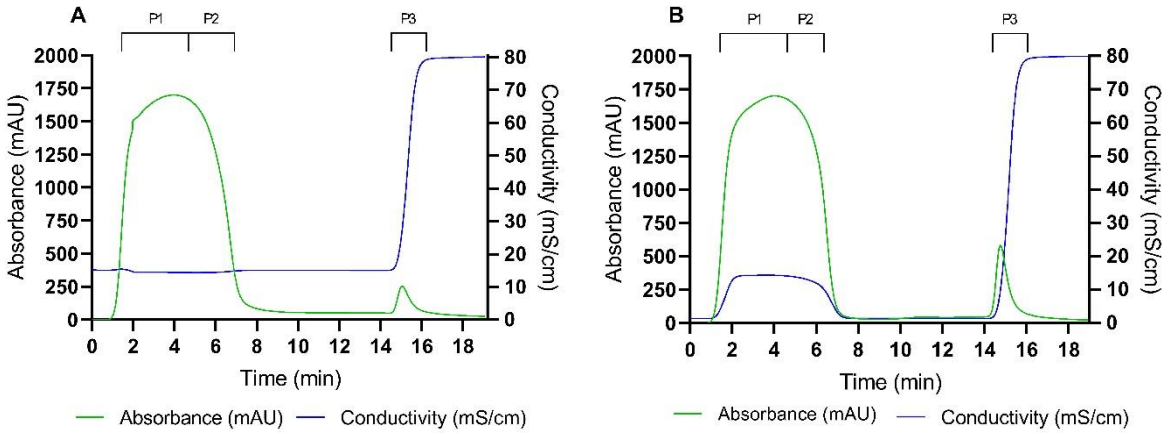

Figure 24- Capto™ Core 700 chromatogram with NaCl (A) or without NaCl (B) in the equilibration buffer. Absorbance (mAU) at 280 nm and conductivity (mS/cm) were measured throughout time (min) at 1 mL/min on the outlet stream of the chromatography column. **(A)** The equilibration/washing buffer was 15 mM Tris-HCl, 150 mM NaCl pH 7.5 and the elution buffer was 15 mM Tris-HCl, 1 M NaCl pH 7.5. **(B)** The equilibration/washing buffer was 15 mM Tris-HCl pH 7.5 and the elution buffer was 15 mM Tris-HCl, 1 M NaCl pH 7.5. Fractions of 1 mL were collected and various pools of fractions were considered for further analysis, which are represented in the upper section of the chromatogram by **PX** (with **X** being the pool number). The following pool composition was devised: **Pool 1** (Fraction 2 to 8), **Pool 2** ((A) Fraction 9 to 11; (B) Fraction 9 to 10), and **Pool 3** (Fraction 18 to 19). The flow-through peak was divided into Pools 1 and 2, while the elution peak is Pool 3.

Figure 24 is similar to the previous chromatogram (Figure 23), with the main difference being in the UV absorbance response of the elution peak (Pool 3). This is the largest when removing the salt from the equilibration buffer. Possibly, the presence of salt in the equilibration buffer prevents the retention of the molecules that penetrate the agarose beads and establish ionic interactions with the ligand. The removal of NaCl permits the same molecules to establish these interactions without being immediately eluted. The larger UV response during the elution phase corresponds to a higher number of molecules eluting. Therefore, the establishment of ionic interactions appears to be fundamental for the successful removal of impurities, considering a negative-mode chromatography. The detailed content composition for each chromatography is represented in Table A.13 (Appendix). The bacteriophage recovery, and the impurities removals, for each chromatography, are represented in Table 22, considering the first part of the flow-through peak (Pool 1).

The first thing that stands out in Table 22 is the bacteriophage recovery above 100% (probably due to the variability of the DLPA), and the minimal protein removal in the chromatography with NaCl in the equilibration buffer. These results greatly stand apart from the previous chromatography, which made use of the same buffer conditions except for the pre-treatment of the bacteriophage lysate. The endotoxin removal increased for both buffer conditions, mainly when supplementing the equilibration

buffer with salt. This confirms the beneficial effect of Tween 20 and EDTA in dissociating endotoxin aggregates and easing their penetration into the agarose beads. The total dsDNA removal increased for both buffer conditions. The reduced size of the remaining dsDNA fragments loaded into the chromatography might explain these results, as they more easily penetrate the beads and interact with the ligand.

Table 22- Bacteriophage recovery and impurities removals in pool 1 of the Capto™ Core 700 chromatography with NaCl or without NaCl in the equilibration buffer. The composition of the equilibration buffer was 15 mM Tris-HCl, 150 mM NaCl pH 7.5, and 15 mM Tris-HCl, 150 mM NaCl pH 7.5. ***** The genomic dsDNA content was not evaluated after Denarase® treatment, thus its injected content onto the chromatography was unknown. For this reason, the genomic dsDNA removal was not determined.

Sample	Bacteriophage recovery (%)	Protein removal (%)	dsDNA removal (%)	Genomic dsDNA removal (%)	Endotoxin removal (%)
Pool 1 with NaCl	115	1.07	42.6	-*	97.1
Pool 1 without NaCl	65.2	16.0	58.0		91.7

The most interesting aspect of Table 22 is the disparity of the bacteriophage yield and impurities removals between the tested chromatography conditions. When analyzing Figure 24, it was predicted that the removal of salt from the equilibration buffer increased the binding of impurities during the equilibration phase. This increase would result in better impurities removals. The protein and dsDNA removals are higher when NaCl is removed from the equilibration buffer. However, the opposite occurs for bacteriophages and endotoxins. The latter may be explained based on hydrophobic interactions and considering most endotoxins are not aggregated due to the Tween 20 treatment. Endotoxins may establish hydrophobic interactions between the lipid A and the octyl chain of the column ligand. If salt is added during the equilibration phase, these interactions are enhanced, resulting in higher column binding. Consequently, the endotoxin removal increases, as fewer molecules are collected during the loading phase. When removing the salt from the equilibration buffer, these interactions are no longer enhanced. Therefore, fewer endotoxins bind to the column ligand, increasing their collection during loading and decreasing the endotoxin removal.

The difference in bacteriophage yield is a bit trickier to explain as bacteriophages are not expected to interact with the column ligand, being collected in the void volume. As a result, the different buffer compositions should not affect bacteriophage recovery in the first half of the flow-through peak. The bacteriophage yield when salt was added to the equilibration phase is abnormal, mainly considering that with the same chromatography conditions, a value of 64.5% (Table 21) was attained. Note that the presence of the bacteriophage lysate pre-treatment might affect this chromatography, but not to the

observed extent. With the data registered in Table 21, a much closer result was obtained when compared with the absence of salt in Table 22. All-in-all, replicas of this study should be made in an attempt to explain the observed results and understand if they could be considered outliers.

3.2.3.2. Conjugation between PBC and Capto™ Core 700 chromatography

The main issue that stands out with the direct loading of bacteriophage lysate onto a Capto™ Core 700 chromatography is the low impurity removal for both proteins and dsDNA. A pre-treatment with Denarase® deals with the latter issue, however a high protein content in the resulting bacteriophage sample is still problematic. Moreover, the use of an enzymatic step at a large scale is not ideal as it implies a great cost. With this in mind, the next devised experiment conjugated the use of PBC with Capto™ Core 700. In this case, the enhancement of hydrophobic interactions in PBC was utilized, with the same chromatographic conditions discussed before (section 3.2.1.3). To gather enough sample volume to load onto Capto™ Core 700, three PBC replicas were performed. For the Capto™ Core 700 chromatography, an equilibration buffer containing 150 mM NaCl was selected. The resulting chromatograms are represented in the Figure A.7 (Appendix). The detailed content composition for each elution pool (Pool 1) for all three PBC replicas is also represented in Table A.14 (Appendix). The resulting elution pools of each PBC replica were pooled together and injected into the Capto™ Core 700 chromatography. The resulting chromatogram is represented in Figure 25.

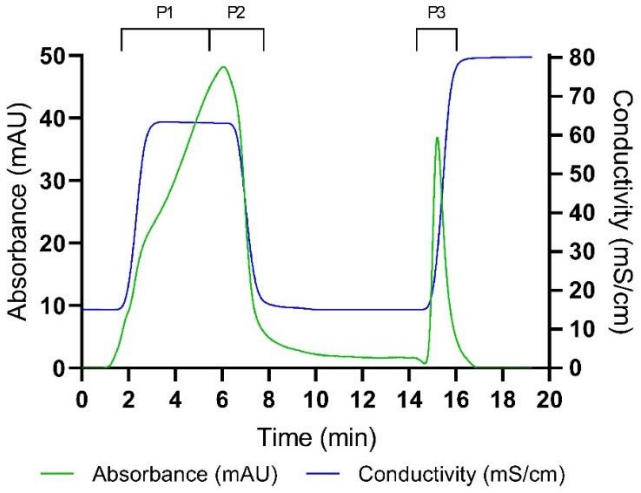

Figure 25- Capto™ Core 700 chromatogram following PBC with enhanced hydrophobic interactions. Absorbance (mAU) at 280 nm and conductivity (mS/cm) were measured throughout time (min) at 1 mL/min on the outlet stream of the chromatography column. The equilibration/washing buffer was 15 mM Tris-HCl, 150 mM NaCl pH 7.5, and the elution buffer was 15 mM Tris-HCl, 1 M NaCl pH 7.5. Fractions of 1 mL were collected and various pools of fractions were considered for further analysis, which are represented in the upper section of the chromatogram by **PX** (with **X** being the pool number). The following pool composition was devised: **Pool 1** (Fraction 3 to 6), **Pool 2** (Fraction 7 to 10), and **Pool 3** (Fraction 18 to 19). The flow-through peak was divided into Pools 1 and 2, while the elution peak is Pool 3.

Figure 25 showcases an overall decrease in absorbance values, seeing that the loaded sample had little protein and dsDNA content. The conductivity spike upon sample injection is associated with a high salt concentration resultant from the previous PBC, which used ammonium sulfate in its equilibration buffer. The detailed content composition of each defined pool is represented in Table 23.

Table 23- Content composition for the PBC pool feed and pools 1-3 of the Capto™ Core 700 chromatography following PBC with enhanced hydrophobic interactions. For each defined pool and the feed, its respective volume (mL), and bacteriophage (PFU/mL), protein (µg/mL), dsDNA (ng/mL), genomic dsDNA (ng/mL), and endotoxin (EU/mL) concentrations are represented

Pools	Volume (mL)	Bacteriophage concentration (PFU/mL)	Protein concentration (µg/mL)	dsDNA concentration (ng/mL)	Genomic dsDNA concentration (ng/mL)	Endotoxin concentration (EU/mL)
Feed	5	(1.87 ± 0.33)E+09	28.9 ± 8.2	280 ± 62	12.2 ± 5.2	(1.08 ± 0.14)E+03
1	4	(2.08 ± 0.31)E+09	16.0 ± 6.7	213 ± 65	-	(1.85 ± 0.07)E+03
2	3	(6.80 ± 0.92)E+08	37.8 ± 15.2	127 ± 22	3.26	(1.97 ± 0.010)+03
3	2	9.50E+05	13.8	201 ± 70	2.71	(1.14 ± 0.15)E+02

In a similar manner to the previous chromatography studies with this resin, most bacteriophages appeared to be collected in the first half of the flow-through peak. Table 24 summarizes the bacteriophage recovery and the impurities removals for each chromatography, as well as for the overall process yield.

Table 24- Bacteriophage recovery and impurities removals of the enhanced hydrophobic interactions in PBC, the following Capto™ Core 700 chromatography, and the overall process. * The genomic dsDNA removal in Capto™ Core 700 chromatography was not able to be determined (due to the formation of secondary products), thus the overall genomic dsDNA removal was considered equal to the removal during the first step. **** The endotoxin content in Capto™ Core 700 chromatography exceeded what was loaded onto this chromatography, thus the overall endotoxin removal rate was considered equal to the removal during the first step.

Process	Bacteriophage recovery (%)	Protein removal (%)	dsDNA removal (%)	Genomic dsDNA removal (%)	Endotoxin removal (%)
Phenyl boronate chromatography	68.4 ± 6.7	98.8 ± 0.1	94.5 ± 0.4	96.8 ± 1.4	98.0 ± 0.2
Capto™ Core 700 chromatography	88.8	55.7	37.0	-*	< 0%**
Overall	67.0	99.7	96.3	96.8 ± 1.4	98.0 ± 0.2

When analyzing Table 24, it is possible to observe reproducible results between the previously performed PBC with enhanced hydrophobic interactions and the three replicas executed for this experiment's purpose. The high protein and dsDNA removals in PBC are beneficial for the subsequent

Capto™ Core 700 chromatography, which as previously observed, displays low removals for both impurities. The dsDNA removal in Capto™ Core 700 is close to what was seen in the initially tested chromatography conditions (Table 21), while the bacteriophage yield (88.8% vs 64.5%) and protein removal (55.7% vs 37.4%) are higher. It is important to understand that the composition of the loaded sample in a chromatography is a critical factor in its performance. A chromatography with a loaded crude sample presents different recoveries compared to a chromatography with a loaded partially purified sample. A peculiar finding in the Capto™ Core 700 chromatography results is the endotoxin removal, which was deemed to be lower than 0, as the endotoxin content recovered exceeded what was loaded into the column. A similar situation occurred in section 3.2.2.3, with the use of a SEC following a previous high-endotoxin-removal chromatography step. The disparity in results observed in both cases mas be associated with the reproducibility issues inherent to the endotoxin quantification kit, under the set non-ideal experimental conditions. Alternatively, an endotoxin contamination could be at the core of this issue. If the resin or the chromatography buffers utilized were contaminated by endotoxins, its content collected at the end of the chromatography run could be higher than was what loaded.

All-in-all, the use of Capto™ Core 700 chromatography as a second purification step brought little to no benefits compared to the sole use of PBC. The dsDNA and protein removals were low and did not greatly alter the final concentration values of these impurities. While the endotoxin and genomic dsDNA removals were not able to be determined, the loaded content of these impurities was already reduced. Although the bacteriophage yield was high, the lost virus's fraction was not compensated by a high removal of any other impurity. Capto™ Core 700 chromatography most likely works better as a polishing step in the DSP of viruses than in their intermediate purification as the direct loading of a clarified bacteriophage lysate worked poorly (Table 21). Processed samples with a previous purification step (Table 24) are also not efficiently purified with this chromatography.

3.3. Product specifications in a phage therapy context

Throughout the developed experimental work in this thesis, many purification alternatives for the T4 bacteriophage were presented. One of the main aims of this work was to devise a DSP scheme that was able to efficiently remove host impurities, compelling common therapeutic practice, whilst maintaining the bacteriophage yield. Different chromatography operations were discussed, compared with each other, and deemed one better than the other. To finish this thesis work, a more theoretical and hypothetical approach will be taken. The best experimental conditions will be put against each other if a bacteriophage therapy with the resulting bacteriophage was envisioned. It is important to notice that most of the acquired samples would need further processing, for formulation purposes or buffer exchange. Nonetheless, alongside the aim of this section, only a simple bacteriophage therapy prediction was looked to be done.

One of the initially set criteria was that a bacteriophage therapy for case reports or clinical trials was to be done. Therefore, animal models were not considered. Secondly, it is important to notice that most case studies utilize bacteriophage cocktails due to their broad and enhanced efficacy. These cocktails are often not characterized in terms of composition and contain bacteriophages with different

concentrations. The first challenge was to gather data regarding clinical experience with bacteriophage treatments. Many parameters are described for each case report/clinical trial, but the most important ones for this work were the bacteriophage dose and the number of doses in the treatment. Two examples regarding the clinical use of bacteriophages and controlled clinical trials are represented in Table 25. It should be noted that no examples utilizing the T4 bacteriophage were found.

Table 25- Case studies and clinical trials related to bacteriophage therapy.

Type of study	Bacterial infection	Bacteriophage dose (PFU)	Number of doses
Case report (Khawaldeh *et al*.[136])	*Pseudomonas aeruginosa*	2.0×10^7	20
Clinical trial (Rhoads *et al*.[126])	*Pseudomonas aeruginosa*, *Staphylococcus aureus*, and *E. coli*	1.0×10^9	12

Although Table 25 includes only a few examples of the current paradigm surrounding bacteriophage therapy, it paints an appropriate picture regarding the common bacteriophage doses and bacterial infections targeted. In combination with this information, it is also crucial to keep in mind the acceptance criteria present in bacteriophage therapy. Unfortunately, no standardized host impurities parameters have been made public for this purpose. Most of the available clinical trials or case reports do not fully disclose the characterization of their bacteriophage solution, mainly when it comes to host impurities. What is known for endotoxins is that the acceptable content for IV administration is 5 EU/kg/h. Considering that the average human adult has between 60-80 kg, this would translate into about 300-400 EU/h of acceptable administration. João *et al*.[70] considered an appropriate bacterial DNA threshold of 0.01 µg per dose. No indication for IV treatment was done. Although the authors do not include bacteriophage DNA, it is possible to consider both equal when it comes to toxicity levels due to their identical double-strand nature. In the paper published by Rhoads *et al*.[126], a rare example of the partial characterization of the bacteriophage cocktail used in a Phase I clinical trial is represented. The administered content in terms of host impurities for each participant is represented in Table 26. Note that an IV administration of 200 mL/h was done, with a final solution of 50 mL (4 mL bacteriophage cocktail + 46 mL sterile saline).

Table 26- Content characterization of the bacteriophage cocktail administered to treat venous leg ulcers in a Phase I clinical trial. [126] The administered content was determined by knowing the concentration of each host impurity in the product, alongside the injected volume.

Specification	Administered content
DNA	0.4 µg
Protein	400 µg
LPS	4000 EU

According to Table 26, the delivered endotoxin number was high as its concentration in the bacteriophage cocktail was 1000 EU/mL. No safety concerns were detected among the test group. The IV treatment also appears to allow for a higher DNA mass to be administered to the patient, compared to the one presented by João *et al*.[70].

The next step was to select the most favorable chromatography conditions explored in this thesis and then to compare them between each other and the acceptance criteria in Table 26. The summary of the processes in terms of contents was represented in Table 27. To further ease the discussion between chromatography operations, a number (1-4) was given to each selected process.

Table 27- Optimal selected chromatography processes (1-4) for the purification of the T4 bacteriophage. The bacteriophage (PFU/mL), protein (µg/mL), dsDNA (ng/mL), and endotoxin (EU/mL) concentrations are represented.

Chromatography process	Process number	Bacteriophage concentration (PFU/mL)	Protein concentration (µg/mL)	dsDNA concentration (ng/mL)	Endotoxin concentration (EU/mL)
PBC with enhanced hydrophobic interactions (Pool 2)	1	1.58×10^9	7.12×10^1	3.00×10^2	7.05×10^2
HIC with 1.0 M ammonium sulfate	2	4.43×10^9	2.01×10^2	9.84×10^2	3.48×10^3
Process 3 of HIC (Pools 2 + 3)	3	1.86×10^9	1.14×10^2	4.36×10^2	7.11×10^2
Process 3 of HIC (Pool 2)	4	2.15×10^9	1.17×10^2	4.54×10^2	4.71×10^2

Knowing the common bacteriophage dosage utilized in human therapy (Table 25), it is possible to predict the amount of host impurities each of the chromatography processes in Table 27 would carry if administered. The described comparison is represented in Table 28, in terms of host impurity masses and sample volume to be administered.

From the selected chromatography processes in Table 27, the absence of the single-step-gradient elution HIC with 1.5 M ammonium sulfate in the equilibration buffer could come as a surprise. The reason behind this choice was the high endotoxin content to be administered (38.4 EU in the case report and 1.92×10^3 EU in the clinical trial), compared to the remaining processes in Table 28. This example portrays that the ideal solution for the presented hypothesis is not the one with the highest product recovery. Although a 90.7% bacteriophage yield was registered in this chromatography, the relatively low removal of impurities prevented this condition to be further selected. The difference in percentage regarding other HIC conditions, such as the ones varying the ammonium sulfate concentration, was

small but significant enough to imply a higher administration of host impurities in a to-be therapeutic product.

Table 28- Bacteriophage therapy performance prediction of each selected chromatography process (1-4) for a case report and a clinical trial. The bacteriophage dose for the case report or the clinical trial is represented in PFU. The therapy performance for each chromatography is composed by the volume to be administered (µL), protein mass (µg), dsDNA mass (µg), and endotoxin number (EU).

Chromatography process	Volume do be administered (µL)	Protein mass (µg)	dsDNA mass (µg)	Endotoxin number (EU)
Case report (Bacteriophage dose of 2.0×10^7 PFU)				
1	12.7	0.901	3.80×10^{-3}	8.92
2	4.51	0.901	4.44×10^{-3}	15.7
3	10.8	1.23	4.68×10^{-3}	7.64
4	9.30	1.09	4.22×10^{-3}	4.38
Clinical trial (Bacteriophage dose of 1.0×10^9 PFU)				
1	633	45.1	0.190	4.46×10^2
2	226	45.4	0.222	7.85×10^2
3	538	61.6	0.234	3.82×10^2
4	465	54.4	0.211	2.19×10^2

Either for the case report or the clinical trial predictions, no process would result in an endotoxin number higher than 1000 EU. The same can be said for the protein and DNA contents, which would never surpass 400 µg and 0.4 µg. According to the criteria set by João *et al*.[70], no process would be viable for the clinical trial as the DNA dose would be higher than 0.01 µg. Only for the case report would any process be viable. Selecting the best process is a complex task as many parameters may be considered. As for the clinical trial, all processes are viable according to Rhoads *et al*.[126]. Possibly, the one requiring the least amount of volume would be best (Process 2), mainly if numerous doses were to be administered. This is associated with the fact that Process 2 presents the highest bacteriophage concentration, and thus requires the least volume to meet the criteria present either in the case report or the clinical trial. If endotoxin toxicity would be a concern, Process 4 is the safest choice. In terms of DNA and proteins, all processes present similar doses. One interesting aspect present in Table 28 is that the final multi-step-gradient HIC is more efficient if only pool 2 is considered, and not the combination of pools 2 and 3. Process 4 presents less impurities delivered across the board, as well as a reduced volume to be administered. The same situation was observed with the enhanced hydrophobic

interactions PBC, where the combination of pools 2 and 3 was detrimental compared to the sole presence of pool 2 (data not shown). In both cases, the pooling together of fractions for the increased recovery of bacteriophages does not compensate for the consequent recovery of host impurities.

All-in-all, a more concentrated initial bacteriophage lysate would require a lesser volume to be administered, reducing the number of impurities delivered. Additionally, some case reports and clinical trials utilize bacteriophage doses higher than the ones present in this work, thus rendering the processes in Table 28 inadequate. An appropriate limit appears to be at 10^9 PFU dose, while any of the processes work efficiently for lower bacteriophage doses. To finalize, it is critical to understand that these processes were not finished from a therapeutic point of view. Although presenting adequate impurities values, further DSP in terms of sterilization and/or formulation could change the bacteriophage titer. More importantly, an efficient method to remove the salt present in the final bacteriophage samples would have to be addressed.

4. Conclusion and future prospects

Bacteriophages are currently viewed as efficient alternatives to antibiotics in the everlasting fight against antibiotic-resistant bacteria. What prevents these viral particles from overtaking the industry is a standardized, efficient, downstream processing scheme, which contemplates all host impurities. The traditional CsCl density gradient ultracentrifugation is not capable of answering the modern industrial standards for the purification of bacteriophages due to its low productivity and high price.

Several novel alternative chromatography modes were tested for the purification of T4 bacteriophages. To understand how the T4 bacteriophages were interacting with the Phenyl Boronate Chromatography (PBC) column, various chromatography conditions were tested. The hampering of the *cis*-diol esterification and charge-transfer interactions in PBC were found most likely not to be responsible for the adsorption of T4 bacteriophages to a PBC column. On the other hand, the adsorption of bacteriophages by hydrophobic interactions between surface viral proteins and the aminophenyl boronic acid was found to be successful. The enhancement of these interactions with ammonium sulfate leads to a bacteriophage yield of 54.5% and a removal of proteins, dsDNA, and endotoxins of 94.9%, 95.8%, and 98.1%, respectively. The establishment of hydrophobic interactions was believed to be based on tail protein complexes such as the cell-puncturing device, the outer tail sheath, and the bacteriophage whisker fibers. The PBC data motivated the use a Hydrophobic Interaction Chromatography (HIC) for the purification of T4 bacteriophages, which required extensive optimization. Various ammonium sulfate concentrations in the equilibration/washing buffer were tested with a single-step-gradient elution. With 0.75 M, the highest bacteriophage recovery was attained (93.0%), alongside a removal of proteins, dsDNA, and endotoxins of 98.3%, 88.3%, and 93.3%, respectively. It was found that a decrease in salt concentration in the equilibration buffer decreased the enhancement of hydrophobic interactions, but also lead to an increase in the number of available ligands that could benefit bacteriophage recovery. Based on an initial linear gradient HIC, multi-step gradients were devised to improve impurity removal whilst maintaining a high bacteriophage yield. The best process used 0.75 M ammonium sulfate in the equilibration buffer and attained a bacteriophage recovery of 70.2%, with a removal of proteins, dsDNA, and endotoxins of 96.8%, 92.5%, and 98.8%, respectively. From the beginning to the end of this work, host impurities and the imperative need for their quantification were emphasized. Many available papers discuss alternative bacteriophage purification techniques, however, almost none fully address this issue. In this work, the quantification of the host impurity content at each chromatography step was key to understand the best possible choice for bacteriophage purification. With this, PBC and HIC appeared to be unrecognized crucial tools for the purification of T4 bacteriophages.

Many key points in this work required further studying. Firstly, the multi-step gradient HIC Process 3 could be further improved if pools 2 and 3 were to be combined in a single elution step. This may represent an additional alternative, although, in the bacteriophage therapy prediction, the sole use of pool 2 was concluded to be best. As discussed thoroughly, HIC requires extensive optimization that was far from being complete in this work. It would be narrow-minded to assume that the use of phenyl as the column ligand and ammonium sulfate as the equilibration salt are the best choices. Alternative ligands should be tested, such as the linear chain alkaline ligands octyl or butyl. Although ammonium sulfate is

generally seen as the best salt for HIC, other alternatives could be better for the product in hand. The use of citrate or ammonium phosphate should be tested. One of the main reasons preventing the industrial implementation of HIC is the high salt concentration needed, both economically and environmentally concerning. No efficient technique was presented for the removal of salt from the final bacteriophage samples. While SEC was already known to be suboptimal for buffer exchange, diafiltration surprisingly resulted in a great loss of bacteriophages. The use of UF/DF operations in an industrial setting is inevitable. The reason why this operation is detrimental to the T4 bacteriophage titer must be investigated. Large-scale processes were suggested to increase this titer. However, the material of the diafiltration membrane may also be at the core of the problem, and thus other materials could be researched. All-in-all, one of the main points that could be explored in the future is the use of the depicted chromatography processes with other bacteriophages. This is the key to create a standardized bacteriophage purification process. That is, the ability to prove that the findings for the T4 bacteriophage could be replicated for other bacteriophage species.

5. References

1. Tacconelli E, Carrara E, Savoldi A, et al. Discovery, research, and development of new antibiotics: the WHO priority list of antibiotic-resistant bacteria and tuberculosis. *Lancet Infectious Diseases*. 2018;18(3):318-327. doi:10.1016/s1473-3099(17)30753-3

2. Boucher HW, Talbot GH, Bradley JS, et al. Bad bugs, no drugs: No ESKAPE! An update from the Infectious Diseases Society of America. *Clinical Infectious Diseases*. 2009;48(1):1-12. doi:10.1086/595011

3. Romero-Calle D, Benevides RG, Góes-Neto A, Billington C. Bacteriophages as alternatives to antibiotics in clinical care. *Antibiotics*. 2019;8(3). doi:10.3390/antibiotics8030138

4. Viertel TM, Ritter K, Horz HP. Viruses versus bacteria-novel approaches to phage therapy as a tool against multidrug-resistant pathogens. *Journal of Antimicrobial Chemotherapy*. 2014;69(9):2326-2336. doi:10.1093/jac/dku173

5. Wittebole X, de Roock S, Opal SM. A historical overview of bacteriophage therapy as an alternative to antibiotics for the treatment of bacterial pathogens. *Virulence*. 2014;5(1):226-235. doi:10.4161/viru.25991

6. Hankin EH. L'action bactericide des eaux de la Jumna et du Gange sur le vibrion du cholera. *Ann Inst Pasteur*. 1896;10:511-523.

7. Chanishvili N. Phage Therapy-History from Twort and d'Herelle Through Soviet Experience to Current Approaches. *Adv Virus Res*. 2012;83:3-40. doi:10.1016/b978-0-12-394438-2.00001-3

8. Twort FW, Lond LRCP. An investigation on the nature of ultra-microscopic viruses. *The Lancet*. 1915;186(4814):1241-1243. doi:10.1016/s0140-6736(01)20383-3

9. d'Herelle F. Sur un microbe invisible antagoniste des bacilles dysente´riques. *CR Acad Sci*. 1917;(165):373-375.

10. Summers WC. History of Virology: Bacteriophages. In: *Encyclopedia of Virology*. Elsevier Inc.; 2021:3-9. doi:10.1016/b978-0-12-809633-8.20950-3

11. Salmond GPC, Fineran PC. A century of the phage: Past, present and future. *Nat Rev Microbiol*. 2015;13(12):777-786. doi:10.1038/nrmicro3564

12. d'Herelle F. Studies Upon Asiatic Cholera. *Yale J Biol Med*. 1929;1(4):195-219.

13. d'Herelle F. The Bacteriophage and its Behaviour. *Nature*. 1926;118(2962):183-185. doi:10.1038/118183a0

14. Davison WC. Das le bacteriophage dans le traitment de la fievre typhoid. *Am J Dis Child*. 1922;23:531-534.

15. Summers WC. Bacteriophage therapy. *Annu Rev Microbiol*. 2001;55:437-451. doi:10.1146/annurev.micro.55.1.437

16. Clark JR. Bacteriophage therapy: History and future prospects. *Future Virol*. 2015;10(4):449-461. doi:10.2217/fvl.15.3

17. Merril CR, Scholl D, Adhya SL. The prospect for bacteriophage therapy in Western medicine. *Nature Reviews*. 2003;2(6):486-497. doi:10.1038/nrd1111

18. Sulakvelidze A, Alavidze Z, Morris JG. Bacteriophage Therapy. *Antimicrob Agents Chemother*. 2001;45(3):649-659. doi:10.1128/aac.45.3.649-659.2001

19. Alisky J, Iczkowski K, Rapoport A, Troitsky N. Bacteriophages show promise as antimicrobial agents. *Journal of Infection*. 1998;36(1):5-15. doi:10.1016/s0163-4453(98)92874-2

20. Eaton MD, Bayne-Jones S. Review of the principles and results of the use of bacteriophage in the treatment of infections. *J Am Med Assoc*. 1934;103(23):1769. doi:10.1001/jama.1934.72750490003007

21. Ruska H. Versuch zu einer Ordnung der Virusarten. *Archives of Virology 1943 2:5*. 1943;2(5):480-498. doi:10.1007/bf01244584

22. Ackermann H. Bacteriophage Classification. In: *Bacteriophages: Biology and Applications*. CRC Press; 2005:67-90. doi:10.1201/9780203491751.ch4

23. Sanger F, Air GM, Barrell BG, et al. Nucleotide sequence of bacteriophage phi X174 DNA. *Nature*. 1977;265(5596):687-695. doi:10.1038/265687a0

24. Brüssow H, Hendrix RW. Phage Genomics: Small Is Beautiful. *Cell*. 2002;108(1):13-16. doi:10.1016/s0092-8674(01)00637-7

25. Shang J, Jiang J, Sun Y. Bacteriophage classification for assembled contigs using graph convolutional network. *Bioinformatics*. 2021;37:I25-I33. doi:10.1093/bioinformatics/btab293

26. ICTV. Taxonomy Release History. Accessed December 1, 2021. https://talk.ictvonline.org/taxonomy/p/taxonomy_releases

27. Ackermann HW. Tailed bacteriophages: The order Caudovirales. *Adv Virus Res*. 1998;51:135-201. doi:10.1016/s0065-3527(08)60785-x

28. Iranzo J, Krupovic M, Koonin E v. The Double-Stranded DNA Virosphere as a Modular Hierarchical Network of Gene Sharing. *mBio*. 2016;7(4). doi:10.1128/mbio.00978-16

29. Michen B, Graule T. Isoelectric points of viruses. *J Appl Microbiol*. 2010;109(2):388-397. doi:10.1111/j.1365-2672.2010.04663.x

30. Dion MB, Oechslin F, Moineau S. Phage diversity, genomics and phylogeny. *Nat Rev Microbiol*. 2020;18(3):125-138. doi:10.1038/s41579-019-0311-5

31. Guttman B, Raya R, Kutter E. Basic Phage Biology. In: *Bacteriophages: Biology and Applications*. CRC Press; 2005:29-66. doi:10.1201/9780203491751.ch3

32. Orlova E v. Bacteriophages and Their Structural Organisation. In: *Bacteriophages*. ; 2012:3-30. doi:10.5772/34642

33. Rakhuba D, Kolomiets E, Dey E, Novik G. Bacteriophage Receptors, Mechanisms of Phage Adsorption and Penetration into Host Cell. *Pol J Microbiol*. 2010;59(3):145-155. doi:10.1016/j.micres.2015.01.008.1.94

34. Harada LK, Silva EC, Campos WF, et al. Biotechnological applications of bacteriophages: State of the art. *Microbiol Res*. 2018;212-213:38-58. doi:10.1016/j.micres.2018.04.007

35. Sharma S, Chatterjee S, Datta S, et al. Bacteriophages and its applications: an overview. *Folia Microbiol (Praha)*. 2017;62(1):17-55. doi:10.1007/s12223-016-0471-x

36. Kutter E, Raya R, Carlson K. Molecular Mechanisms of Phage Infection. In: *Bacteriophages: Biology and Applications*. CRC Press; 2005:165-222. doi:10.1201/9780203491751.ch7

37. Leiman PG, Shneider MM. Contractile tail machines of bacteriophages. *Adv Exp Med Biol*. 2012;726:93-114. doi:10.1007/978-1-4614-0980-9_5

38. Casjens SR, Molineux IJ. Short noncontractile tail machines: adsorption and DNA delivery by podoviruses. *Adv Exp Med Biol*. 2012;726:143-179. doi:10.1007/978-1-4614-0980-9_7

39. Silhavy TJ, Kahne D, Walker S. The bacterial cell envelope. *Cold Spring Harb Perspect Biol*. 2010;2(5). doi:10.1101/cshperspect.a000414

40. Maura D, Debarbieux L. Bacteriophages as twenty-first century antibacterial tools for food and medicine. *Appl Microbiol Biotechnol*. 2011;90(3):851-859. doi:10.1007/s00253-011-3227-1

41. Zahler SA. Temperate Bacteriophages of Bacillus subtilis. In: *The Bacteriophages*. Springer US; 1988:559-592. doi:10.1007/978-1-4684-5424-6_13

42. O'Flaherty S, Ross RP, Coffey A. Bacteriophage and their lysins for elimination of infectious bacteria. *FEMS Microbiol Rev*. 2009;33(4):801-819. doi:10.1111/j.1574-6976.2009.00176.x

43. Boyd EF, Brüssow H. Common themes among bacteriophage-encoded virulence factors and diversity among the bacteriophages involved. *Trends Microbiol*. 2002;10(11):521-529. doi:10.1016/s0966-842x(02)02459-9

44. Keen EC. Paradigms of pathogenesis: targeting the mobile genetic elements of disease. *Front Cell Infect Microbiol*. 2012;161(2). doi:10.3389/fmicb.2012.00161

45. Hyman P, Abedon ST. Bacteriophage (Overview). In: *Desk Encyclopedia of Microbiology*. Elsevier Inc.; 2009:166-182.

46. Young R, Wang IN, Roof WD. Phages will out: strategies of host cell lysis. *Trends Microbiol*. 2000;8(3):120-128. doi:10.1016/S0966-842X(00)01705-4

47. Wang IN, Smith DL, Young R. Holins: the protein clocks of bacteriophage infections. *Annu Rev Microbiol*. 2000;54:799-825. doi:10.1146/annurev.micro.54.1.799

48. BioRender. Lytic and Lysogenic Cycle. Published 2021. Accessed December 18, 2021. https://app.biorender.com/biorender-templates

49. Wang IN, Deaton J, Young R. Sizing the holin lesion with an endolysin-beta-galactosidase fusion. *J Bacteriol*. 2003;185(3):779-787. doi:10.1128/jb.185.3.779-787.2003

50. Vollmer W, Blanot D, de Pedro MA. Peptidoglycan structure and architecture. *FEMS Microbiol Rev*. 2008;32(2):149-167. doi:10.1111/j.1574-6976.2007.00094.x

51. Chhibber S, Kumari S. Application of Therapeutic Phages in Medicine. In: *Bacteriophages*. InTech; 2012:139-158. doi:10.5772/34296

52. Kutter E, de Vos D, Gvasalia G, et al. Phage Therapy in Clinical Practice: Treatment of Human Infections. *Curr Pharm Biotechnol*. 2010;11(1):69-86. doi:10.2174/138920110790725401

53. Abedon ST, Kuhl SJ, Blasdel BG, Kutter EM. Phage treatment of human infections. *Bacteriophage*. 2011;1(2):66-85. doi:10.4161/bact.1.2.15845

54. Coates AR, Halls G, Hu Y. Novel classes of antibiotics or more of the same? *Br J Pharmacol*. 2011;163(1):184. doi:10.1111/j.1476-5381.2011.01250.x

55. Parisien A, Allain B, Zhang J, Mandeville R, Lan CQ. Novel alternatives to antibiotics: Bacteriophages, bacterial cell wall hydrolases, and antimicrobial peptides. *J Appl Microbiol*. 2008;104(1):1-13. doi:10.1111/j.1365-2672.2007.03498.x

56. Gerstmans H, Criel B, Briers Y. Synthetic biology of modular endolysins. *Biotechnol Adv*. 2018;36(3):624-640. doi:10.1016/j.biotechadv.2017.12.009

57. Krylov V, Shaburova O, Pleteneva E, et al. Modular Approach to Select Bacteriophages Targeting Pseudomonas aeruginosa for Their Application to Children Suffering With Cystic Fibrosis. *Front Microbiol*. 2016;7. doi:10.3389/fmicb.2016.01631

58. Breidenstein EBM, de la Fuente-Núñez C, Hancock REW. Pseudomonas aeruginosa: all roads lead to resistance. *Trends Microbiol*. 2011;19(8):419-426. doi:10.1016/j.tim.2011.04.005

59. Chegini Z, Khoshbayan A, Taati Moghadam M, Farahani I, Jazireian P, Shariati A. Bacteriophage therapy against Pseudomonas aeruginosa biofilms: a review. *Ann Clin Microbiol Antimicrob*. 2020;19(1). doi:10.1186/S12941-020-00389-5

60. Liu YY, Wang Y, Walsh TR, et al. Emergence of plasmid-mediated colistin resistance mechanism MCR-1 in animals and human beings in China: a microbiological and molecular biological study. *Lancet Infectious diseases*. 2016;16(2):161-168. doi:10.1016/s1473-3099(15)00424-7

61. Armata Pharmaceuticals. Ph 1/2 Study Evaluating Safety and Tolerability of Inhaled AP-PA02 in Subjects With Chronic Pseudomonas Aeruginosa Lung Infections and Cystic Fibrosis (SWARM-Pa). Published 2021. Accessed November 25, 2021. https://clinicaltrials.gov/ct2/show/NCT04596319?term=bacteriophage&draw=4&rank=26

62. Law N, Logan C, Yung G, et al. Successful adjunctive use of bacteriophage therapy for treatment of multidrug-resistant Pseudomonas aeruginosa infection in a cystic fibrosis patient. *Infection*. 2019;47(4):665-668. doi:10.1007/s15010-019-01319-0

63. Bruttin A, Brüssow H. Human volunteers receiving Escherichia coli phage T4 orally: a safety test of phage therapy. *Antimicrob Agents Chemother*. 2005;49(7):2874-2878. doi:10.1128/aac.49.7.2874-2878.2005

64. Nilsson AS. Phage therapy--constraints and possibilities. *Ups J Med Sci*. 2014;119(2):192-198. doi:10.3109/03009734.2014.902878

65. Goodridge L. Designing phage therapeutics. *Curr Pharm Biotechnol*. 2010;11(1):15-27. doi:10.2174/138920110790725348

66. Moradpour Z, Ghasemian A. Modified phages: Novel antimicrobial agents to combat infectious diseases. *Biotechnol Adv*. 2011;29(6):732-738. doi:10.1016/j.biotechadv.2011.06.003

67. Levin BR, Bull JJ. Population and evolutionary dynamics of phage therapy. *Nat Rev Microbiol*. 2004;2(2):166-173. doi:10.1038/nrmicro822

68. Bondy-Denomy J, Pawluk A, Maxwell KL, Davidson AR. Bacteriophage genes that inactivate the CRISPR/Cas bacterial immune system. *Nature*. 2013;493(7432):429-432. doi:10.1038/nature11723

69. Sargeant K. Large-Scale Bacteriophage Production. *Adv Appl Microbiol*. 1970;13(C):121-137. doi:10.1016/s0065-2164(08)70402-7

70. João J, Lampreia J, Prazeres DMF, Azevedo AM. Manufacturing of bacteriophages for therapeutic applications. *Biotechnol Adv*. 2021;49(107758). doi:10.1016/j.biotechadv.2021.107758

71. Tanir T, Orellana M, Escalante A, de Souza CM, Koeris MS. Manufacturing Bacteriophages (Part 1 of 2): Cell Line Development, Upstream, and Downstream Considerations. *Pharmaceuticals*. 2021;14(9). doi:10.3390/ph14090934

72. Agboluaje M, Sauvageau D. Bacteriophage Production in Bioreactors. *Methods in Molecular Biology* . 2018;1693:173-193. doi:10.1007/978-1-4939-7395-8_15

73. Bonilla N, Rojas MI, Cruz GNF, Hung SH, Rohwer F, Barr JJ. Phage on tap-a quick and efficient protocol for the preparation of bacteriophage laboratory stocks. *PeerJ*. 2016;2016(7). doi:10.7717/peerj.2261

74. García R, Latz S, Romero J, Higuera G, García K, Bastías R. Bacteriophage production models: An overview. *Front Microbiol*. 2019;10(JUN):1187. doi:10.3389/fmicb.2019.01187

75. Jurač K, Nabergoj D, Podgornik A. Bacteriophage production processes. *Appl Microbiol Biotechnol*. 2019;103(2):685-694. doi:10.1007/s00253-018-9527-y

76. Sauvageau D, Cooper DG. Two-stage, self-cycling process for the production of bacteriophages. *Microb Cell Fact*. 2010;9(81). doi:10.1186/1475-2859-9-81

77. Gill J, Hyman P. Phage choice, isolation, and preparation for phage therapy. *Curr Pharm Biotechnol*. 2010;11(1):2-14. doi:10.2174/138920110790725311

78. Bourdin G, Schmitt B, Guy LM, et al. Amplification and purification of T4-like escherichia coli phages for phage therapy: from laboratory to pilot scale. *Appl Environ Microbiol*. 2013;80(4):1469-1476. doi:10.1128/aem.03357-13

79. Regulski K, Champion-Arnaud P, Gabard J. Bacteriophage Manufacturing: From Early Twentieth-Century Processes to Current GMP. In: *Bacteriophages*. Springer, Cham; 2018:1-31. doi:10.1007/978-3-319-40598-8_25-1

80. Mutti M, Corsini L. Robust Approaches for the Production of Active Ingredient and Drug Product for Human Phage Therapy. *Front Microbiol*. 2019;10(2289). doi:10.3389/fmicb.2019.02289

81. Carslon K. Working with Bacteriophages: Common Techniques and Methodological Approaches. In: *Bacteriophages: Biology and Applications*. CRC Press; 2004:437-495.

82. Nasukawa T, Uchiyama J, Taharaguchi S, et al. Virus purification by CsCl density gradient using general centrifugation. *Arch Virol*. 2017;162(11):3523-3528. doi:10.1007/s00705-017-3513-z

83. Hietala V, Horsma-Heikkinen J, Carron A, Skurnik M, Kiljunen S. The Removal of Endo- and Enterotoxins From Bacteriophage Preparations. *Front Microbiol*. 2019;10. doi:10.3389/fmicb.2019.01674

84. Wolf MW, Reichl U. Downstream processing of cell culture-derived virus particles. *Expert Rev Vaccines*. 2011;10(10):1451-1475. doi:10.1586/erv.11.111

85. Kramberger P, Urbas L, Štrancar A. Downstream processing and chromatography based analytical methods for production of vaccines, gene therapy vectors, and bacteriophages. *Hum Vaccin Immunother*. 2015;11(4):1010. doi:10.1080/21645515.2015.1009817

86. Food and Drug Administration. FDA alerts health care professionals of significant safety risks associated with cesium chloride | FDA. Published 2018. Accessed December 15, 2021. https://www.fda.gov/drugs/human-drug-compounding/fda-alerts-health-care-professionals-significant-safety-risks-associated-cesium-chloride

87. Branston S, Stanley E, Keshavarz-Moore E, Ward J. Precipitation of filamentous bacteriophages for their selective recovery in primary purification. *Biotechnol Prog*. 2012;28(1):129-136. doi:10.1002/btpr.705

88. Branston SD, Wright J, Keshavarz-Moore E. A non-chromatographic method for the removal of endotoxins from bacteriophages. *Biotechnol Bioeng*. 2015;112(8):1714-1719. doi:10.1002/bit.25571

89. Yamamoto KR, Alberts BM, Benzinger R, Lawhorne L, Treiber G. Rapid bacteriophage sedimentation in the presence of polyethylene glycol and its application to large-scale virus purification. *Virology*. 1970;40(3):734-744. doi:10.1016/0042-6822(70)90218-7

90. Monjezi R, Tey BT, Sieo CC, Tan WS. Purification of bacteriophage M13 by anion exchange chromatography. *Journal of chromatography B*. 2010;878(21):1855-1859. doi:10.1016/j.jchromb.2010.05.028

91. Mi X, Fuks P, Wang S ching, Winters MA, Carta G. Protein Adsorption on Core-shell Particles: Comparison of Capto™ Core 400 and 700 Resins. *J Chromatogr A*. 2021;1651(462314). doi:10.1016/j.chroma.2021.462314

92. Smrekar F, Ciringer M, Peterka M, Podgornik A, Štrancar A. Purification and concentration of bacteriophage T4 using monolithic chromatographic supports. *Journal of Chromatography B*. 2008;861(2):177-180. doi:10.1016/j.jchromb.2007.05.048

93. Smrekar F, Ciringer M, Štrancar A, Podgornik A. Characterisation of methacrylate monoliths for bacteriophage purification. *J Chromatogr A*. 2011;1218(17):2438-2444. doi:10.1016/j.chroma.2010.12.083

94. Smrekar F, Ciringer M, Jančar J, Raspor P, Štrancar A, Podgornik A. Optimization of lytic phage manufacturing in bioreactor using monolithic supports. *J Sep Sci*. 2011;34(16-17):2152-2158. doi:10.1002/jssc.201100182

95. Kramberger P, Honour RC, Herman RE, Smrekar F, Peterka M. Purification of the Staphylococcus aureus bacteriophages VDX-10 on methacrylate monoliths. *J Virol Methods*. 2010;166(1-2):60-64. doi:10.1016/j.jviromet.2010.02.020

96. Queiroz JA, Tomaz CT, Cabral JMS. Hydrophobic interaction chromatography of proteins. *J Biotechnol*. 2001;87(2):143-159. doi:10.1016/s0168-1656(01)00237-1

97. Weigel T, Soliman R, Wolff MW, Reichl U. Hydrophobic-interaction chromatography for purification of influenza A and B virus. *Journal of Chromatography B*. 2019;1117:103-117. doi:10.1016/j.jchromb.2019.03.037

98. Kennedy RM. Hydrophobic-Interaction Chromatography. *Curr Protoc Protein Sci*. 1995;00(1):8.4.1-8.4.21. doi:10.1002/0471140864.ps0804s00

99. McCue JT. Theory and Use of Hydrophobic Interaction Chromatography in Protein Purification Applications. In: *Methods in Enzymology*. Vol 463. Academic Press; 2009:405-414. doi:10.1016/s0076-6879(09)63025-1

100. Fekete S, Veuthey JL, Beck A, Guillarme D. Hydrophobic interaction chromatography for the characterization of monoclonal antibodies and related products. *J Pharm Biomed Anal*. 2016;130:3-18. doi:10.1016/j.jpba.2016.04.004

101. Azevedo AM, Rosa PAJ, Ferreira IF, Aires-Barros MR. Integrated process for the purification of antibodies combining aqueous two-phase extraction, hydrophobic interaction chromatography and size-exclusion chromatography. *J Chromatogr A*. 2008;1213(2):154-161. doi:10.1016/j.chroma.2008.09.115

102. Wolff MW, Siewert C, Hansen SP, Faber R, Reichl U. Purification of cell culture-derived modified vaccinia ankara virus by pseudo-affinity membrane adsorbers and hydrophobic interaction chromatography. *Biotechnol Bioeng*. 2010;107(2):312-320. doi:10.1002/bit.22797

103. Oślizło A, Miernikiewicz P, Piotrowicz A, et al. Purification of phage display-modified bacteriophage T4 by affinity chromatography. *BMC Biotechnol*. 2011;11(59). doi:10.1186/1472-6750-11-59

104. Nídia Raquel da Silva Viúla. *Design of a Scalable Strategy for the Initial Recovery and Capture of Bacteriophages: Nuclease Digestion and Phenyl Boronate Chromatography*. IBB – Institute for Biotechnology and Bioengineering, Centre for Biological and Chemical Engineering; 2021.

105. Gomes AG, Azevedo AM, Aires-Barros MR, Prazeres DMF. Clearance of host cell impurities from plasmid-containing lysates by boronate adsorption. *J Chromatogr A*. 2010;1217(15):2262-2266. doi:10.1016/j.chroma.2010.02.015

106. Azevedo AM, Gomes AG, Borlido L, Santos IFS, Prazeres DMF, Aires-Barros MR. Capture of human monoclonal antibodies from a clarified cell culture supernatant by phenyl boronate chromatography. *Journal of Molecular Recognition*. 2010;23(6):569-576. doi:10.1002/jmr.1068

107. Carvalho RJ, Woo J, Aires-Barros MR, Cramer SM, Azevedo AM. Phenylboronate chromatography selectively separates glycoproteins through the manipulation of electrostatic, charge transfer, and cis-diol interactions. *Biotechnol J*. 2014;9(10):1250-1258. doi:10.1002/biot.201400170

108. Gomes AG, Azevedo AM, Aires-Barros MR, Prazeres DMF. Validation and scale-up of plasmid DNA purification by phenyl-boronic acid chromatography. *J Sep Sci*. 2012;35(22):3190-3196. doi:10.1002/jssc.201200225

109. Liu XC, Scouten WH. Boronate Affinity Chromatography. In: *Methods in Molecular Biology* . Vol 147. Humana Press; 2000:119-128. doi:10.1007/978-1-60327-261-2_12

110. Zakharova MY, Kozyr A v., Ignatova AN, Vinnikov IA, Shemyakin IG, Kolesnikov A v. Purification of filamentous bacteriophage for phage display using size-exclusion chromatography. *Biotechniques*. 2005;38(2):194-198. doi:10.2144/05382bm04

111. Boratyński J, Syper D, Weber-Dabrowska B, Łusiak-Szelachowska M, Poźniak G, Górski A. Preparation of endotoxin-free bacteriophages. *Cell Mol Biol Lett*. 2004;9(2):253-259.

112. James KT, Cooney B, Agopsowicz K, et al. Novel High-throughput Approach for Purification of Infectious Virions. *Sci Rep*. 2016;6(36826). doi:10.1038/SREP36826

113. Schneier M, Razdan S, Miller AM, Briceno ME, Barua S. Current technologies to endotoxin detection and removal for biopharmaceutical purification. *Biotechnol Bioeng*. 2020;117(8):2588-2609. doi:10.1002/bit.27362

114. Petsch D, Anspach FB. Endotoxin removal from protein solutions. *J Biotechnol*. 2000;76(2-3):97-119. doi:10.1016/s0168-1656(99)00185-6

115. Jang H, Kim HS, Moon SC, et al. Effects of protein concentration and detergent on endotoxin reduction by ultrafiltration. *BMB Rep*. 2009;42(7):462-466. doi:10.5483/bmbrep.2009.42.7.462

116. Razdan S, Wang JC, Barua S. PolyBall: A new adsorbent for the efficient removal of endotoxin from biopharmaceuticals. *Scientific Reports 2019 9:1*. 2019;9(1):1-15. doi:10.1038/s41598-019-45402-w

117. Merabishvili M, Pirnay JP, Verbeken G, et al. Quality-Controlled Small-Scale Production of a Well-Defined Bacteriophage Cocktail for Use in Human Clinical Trials. *PLoS One*. 2009;4(3). doi:10.1371/journal.pone.0004944

118. Lionex. Endotoxin Removal Resin EndoTrap | Lionex. Accessed December 15, 2021. https://lionex.de/product/endotoxin-removal-resin/

119. Hashemi H, Pouyanfard S, Bandehpour M, et al. Efficient endotoxin removal from T7 phage preparations by a mild detergent treatment followed by ultrafiltration. *Acta Virol*. 2013;57(3):373-374. doi:10.4149/av_2013_03_373

120. European Chemicals Agency. Lista de Substâncias Sujeitas a Autorização - ECHA. Accessed December 18, 2021. https://echa.europa.eu/pt/authorisation-list

121. Kropinski AM, Mazzocco A, Waddell TE, Lingohr E, Johnson RP. Enumeration of bacteriophages by double agar overlay plaque assay. In: *Methods in Molecular Biology* . Vol 501. Methods Mol Biol; 2009:69-76. doi:10.1007/978-1-60327-164-6_7

122. Pecota DC, Wood TK. Exclusion of T4 phage by the hok/sok killer locus from plasmid R1. *J Bacteriol*. 1996;178(7):2044. doi:10.1128/jb.178.7.2044-2050.1996

123. Longin C, Guilloux-Benatier M, Alexandre H. Design and Performance Testing of a DNA Extraction Assay for Sensitive and Reliable Quantification of Acetic Acid Bacteria Directly in Red Wine Using Real Time PCR. *Front Microbiol*. 2016;7:831. doi:10.3389/fmicb.2016.00831

124. Monk AB, Rees CD, Barrow P, Hagens S, Harper DR. Bacteriophage applications: Where are we now? *Lett Appl Microbiol*. 2010;51(4):363-369. doi:10.1111/j.1472-765x.2010.02916.x

125. Gomes AG, Azevedo AM, Aires-Barros MR, Prazeres DMF. Studies on the adsorption of cell impurities from plasmid-containing lysates to phenyl boronic acid chromatographic beads. *J Chromatogr A*. 2011;1218(48):8629-8637. doi:10.1016/j.chroma.2011.10.004

126. Rhoads DD, Wolcott RD, Kuskowski MA, Wolcott BM, Ward LS, Sulakvelidze A. Bacteriophage therapy of venous leg ulcers in humans: results of a phase I safety trial. *J Wound Care*. 2009;18(6):237-243. doi:10.12968/jowc.2009.18.6.42801

127. Yap ML, Rossmann MG. Structure and function of bacteriophage T4. *Future Microbiol*. 2014;9(12):1319. doi:10.2217/fmb.14.91

128. Kanamaru S, Leiman PG, Kostyuchenko VA, et al. Structure of the cell-puncturing device of bacteriophage T4. *Nature*. 2002;415(6871):553-557. doi:10.1038/415553a

129. Rossmann MG, Mesyanzhinov V v., Arisaka F, Leiman PG. The bacteriophage T4 DNA injection machine. *Curr Opin Struct Biol*. 2004;14(2):171-180. doi:10.1016/j.sbi.2004.02.001

130. Aksyuk AA, Leiman PG, Kurochkina LP, et al. The tail sheath structure of bacteriophage T4: a molecular machine for infecting bacteria. *EMBO J*. 2009;28(7):821-829. doi:10.1038/emboj.2009.36

131. Tao Y, Strelkov S v., Mesyanzhinov V v., Rossmann MG. Structure of bacteriophage T4 fibritin: a segmented coiled coil and the role of the C-terminal domain. *Structure* . 1997;5(6):789-798. doi:10.1016/s0969-2126(97)00233-5

132. Freitas SS, Santos JAL, Prazeres DMF. Plasmid purification by hydrophobic interaction chromatography using sodium citrate in the mobile phase. *Sep Purif Technol*. 2009;65(1):95-104. doi:10.1016/j.seppur.2008.04.001

133. Engelbrecht KC, Putonti C, Koenig DW, Wolfe AJ. Draft Genome Sequence of Escherichia coli K-12 (ATCC 29425). *Genome Announc*. 2017;5(27):574-591. doi:10.1128/genomea.00574-17

134. Miller ES, Kutter E, Mosig G, Arisaka F, Kunisawa T, Rüger W. Bacteriophage T4 genome. *Microbiology and Molecular Biology* . 2003;67(1):86-156. doi:10.1128/mmbr.67.1.86-156.2003

135. Trabelsi K, ben Zakour M, Kallel H. Purification of rabies virus produced in Vero cells grown in serum free medium. *Vaccine*. 2019;37(47):7052-7060. doi:10.1016/j.vaccine.2019.06.072

136. Khawaldeh A, Morales S, Dillon B, et al. Bacteriophage therapy for refractory Pseudomonas aeruginosa urinary tract infection. *Journal of Medical Microbiology* . 2011;60(Pt 11):1697-1700. doi:10.1099/jmm.0.029744-0

Appendix

A.1 Methods

A.1.1 Solid medium T4 bacteriophage revitalization

Initially, an *E. coli* pre-inoculum in 5 mL of TSB medium was grown overnight, at 37ºC and under agitation (250 rpm). On the following day (16-18 h), 100 µL of the pre-inoculum was added to a 15 mL falcon. Additionally, the top agar must be fully melted and thermostated at 64ºC in the suitable incubator. Following its removal from the incubator, the top agar is supplemented with 10 mM $MgCl_2$. 3 mL of the top agar is added to the bacteria-containing falcon, which was then gently mixed and poured onto a TSA plate. When the upper top agar layer solidifies, one of the halves of the T4 bacteriophage-dried filter paper was placed in the middle of the plate, followed by the addition of 100 µL of TSB medium on the surface of the filter paper. This plate was incubated overnight at 37ºC without agitation in the incubator.

On the next day, a clear zone surrounding the filter paper was observed, associated with bacteria lysis by the T4 bacteriophage. 4 mL of SM buffer was added to the plate, which was slowly rotated at room temperature in the orbital for 4 hours. With the time elapsed, the phage suspension was clarified using a centrifugation followed by a microfiltration. Centrifugation was done at 8000 *g*, with a temperature of 4ºC and lasting 10 min. The recovered supernatant was filtered with a syringe filter. A final volume of about 2 mL was attained and the bacteriophage titer was evaluated via a DLPA. A single MFB was done using the clarified phage lysate. For this, 700 µL of clarified phage lysate was added to 300 µL of glycerol (50% w/v). The remaining volume was stored at 4 ºC. It was considered as a standard procedure to construct, for any T4 bacteriophage lysate, a small number of MFBs, as a safeguard for emergency purposes. A complete MFB was only generated for the final T4 bacteriophage lysate.

A.1.2 Liquid medium T4 bacteriophage revitalization

The liquid medium T4 bacteriophage revitalization was initiated by the overnight pre-inoculation of *E. coli* in 30 mL of TSB medium at 37ºC and under agitation, at 250 pm in an incubator. On the next day (16-18 h), 200 mL of TSB medium was inoculated with the previously prepared pre-inoculum, knowing that a final $OD_{600\ nm}$ of 0.1 was intended to attain in the inoculum (200 mL of TSB medium). Next, the inoculum was grown at 37ºC and under agitation, at 250 rpm. $OD_{600\ nm}$ was measured every 15 minutes until the beginning of the exponential phase.[78,81] At this stage, T4 bacteriophage infection is performed by the addition of the other half of the T4 bacteriophage-dried filter paper to the cell culture. Upon infection, 10 mM $MgCl_2$ was also added to the bacteria culture. From this stage onwards, the same incubation conditions were resumed and $OD_{600\ nm}$ was measured every 30 minutes. Incubation with the agitation was maintained for an additional 90 minutes, followed by an incubation period of 90 minutes, at 37 ºC, without agitation. In a traditional liquid bacteriophage amplification, after infection, $OD_{600\ nm}$ should eventually decrease, due to the bacteriophage propagation associated with cell lysis. In the performed work, 180 minutes after T4 bacteriophage infection, the $OD_{600\ nm}$ did not decrease, instead increasing. This might have been associated with the aforementioned deviation from the DSMZ guidelines, which included an incubation period without agitation, upon infection. Nonetheless, the liquid medium revitalization of the T4 bacteriophages was discarded from further use.

A.1.3 Impurities quantification assays

Table A.1- BSA standards. The BSA standards are represented as vials from A to I. The BSA stock solution had a concentration of 2 mg/mL. The volume of PBS 1X (µL), the volume and source of BSA (µL), and the final BSA concentration (µg/mL) are represented.

Vial	Volume of PBS 1X (µL)	Volume and Source of BSA (µL)	Final BSA concentration (µg/mL)
A	800	200 of Stock	400
B	125	375 of vial A	300
C	325	325 of vial A	200
D	175	175 of vial B	150
E	325	325 of vial C	100
F	325	325 of vial E	50
G	325	325 of vial F	25
H	400	100 of vial G	5
I (Blank)	400	0	0

Table A.2- dsDNA standards. The PicoGreen™ dsDNA standards are represented as vials from 1 to 5. The lambda DNA stock solution had a concentration of 100 µg/mL. The volume of TE 1X (µL), the volume of lambda DNA stock (µL), and the final DNA concentration are represented.

Vial	Volume of TE 1X (µL)	Volume of DNA stock (µL)	Final DNA concentration
1	0	1000	1 µg/mL
2	900	100	100 ng/mL
3	990	10	10 ng/mL
4	999	1	1 ng/mL
5 (Blank)	1000	0	0

Table A.3- Endotoxin standards. The endotoxin standards are represented as vials from 1 to 5. The endotoxin standard solution had a final concentration of 10 EU/mL. The volume of endotoxin standard solution (mL), the volume of vial 1 (mL), the volume of EFW (mL), and the final endotoxin concentration (EU/mL) are represented.

Vial	Volume of endotoxin standard solution (mL)	Volume of vial 1 (mL)	Endotoxin-free water (mL)	Final endotoxin concentration (EU/mL)
1	0.20	-	1.80	1.00
2	-	1.00	1.00	0.50
3	-	0.50	1.50	0.25
4	-	0.20	1.80	0.1
5 (Blank)	.	-	0.50	0

Table A.4- Forward and reverse primer sequence for *E. coli* K-12.

Primer	Sequence 5' → 3'
Forward	CATAAGCGTCGCTGCCG
Reverse	AAAGAAAGCGTAATAGCTCACTGGTC

Table A.5- qPCR cycling conditions using the LightCycler 2.0.

Cycle step	Temperature (ºC)	Time (s)	Cycles
Initial Denaturation	95	60	1
Denaturation	95	15	40-45
Extension	60	30	
Melt Curve	60-95	0.05º C/s	

A.2 Results

A.2.1 Host cell growth and T4 bacteriophage amplification

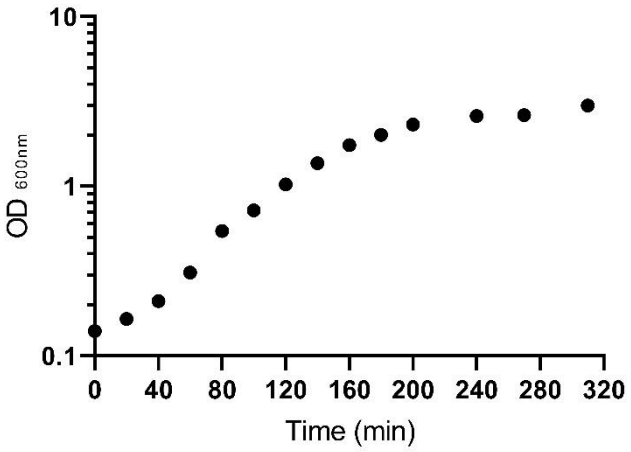

Figure A.1- Growth curve for *E. coli* 613. Bacteria were grown at 37ºC in 200 mL of TSB medium. The $OD_{600\ nm}$ is represented in a logarithmic scale, over a time course of 310 min. The initial host density was 0.14. Cell growth was halted when the stationary phase was attained.

Table A.6- Cell concentration (CFU/mL) of *E. coli* 613 throughout time (min).

Time (min)	CFU/mL
0	7.00E+07
20	9.05E+07
40	1.17E+08
140	3.20E+08
160	5.50E+08
180	8.20E+08

Table A.7- Cell concentration (CFU/mL) of *E. coli* K-12 throughout time (min).

Time (min)	CFU/mL
0	-
30	(3.60 ± 0.90)E+07
60	(1.08 ± 0.14)E+08
90	(2.12 ± 0.44)E+08
120	2.5E+08
150	(3.08 ± 0.28)E+08
180	(6.10 ± 0.30)E+08
220	(1.60 ± 0.23)E+09
260	(2.41 ± 0.24)E+09
300	2.63E+09
360	(4.05 ± 0.75)E+08

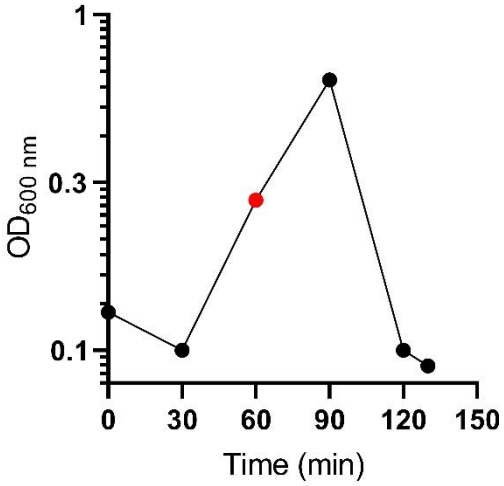

Figure A.2- T4 bacteriophage amplification curve for the host *E. coli* 613. The $OD_{600\ nm}$ is represented in a logarithmic scale, over a time course of 130 min. The initial host density was 0.13. Bacteriophage infection was performed with a MOI of 0.1 and is represented by a red dot. This occurred at 60 minutes with an $OD_{600\ nm}$ = 0.28. The bacteriophage amplification process was halted when cell growth abruptly decreased and $OD_{600\ nm}$ was below 0.1.

A.2.1.1 Infection volume determination

As described in section 3.1 (Results), various T4 bacteriophage stock lysates were generated throughout this experimental work. The subsequent calculations are an example of one of these procedures, as all follow the same logic. The following data is needed:

- MOI = 0.1 (1 bacteriophage / 10 host cells)
- Host cell concentration upon infection = 1.1E+08 CFU/mL
- Volume of host cells = 100 mL
- T4 bacteriophage concentration of the lysate used for infection = 2.8E+09 PFU/mL

Firstly, the number of host cells is calculated:

$$n_{bacteria} = 1.1 \times 10^{8} \frac{CFU}{mL} \times 100\ mL = 1.1 \times 10^{10}\ CFU$$

With the pre-defined MOI, the number of bacteriophages needed for infection may be calculated:

$$MOI = \frac{n_{bacteriophages}}{n_{bacteria}}\ (=)\ n_{bacteriophages} = 1.1 \times 10^{10}\ CFU \times 0.1\ (=)\ n_{bacteriophages} = 1.1 \times 10^{9}\ PFU$$

Knowing the concentration of the bacteriophage lysate used for infection, one may calculate the volume needed for this process.

$$Volume_{Infection} = \frac{n_{bacteriophages}}{[Bacteriophage\ concentration]}\ (=)\ Volume_{Infection}$$

$$= \frac{1.1 \times 10^{9}\ PFU}{2.8 \times 10^{9}\ PFU/mL}\ (=)\ Volume_{Infection} = 0.393\ mL$$

A.2.2 Phenyl boronate chromatography

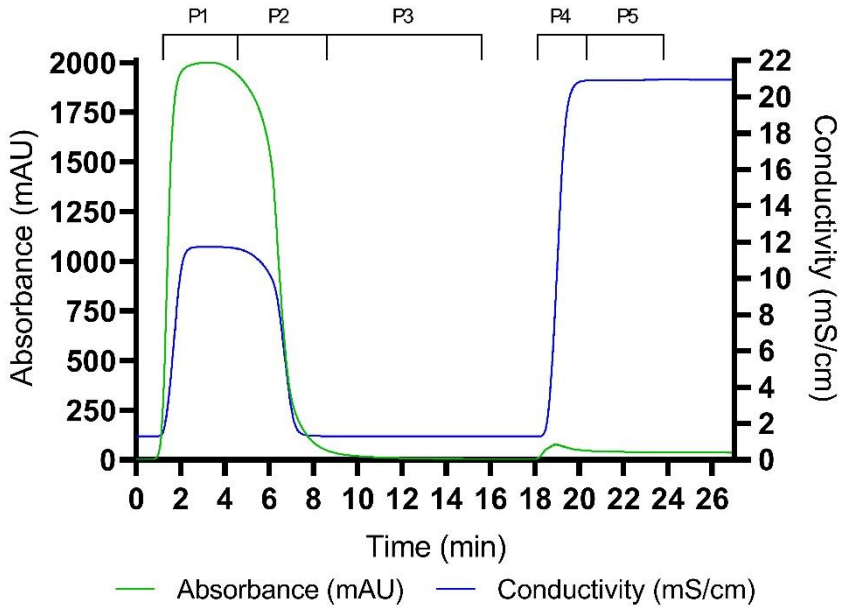

Figure A.3- PBC chromatogram of replica 1 using the previously optimized chromatography conditions. Absorbance (mAU) at 280 nm and conductivity (mS/cm) were measured throughout time (min) at 1 mL/min on the outlet stream of the chromatography column. The equilibration/washing buffer was 15 mM Tris-HCl pH 7.0 and the elution buffer was 1.5 M Tris-HCl pH 8.5. Fractions of 1 mL were collected and various pools of fractions were considered for further analysis, which are represented in the upper section of the chromatogram by **PX** (with **X** being the pool number). The following pool composition was devised: **Pool 1** (Fraction 2 to 6), **Pool 2** (Fraction 7 to 12), **Pool 3** (Fraction 13 to 16), **Pool 4** (Fraction 21 to 24), and **Pool 5** (Fraction 25 to 27). The flow-through peak was divided into Pools 1 and 2, while the elution peak is Pool 4.

Table A.8- Content composition for the feed lysate and pools 1-5 of replica 1 of the previously optimized chromatography conditions in PBC. For each defined pool and the lysate, its respective volume (mL), and bacteriophage (PFU/mL), protein (µg/mL), and dsDNA (ng/mL) concentration are represented.

Pools	Volume (mL)	[Bacteriophage] (PFU/mL)	[Protein] (µg/mL)	[dsDNA] (ng/mL)	[Endotoxin] (EU/mL)
Lysate	5.00	(2.58 ± 0.03)E+09	3926 ± 435	10443 ± 2259	(8.87 ± 0.78)E+04
1	5.00	(3.65 ± 0.45)E+08	2621 ± 97	6147 ± 736	-
2	4.60	(5.95 ± 0.45)E+07	846 ± 110		
3	4.00	(2.50 ± 0.08)E+05	10.4 ± 1.5	-	-
4	4.00	(1.65 ± 0.08)E+09	23.7 ± 2.2	458 ± 53	-
5	3.00	(7.33 ± 3.09)E+07	25.7 ± 2.6	-	-

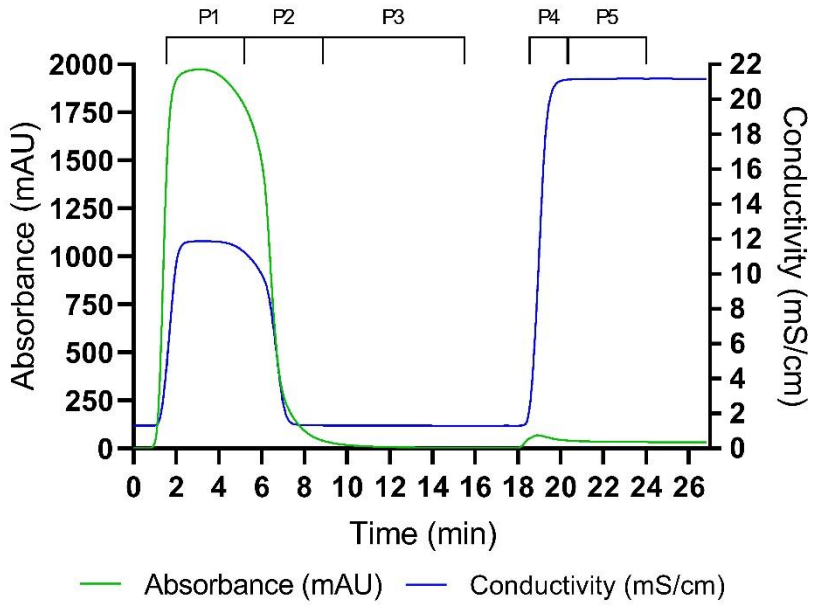

Figure A.4- PBC chromatogram of replica 3 using the previously optimized chromatography conditions. Absorbance (mAU) at 280 nm and conductivity (mS/cm) were measured throughout time (min) at 1 mL/min on the outlet stream of the chromatography column. The equilibration/washing buffer was 15 mM Tris-HCl pH 7.0 and the elution buffer was 1.5 M Tris-HCl pH 8.5. Fractions of 1 mL were collected and various pools of fractions were considered for further analysis, which are represented in the upper section of the chromatogram by **PX** (with **X** being the pool number). The following pool composition was devised: **Pool 1** (Fraction 2 to 6), **Pool 2** (Fraction 7 to 12), **Pool 3** (Fraction 13 to 16), **Pool 4** (Fraction 21 to 24), and **Pool 5** (Fraction 25 to 27). The flow-through peak was divided into Pools 1 and 2, while the elution peak is Pool 4.

Table A.9- Content composition for the feed lysate and pools 1-5 of replica 3 of the previously optimized chromatography conditions in PBC. For each defined pool and the lysate, its respective volume (mL), and bacteriophage (PFU/mL), protein (µg/mL), dsDNA (ng/mL), and endotoxin (EU/mL) concentration are represented. Note that in some cases no dsDNA nor endotoxin quantification were performed due to the shortage of the respective quantification kits.

Pools	Volume (mL)	[Bacteriophage] (PFU/mL)	[Protein] (µg/mL)	[dsDNA] (ng/mL)	[Endotoxin] (EU/mL)
Lysate	5.00	(2.36 ± 0.37)E+09	3926 ± 435	10443 ± 2259	(8.87 ± 0.78)E+04
1	5.00	(1.61 ± 0.17)E+08	2942 ± 216	4397 ± 243	-
2	4.60	(3.20 ± 0.22)E+07	809 ± 97		
3	4.00	(1.91 ± 0.08)E+05	11.8 ± 7.2	-	-
4	4.00	(1.00 ± 0.32)E+09	21.3 ± 3.4	381 ± 38	(2.24 ± 1.42)E+04
5	3.00	(5.65 ± 1.45)E+07	28.5 ± 1.4	-	-

Table A.10- Content composition for the bacteriophage lysate before and after a diafiltration using Vivaspin® 6 100 kDa MWCO centrifuge filters. For each defined sample, its respective bacteriophage (PFU/mL), protein (µg/mL), and dsDNA (ng/mL) concentrations are represented.

	[Bacteriophage] (PFU/mL)	[Protein] (µg/mL)	[dsDNA] (ng/mL)	[Endotoxin] (EU/mL)
Original bacteriophage Lysate	(3.10 ± 0.30)E+09	4687 ± 645	6998 ± 278	(8.17 ± 4.45)E+04
Bacteriophage lysate after diafiltration	(1.07 ± 0.10)E+09	420 ± 79	4646 ± 397	1.60E+09

A.2.3 Phenyl Sepharose FF chromatography

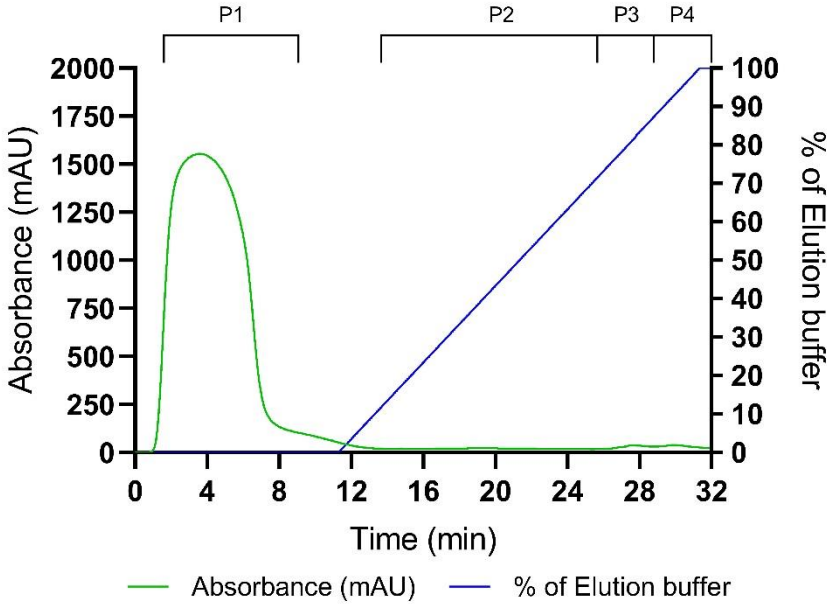

Figure A.5- Phenyl Sepharose FF chromatogram with a 20 min linear-gradient elution. Absorbance (mAU) at 280 nm and % of elution buffer were measured throughout time (min) at 1 mL/min on the outlet stream of the chromatography column. The equilibration/washing buffer was 1.5 M $(NH4)_2SO_4$, 15 mM Tris-HCl pH 7.0, and the elution buffer was 15 mM Tris-HCl pH 7.0. Fractions of 1 mL were collected and various pools of fractions were considered for further analysis, which are represented in the upper section of the chromatogram by **PX** (with **X** being the pool number). The following pool composition was devised: **Pool 1** (Fraction 3 to 11), **Pool 2** (Fraction 18 to 29), **Pool 3** (Fraction 30 to 31), and **Pool 4** (Fraction 33 to 34). Pools 3 and 4 correspond to the elution pools.

Table A.11- T4 bacteriophage lysate content composition for the different ammonium sulfate concentrations (1.0, 0.75, and 0.50 M) in the equilibration buffer of a Phenyl Sepharose FF chromatography. The estimation of the bacteriophage (PFU/mL), protein (µg/mL), dsDNA (ng/mL), genomic dsDNA (ng/mL), and endotoxin (EU/mL) concentration of the injected bacteriophage lysate is represented.

Ammonium sulfate concentration (M)	[Bacteriophage] (PFU/mL)	[Protein] (µg/mL)	[dsDNA] (ng/mL)	[Genomic dsDNA] (EU/mL)	[Endotoxin] (EU/mL)
1.00	(3.10 ± 0.30)E+09	4687 ± 646	6998 ± 278	1199 ± 134	(8.17 ± 4.45)E+04
0.75	(3.70 ± 0.16)E+09	5077 ± 929	8117 ± 440	1199 ± 134	(8.17 ± 4.45)E+04
0.50					

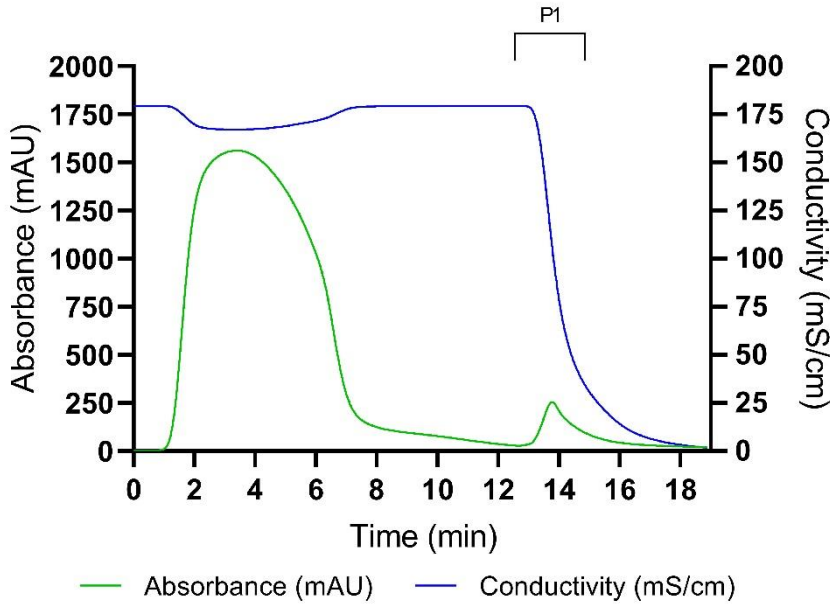

Figure A.6- Single-step-gradient elution Phenyl Sepharose FF chromatogram before a SEC. Absorbance (mAU) at 280 nm and % of elution buffer were measured throughout time (min) at 1 mL/min on the outlet stream of the chromatography column. The equilibration/washing buffer was 1.5 M $(NH4)_2SO_4$, 15 mM Tris-HCl pH 7.0, and the elution buffer was 15 mM Tris-HCl pH 7.0. Fractions of 1 mL were collected and various pools of fractions were considered for further analysis, which are represented in the upper section of the chromatogram by **PX** (with **X** being the pool number). The following pool composition was devised: **Pool 1** (Fraction 16 to 19). Pool 1 corresponds to the elution pool.

Table A.12- Content composition for the feed lysate and the single-step-gradient elution Phenyl Sepharose FF chromatography before a SEC. For the defined elution pool, its respective volume (mL), and bacteriophage (PFU/mL), protein (µg/mL), dsDNA (ng/mL), and endotoxin (EU/mL) concentrations are represented.

Pools	Volume (mL)	[Bacteriophage] (PFU/mL)	[Protein] (µg/mL)	[dsDNA] (ng/mL)	[Genomic dsDNA] (EU/mL)	[Endotoxin] (EU/mL)
Lysate	5.00	(3.50 ± 0.37)E+09	4348 ± 479	6695 ± 326	1199 ± 134	(8.17 ± 4.45)E+04
1	4.00	(3.63 ± 0.21)E+09	122 ± 7	1035 ± 345	-	(2.80 ± 0.80)E+03

A.2.4 Capto™ Core 700 chromatography

Table A.13- Content composition for the feed lysate and pools 1-3 of the Capto™ Core 700 chromatography with or without salt in the equilibration buffer. For each defined pool and the lysate, its respective volume (mL), and bacteriophage (PFU/mL), protein (µg/mL), dsDNA (ng/mL), genomic dsDNA (ng/mL), and endotoxin (EU/mL) concentrations are represented.

Pools	Volume (mL)	[Bacteriophage] (PFU/mL)	[Protein] (µg/mL)	[dsDNA] (ng/mL)	[Genomic dsDNA] (EU/mL)	[Endotoxin] (EU/mL)
Lysate	5.00	(2.19 ± 0.27)E+09	3446 ± 175	5047 ± 363	308 ± 5	(6.13 ± 3.45)E+04
Equilibration buffer with NaCl						
1	6.95	(1.82 ± 0.06)E+09	2452 ± 127	62.8 ± 8.6	33.3	1.30E+03
2	3.00	(3.80 ± 0.85)E+08	533 ± 61	12.1 ± 8.6	9.56	7.82E+02
3	2.00	-	285 ± 14	639 ± 17	3.16	(6.90 ± 4.79)E+02
Equilibration buffer without NaCl						
1	4.50	(1.58 ± 0.23)E+09	3219 ± 371	65.3 ± 4.8	7.30	(5.64 ± 2.60)E+03
2	2.00	(7.77 ± 0.49)E+07	641 ± 68	7.05 ± 0.58	-	(1.72 ± 0.98)E+03
3	2.00	(3.65 ± 0.65)E+05	487 ± 34	123 ± 45	-	(5.33 ± 0.23)E+02

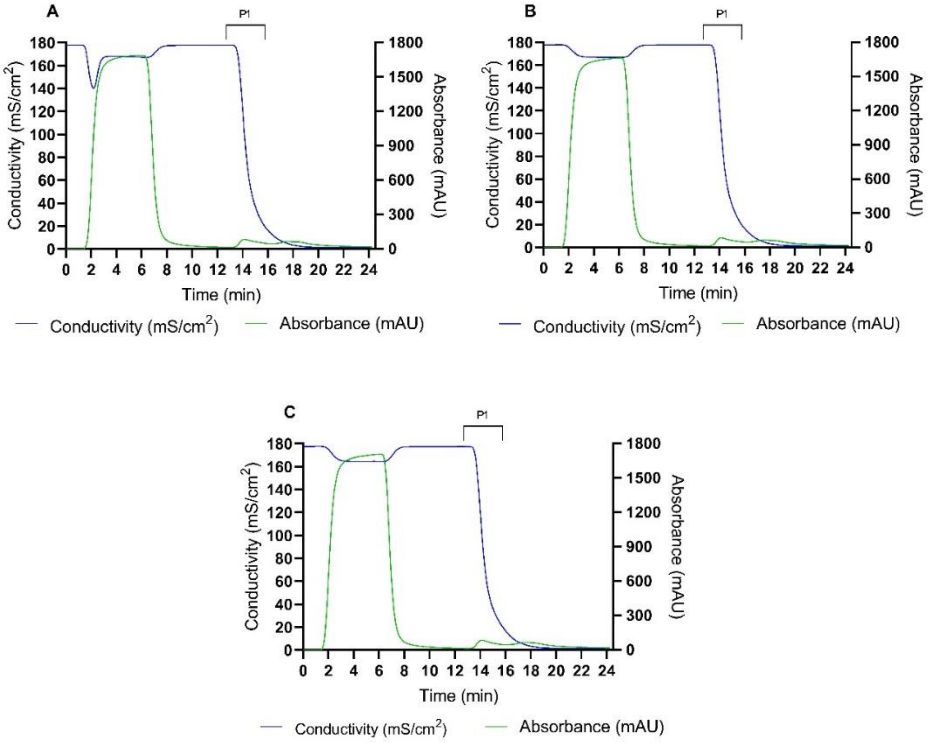

Figure A.7- PBC chromatograms for the three replicas (A, B, and C) exploring the enhanced hydrophobic interactions. Absorbance (mAU) at 280 nm and conductivity (mS/cm) were measured throughout time (min) at 1 mL/min on the outlet stream of the chromatography column. The equilibration/washing buffer was 1.5 M $(NH4)_2SO_4$, 15 mM Tris-HCl pH 7.0, and the elution buffer was 15 mM Tris-HCl pH 7.0. Fractions of 1 mL were collected and one pool of fractions was considered for further analysis, which is represented in the upper section of the chromatogram by **PX** (with **X** being the pool number). The following pool composition was devised: **Pool 1** (Fraction 16 to 19). The elution peak is associated with pool 1.

Table A.14- Content composition for the feed lysate and the three replicas of PBC with enhanced hydrophobic interactions. For each defined pool replica and the lysate, its respective volume (mL), and bacteriophage (PFU/mL), protein (µg/mL), dsDNA (ng/mL), genomic dsDNA (ng/mL), and endotoxin (EU/mL) concentrations are represented. *****The genomic dsDNA concentration for the third replica considers the lowest possible threshold of the qPCR assay, according to a CP value > 35.00.

Elution pool replicas	Volume (mL)	[Bacteriophage] (PFU/mL)	[Protein] (µg/mL)	[dsDNA] (ng/mL)	[Genomic dsDNA] (EU/mL)	[Endotoxin] (EU/mL)
Lysate	5.00	(2.48 ± 0.38)E+09	4528 ± 542	4349 ± 412	308 ± 5	(6.13 ± 3.45)E+04
1	4.00	(1.83 ± 0.31)E+09	79.8 ± 37.1	284 ± 56	17.4	(1.46 ± 0.37)E+03
2		(2.21 ± 0.15)E+09	74.0 ± 34.0	325 ± 69	6.97	1.68E+03
3		(2.31 ± 0.40)E+09	64.9 ± 11.3	338 ± 77	< 11.1*	1.37E+03